Appendix A.10:

Pinewood Ave – CPT 61991

Table 1: Site Description for Pinewood Ave (CC LIQ 5 – CPT 61991).

Attribute	Yes/No			Description/Date	Symbol in Figure 1
	10-m Buffer	20-m Buffer	50-m Buffer		
Near a body of surface water or other free face features?	No	No	No	The center of the site is 810 m away from a swamp (~2.0 m high, N-S free face), 1070 m away from the Pegasus Bay (~6 m high, NW-SE free face), and 1560 m away from the Avon River (~1.5 m high, NW-SE free face).	NA
Lateral spreading observed during the CES?	No	No	No	Absence of ground cracks indicates no lateral spreading, as observed by the mapping team.[1]	NA
Nearby buildings or structures?	Yes	Yes	Yes	Building coverage of the 10-m, 20-m, and 50-m buffers is 26%, 29%, and 22%, respectively.	White Fill + Brown Outline
Sloping land?	No	No	No	Flat land, residential area.	NA
Step changes in the ground surface?	No	No	No	NA	NA
Retaining walls?	No	No	No	NA	NA
Vegetation?	Yes	Yes	Yes	Trees and bushes cover 12% of the 10-m buffer, 10% of the 20-m buffer and 15% of the 50-m buffer. They are spread throughout all quadrants of the three buffers.	White Fill + Green Outline
Anthropogenic changes to the site between the LiDAR surveys?	Yes	Yes	Yes	Vegetation in the SW quadrant was removed between Apr 2009 and Sep 2010. Building in the SW quadrant of the 50-m buffer was removed between Aug 2014 and Sep 2014. Vegetation covered the center of the site from Sep 2013 to Jan 2015. Earthwork was done in the SW quadrant of the 50-m buffer in Aug-Sep 2014.	Vegetation Removal: Green Outline + Orange Crossline; Building Removal: Orange Crossline; Vegetation Addition: Green Outline
Other important factors?	Yes	Yes	Yes	Low to moderate-motor-vehicle-volume, two-way roadways occupy 21% of the 50-m buffer, and are in the NE, NW, and SE quadrants. The same quadrants of the 20-m buffer are affected by the roadway, which covers 21% of the area. Only NE portion of the 10-m buffer is occupied by the roadway that covers 4% of the area. Motor vehicles are occasionally parked on the lawn.	Road: White Fill + Gray Outline

Note: Buffer is the area within a circle of a specified radius with CPT investigations done at its center (172.711272°, -43.488333°).

[1] Canterbury Geotechnical Database. (2012). "Observed Ground Crack Locations", Map Layer CGD0400 - 23 July 2012, retrieved July 09, 2018 from https://canterburygeotechnicaldatabase.projectorbit.com/

Figure 1: Site plan with areas where LiDAR survey data is considered.

Note 1: Ten patches (outlined in red) in the free field were initially selected for settlement assessment as areas free of vegetation and structures. Further analyses such as proximity of a patch to a CPT, proximity of a patch to a property subjected to addition and/or demolition of a structure, front yard/backyard alterations (e.g., ploughing, rubble, scrap), aerial distribution of sediment ejecta, and density of LiDAR points for 2003 resulted in Patches A, B, and C being selected for detailed settlement assessment and other patches being discarded for detailed settlement assessment. In addition, since significant amounts of ejecta were observed on roads in the CES, the entire portion of the road within the 50-m buffer was considered for settlement assessment. Roads as hard, relatively flat surfaces provide many ground-classified points. Therefore, it is very useful to compare settlement estimates on roads with settlement estimates for the unpaved patches.

Table 2: LiDAR flight error adjustments, global adjustments for the difference between average LiDAR point elevations and benchmark survey elevations, and vertical tectonic movement adjustments.

	Adjustments (mm)		
Earthquake Event(s)	LiDAR Flight Error	Global Offset[2]	Tectonic Vertical Movement
Sep-10	-50	-3	0
Feb-11	50	16	-30
Jun-11	0	38	-40
Dec-11	0	-65	-5
CES	0	-14	-75
Any LiDAR survey affected by ejecta?			No

Note: The negative sign indicates the subtraction from the ground surface subsidence, while the positive sign indicates the addition to the ground surface subsidence.

Table 3a: LiDAR Measurement Error for Patch A.

Surveys	Buffer	Area Averaged Difference Indicating Repeat Measurement Error (mm)	$\sigma^*_{\text{individual LiDAR points}}$ (mm)	%Reduction in σ due to Area Averaging of LiDAR Points
Post Feb 2011: Mar 2011 and May 2011	10-m	NA	59	[NA,NA]
	20-m	NA		
	50-m	NA		
Post Dec 2011: Feb 2012 and Oct 2015	10-m	38	70	[54,54]
	20-m	38		
	50-m	38		

*Standard deviation.

[2] Russell, J., & van Ballegooy, S. (2015). *Canterbury Earthquake Sequence: Increased liquefaction vulnerability assessment methodology*. New Zealand: Tonkin & Taylor Ltd.

Table 3b: LiDAR Measurement Error for Patch B.

Surveys	Buffer	Area Averaged Difference Indicating Repeat Measurement Error (mm)	$\sigma^*_{individual\ LiDAR\ points}$ (mm)	%Reduction in σ due to Area Averaging of LiDAR Points
Post Feb 2011: Mar 2011 and May 2011	10-m	NA	59	[NA,NA]
	20-m	NA		
	50-m	NA		
Post Dec 2011: Feb 2012 and Oct 2015	10-m	47	70	[41,67]
	20-m	29		
	50-m	29		

*Standard deviation.

Table 3c: LiDAR Measurement Error for Patch C.

Surveys	Buffer	Area Averaged Difference Indicating Repeat Measurement Error (mm)	$\sigma^*_{individual\ LiDAR\ points}$ (mm)	%Reduction in σ due to Area Averaging of LiDAR Points
Post Feb 2011: Mar 2011 and May 2011	10-m	NA	59	[NA,NA]
	20-m	NA		
	50-m	NA		
Post Dec 2011: Feb 2012 and Oct 2015	10-m	NA	70	[NA,NA]
	20-m	NA		
	50-m	NA		

*Standard deviation; The Oct-2015 LiDAR survey was excluded from the analysis because it is affected by the earthwork that was done in Aug-Sep 2014.

Table 3d: LiDAR Measurement Error for Road.

Surveys	Buffer	Area Averaged Difference Indicating Repeat Measurement Error (mm)	$\sigma^*_{individual\ LiDAR\ points}$ (mm)	%Reduction in σ due to Area Averaging of LiDAR Points
Post Feb 2011: Mar 2011 and May 2011	10-m	NA	59	[NA,NA]
	20-m	NA		
	50-m	NA		
Post Dec 2011: Feb 2012 and Oct 2015	10-m	35	70	[43,53]
	20-m	30		
	50-m	37		

*Standard deviation.

Table 4a: Ground surface subsidence adjustments for Patch A due to LiDAR measurement error.

Earthquake Event(s)	$\sigma_{pre\text{-}EQ\ LiDAR\ survey}$ (mm)	$\sigma_{post\text{-}EQ\ LiDAR\ survey}$ (mm)	σ_{total} (mm)	Area Average Adjusted σ (mm) **
Sep-10	158	56	134	±73
Feb-11	56	59	59	±32
Jun-11	59	61	62	±34
Dec-11	61	70	87	±47
CES	158	70	124	±68

**Based on the highest %Reduction in Table 3a.

Table 4b: Ground surface subsidence adjustments for Patch B due to LiDAR measurement error.

Earthquake Event(s)	$\sigma_{pre\text{-}EQ\ LiDAR\ survey}$ (mm)	$\sigma_{post\text{-}EQ\ LiDAR\ survey}$ (mm)	σ_{total} (mm)	Area Average Adjusted σ (mm) **
Sep-10	158	56	134	±90
Feb-11	56	59	59	±40
Jun-11	59	61	62	±42
Dec-11	61	70	87	±58
CES	158	70	124	±84

**Based on the highest %Reduction in Table 3b.

Table 4c: Ground surface subsidence adjustments for Patch C due to LiDAR measurement error.

Earthquake Event(s)	$\sigma_{\text{pre-EQ LiDAR survey}}$ (mm)	$\sigma_{\text{post-EQ LiDAR survey}}$ (mm)	σ_{total} (mm)	Area Average Adjusted σ (mm) **
Sep-10	158	56	134	NA
Feb-11	56	59	59	NA
Jun-11	59	61	62	NA
Dec-11	61	70	87	NA
CES	158	70	124	NA

**Based on the highest %Reduction in Table 3c.

Table 4d: Ground surface subsidence adjustments for Road due to LiDAR measurement error.

Earthquake Event(s)	$\sigma_{\text{pre-EQ LiDAR survey}}$ (mm)	$\sigma_{\text{post-EQ LiDAR survey}}$ (mm)	σ_{total} (mm)	Area Average Adjusted σ (mm) **
Sep-10	158	56	134	$\pm$71
Feb-11	56	59	59	$\pm$31
Jun-11	59	61	62	$\pm$33
Dec-11	61	70	87	$\pm$46
CES	158	70	124	$\pm$66

**Based on the highest %Reduction in Table 3d.

Table 5a: Raw liquefaction-related ground surface subsidence for Patch A using original LiDAR points.

	Average Ground Surface Subsidence (mm)		
Earthquake Event(s)	10-m Buffer	20-m Buffer	50-m Buffer
Sep-10	67	67	67
Feb-11	143	143	143
Jun-11	32	32	32
Dec-11	136	136	136
CES	378	378	378

Table 5b: Raw liquefaction-related ground surface subsidence for Patch B using original LiDAR points.

	Average Ground Surface Subsidence (mm)		
Earthquake Event(s)	10-m Buffer	20-m Buffer	50-m Buffer
Sep-10	61	54	54
Feb-11	153	157	157
Jun-11	17	17	17
Dec-11	89	96	96
CES	320	324	324

Table 5c: Raw liquefaction-related ground surface subsidence for Patch C using original LiDAR points.

	Average Ground Surface Subsidence (mm)		
Earthquake Event(s)	10-m Buffer	20-m Buffer	50-m Buffer
Sep-10	NA	NA	-7
Feb-11	NA	NA	91
Jun-11	NA	NA	-9
Dec-11	NA	NA	94
CES	NA	NA	169

Table 5d: Raw liquefaction-related ground surface subsidence for Road using original LiDAR points.

	Average Ground Surface Subsidence (mm)		
Earthquake Event(s)	10-m Buffer	20-m Buffer	50-m Buffer
Sep-10	NA	59	34
Feb-11	123	142	154
Jun-11	45	46	73
Dec-11	131	121	111
CES	NA	368	373

Table 6a: Corrected liquefaction-related ground surface subsidence for Patch A using original LiDAR points with the calculated adjustments in Table 2.

	Average Calculated Ground Surface Subsidence (mm)		
Earthquake Event(s)	10-m Buffer	20-m Buffer	50-m Buffer
Sep-10	14 ± 75	14 ± 75	14 ± 75
Feb-11	179 ± 25	179 ± 25	179 ± 25
Jun-11	30 ± 25	30 ± 25	30 ± 25
Dec-11	66 ± 50	66 ± 50	66 ± 50
CES	289 ± 75	289 ± 75	289 ± 75

Notes: Plus/minus values are same as those in Table 4a, but rounded to the nearest 25; Positive overall values indicate ground surface subsidence, while negative overall values indicate ground surface uplift.

Table 6b: Corrected liquefaction-related ground surface subsidence for Patch B using original LiDAR points with the calculated adjustments in Table 2.

	Average Calculated Ground Surface Subsidence (mm)		
Earthquake Event(s)	10-m Buffer	20-m Buffer	50-m Buffer
Sep-10	8 ± 100	1 ± 100	1 ± 100
Feb-11	189 ± 50	193 ± 50	193 ± 50
Jun-11	15 ± 50	15 ± 50	15 ± 50
Dec-11	19 ± 50	26 ± 50	26 ± 50
CES	231 ± 75	235 ± 75	235 ± 75

Notes: Plus/minus values are same as those in Table 4b, but rounded to the nearest 25; Positive overall values indicate ground surface subsidence, while negative overall values indicate ground surface uplift.

Table 6c: Corrected liquefaction-related ground surface subsidence for Patch C using original LiDAR points with the calculated adjustments in Table 2.

	Average Calculated Ground Surface Subsidence (mm)		
Earthquake Event(s)	10-m Buffer	20-m Buffer	50-m Buffer
Sep-10	NA	NA	-60 ± NA
Feb-11	NA	NA	127 ± NA
Jun-11	NA	NA	-11 ± NA
Dec-11	NA	NA	24 ± NA
CES	NA	NA	80 ± NA

Notes: Plus/minus values are same as those in Table 4c, but rounded to the nearest 25; Positive overall values indicate ground surface subsidence, while negative overall values indicate ground surface uplift.

Table 6d: Corrected liquefaction-related ground surface subsidence for Road using original LiDAR points with the calculated adjustments in Table 2.

	Average Calculated Ground Surface Subsidence (mm)		
Earthquake Event(s)	10-m Buffer	20-m Buffer	50-m Buffer
Sep-10	NA ± 75	6 ± 75	-19 ± 75
Feb-11	159 ± 25	178 ± 25	190 ± 25
Jun-11	43 ± 25	44 ± 25	71 ± 25
Dec-11	61 ± 50	51 ± 50	41 ± 50
CES	NA ± 75	279 ± 75	284 ± 75

Notes: Plus/minus values are same as those in Table 4a, but rounded to the nearest 25; Positive overall values indicate ground surface subsidence, while negative overall values indicate ground surface uplift.

Table 7a: Corrected liquefaction-related ground surface subsidence for Patch A using LiDAR DEMs.

	Estimated Ground Surface Subsidence (mm)								
	10-m Buffer			20-m Buffer			50-m Buffer		
Earthquake Event(s)	16th %ile	50th %ile	84th %ile	16th %ile	50th %ile	84th %ile	16th %ile	50th %ile	84th %ile
Sep-10	50	50	50	50	50	50	50	50	50
Feb-11	200	200	200	200	200	200	200	200	200
Jun-11	50	50	50	50	50	50	50	50	50
Dec-11	50	50	50	50	50	50	50	50	50
CES	350	350	350	350	350	350	350	350	350

Note: These percentiles are not the exact statistical measures; they indicate the spatial variability of ground surface subsidence.

Table 7b: Corrected liquefaction-related ground surface subsidence for Patch B using LiDAR DEMs.

	Estimated Ground Surface Subsidence (mm)								
	10-m Buffer			20-m Buffer			50-m Buffer		
Earthquake Event(s)	16th %ile	50th %ile	84th %ile	16th %ile	50th %ile	84th %ile	16th %ile	50th %ile	84th %ile
Sep-10	<50	<50	50	<50	<50	50	<50	<50	50
Feb-11	150	200	200	150	200	200	150	200	200
Jun-11	50	50	50	50	50	50	50	50	50
Dec-11	50	50	50	50	50	50	50	50	50
CES	250	300	350	250	300	350	250	300	350

Note: These percentiles are not the exact statistical measures; they indicate the spatial variability of ground surface subsidence.

Table 7c: Corrected liquefaction-related ground surface subsidence for Patch C using LiDAR DEMs.

	Estimated Ground Surface Subsidence (mm)								
	10-m Buffer			20-m Buffer			50-m Buffer		
Earthquake Event(s)	16th %ile	50th %ile	84th %ile	16th %ile	50th %ile	84th %ile	16th %ile	50th %ile	84th %ile
Sep-10	NA	NA	NA	NA	NA	NA	<50	50	50
Feb-11	NA	NA	NA	NA	NA	NA	150	150	200
Jun-11	NA	NA	NA	NA	NA	NA	50	50	50
Dec-11	NA	NA	NA	NA	NA	NA	50	100	100
CES	NA	NA	NA	NA	NA	NA	300	350	400

Note: These percentiles are not the exact statistical measures; they indicate the spatial variability of ground surface subsidence.

Table 7d: Corrected liquefaction-related ground surface subsidence for Road using LiDAR DEMs.

	Estimated Ground Surface Subsidence (mm)								
	10-m Buffer			20-m Buffer			50-m Buffer		
Earthquake Event(s)	16th %ile	50th %ile	84th %ile	16th %ile	50th %ile	84th %ile	16th %ile	50th %ile	84th %ile
Sep-10	50	50	50	<50	50	50	<50	50	50
Feb-11	200	200	200	100	200	200	100	200	200
Jun-11	50	50	50	50	50	50	50	50	50
Dec-11	50	50	50	50	50	150	50	50	150
CES	350	350	350	250	350	350	250	350	450

Note: These percentiles are not the exact statistical measures; they indicate the spatial variability of ground surface subsidence.

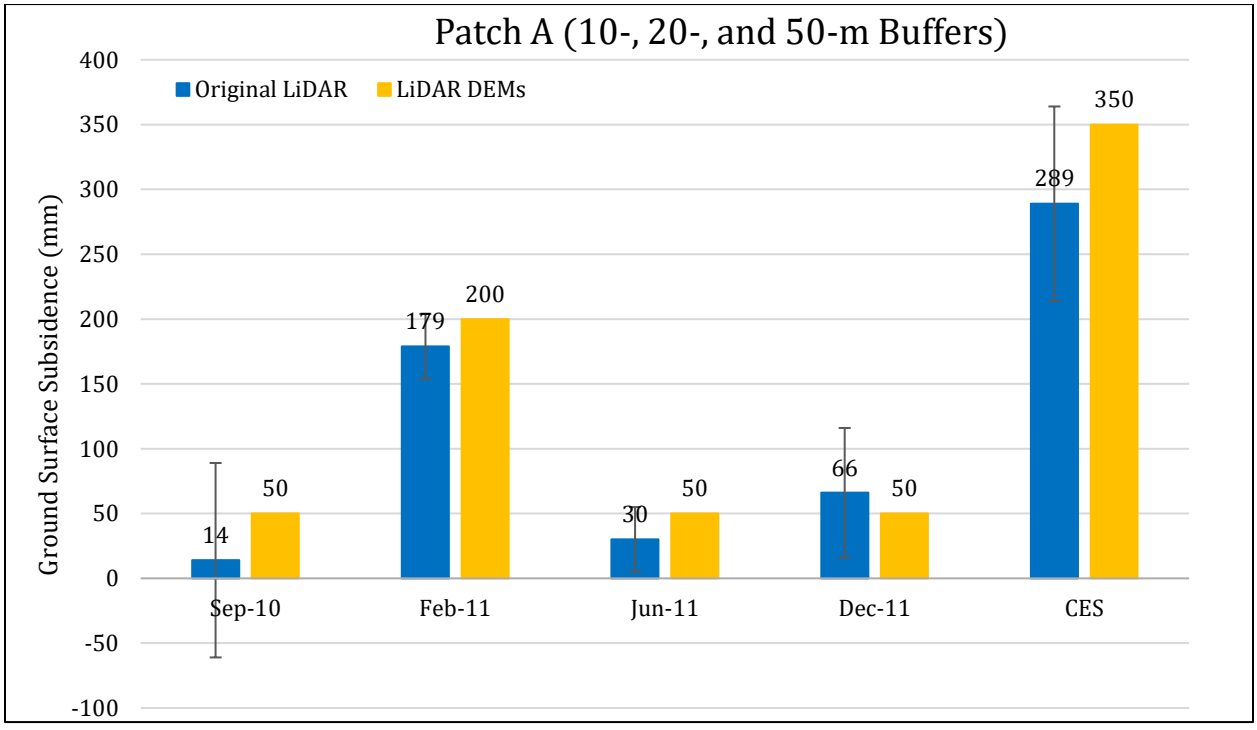

Figure 2: Comparison between ground surface subsidence determined from original LiDAR survey points and ground surface subsidence (50th %ile) estimated using LiDAR DEMs for Patch A.

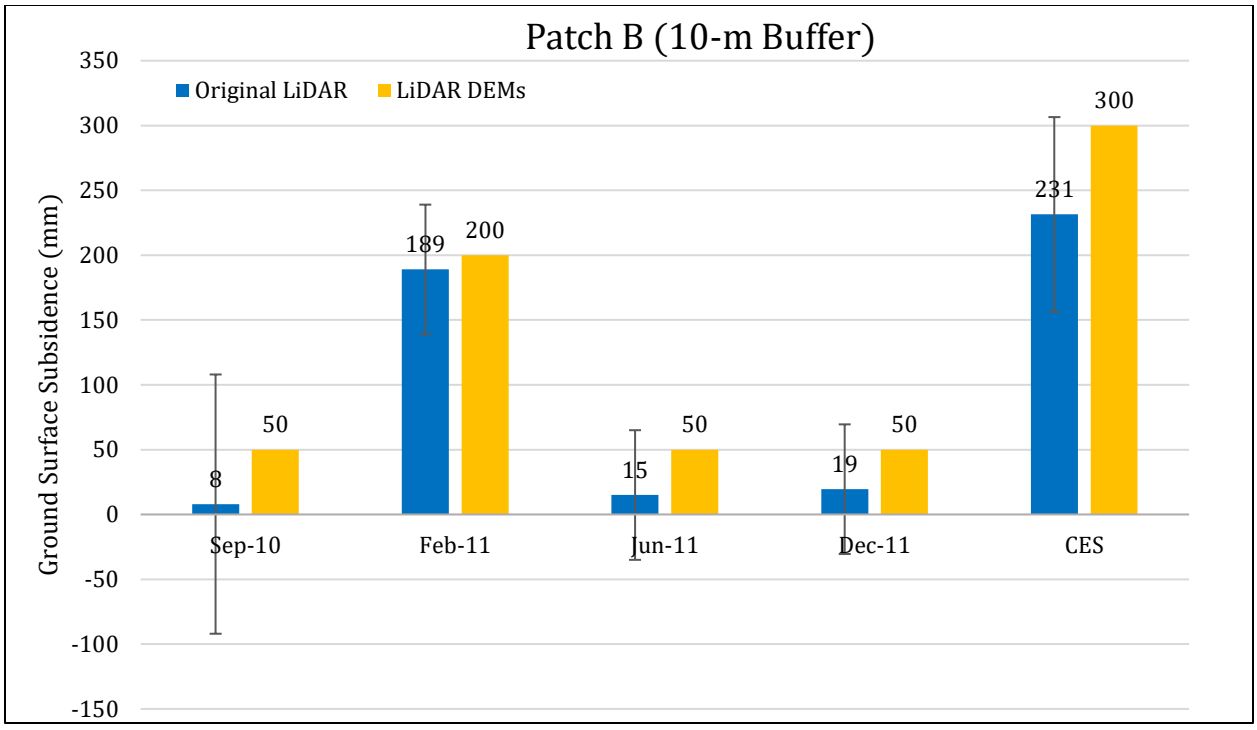

Figure 3: Comparison between ground surface subsidence determined from original LiDAR survey points and ground surface subsidence (50th %ile) estimated using LiDAR DEMs for Patch B for the 10-m buffer.

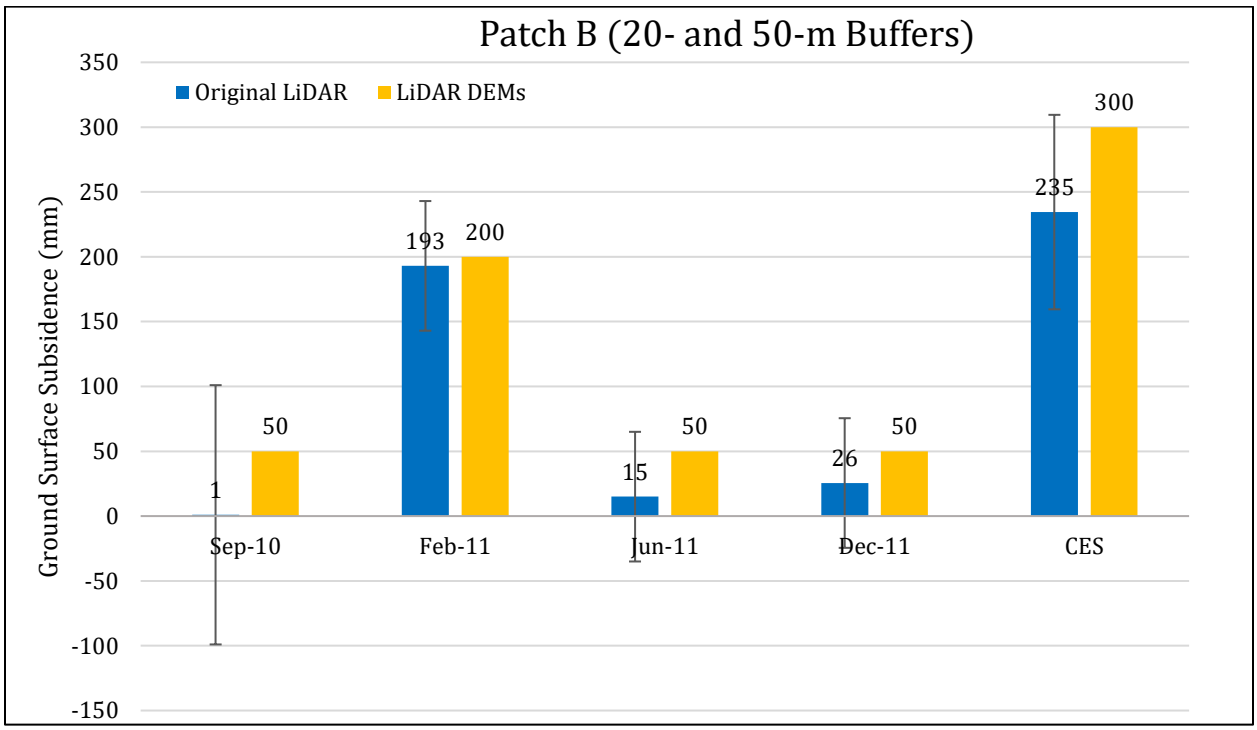

Figure 4: Comparison between ground surface subsidence determined from original LiDAR survey points and ground surface subsidence (50th %ile) estimated using LiDAR DEMs for Patch B for the 20-m and 50-m buffers.

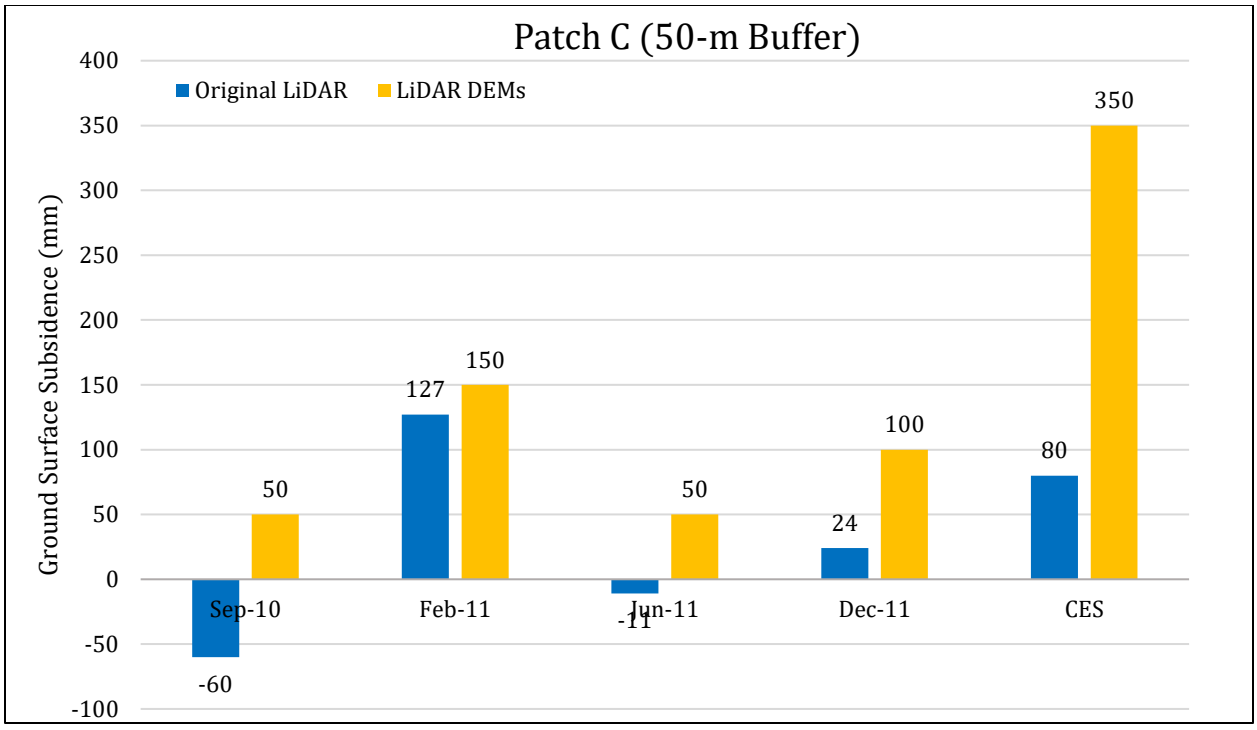

Figure 5: Comparison between ground surface subsidence determined from original LiDAR survey points and ground surface subsidence (50th %ile) estimated using LiDAR DEMs for Patch C for the 50-m buffer.

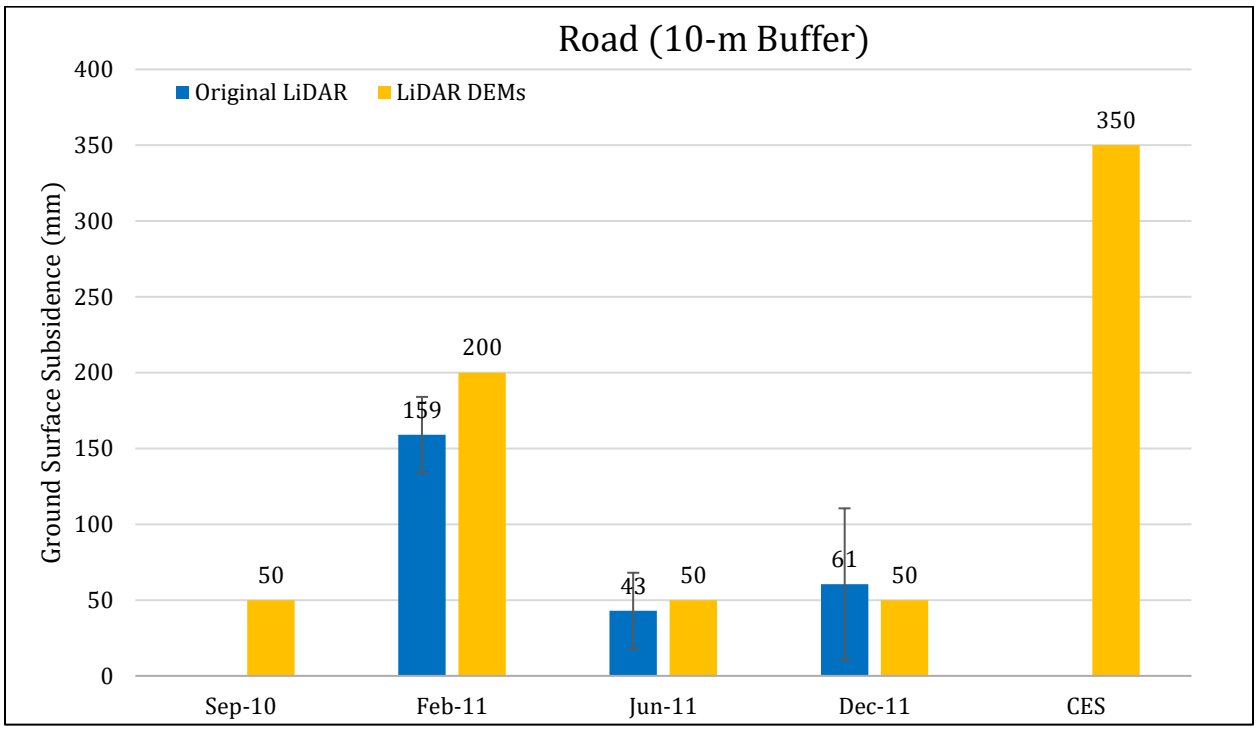

Figure 6: Comparison between ground surface subsidence determined from original LiDAR survey points and ground surface subsidence (50th %ile) estimated using LiDAR DEMs for Road for the 10-m buffer.

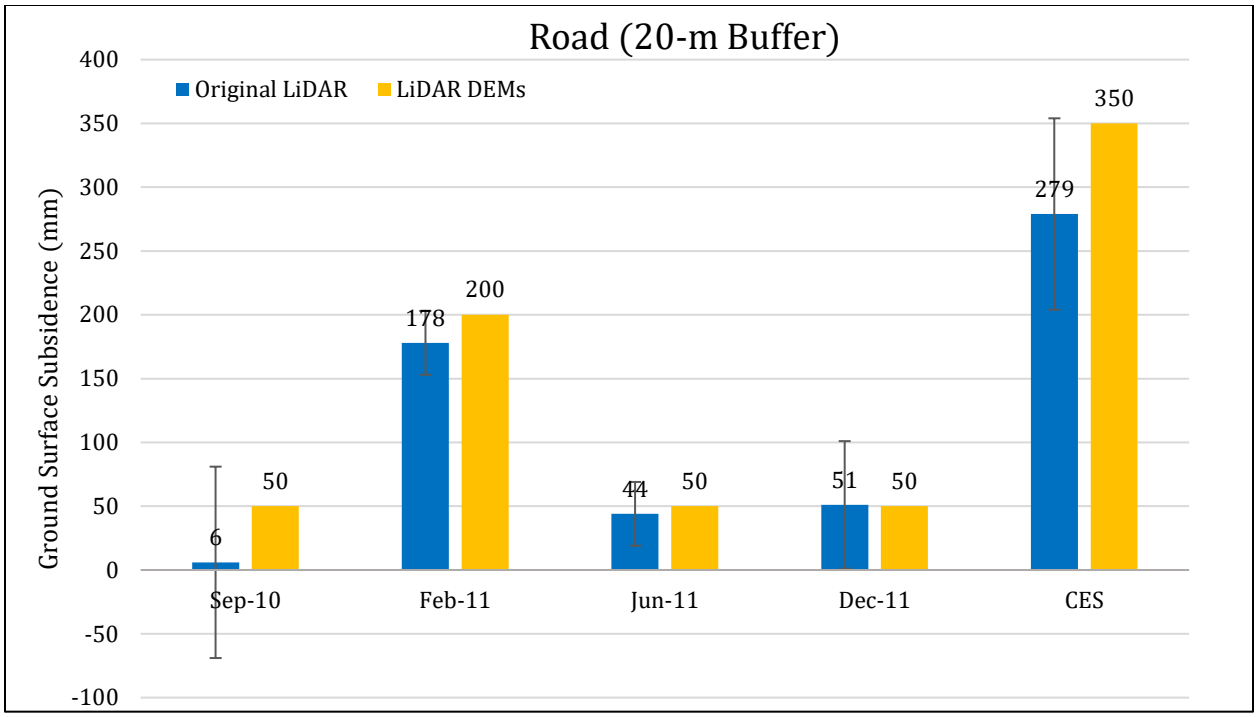

Figure 7: Comparison between ground surface subsidence determined from original LiDAR survey points and ground surface subsidence (50th %ile) estimated using LiDAR DEMs for Road for the 20-m buffer.

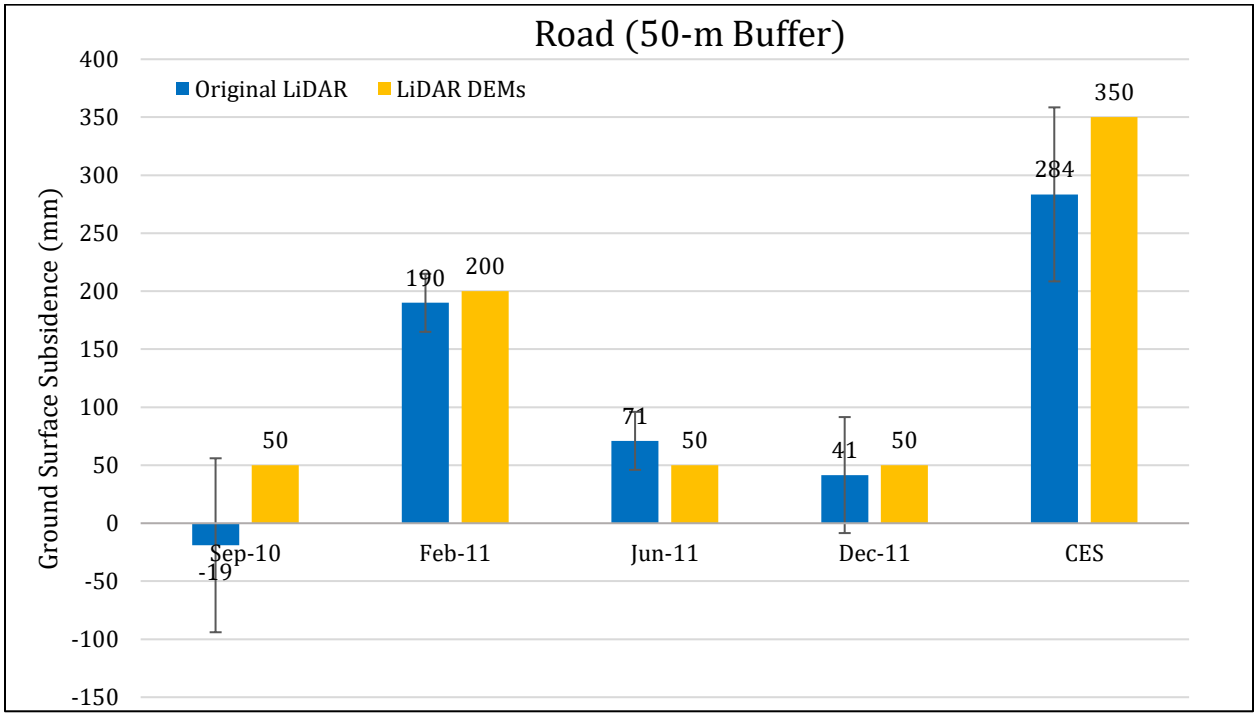

Figure 8: Comparison between ground surface subsidence determined from original LiDAR survey points and ground surface subsidence (50th %ile) estimated using LiDAR DEMs for Road for the 50-m buffer.

Note 2: The ground surface subsidence values determined from original LiDAR survey points are similar to the ground surface subsidence values estimated using LiDAR DEMs for all earthquake events.

Table 8a: Ejecta-induced settlement for the top 20-m of the soil profile for Patch A for the 50th %ile PGA and P_L=50% using BI-2014, ZRB-2002, C_{FC} = 0.13, and I_C cutoff of 2.6.

Earthquake Event(s)	M_W	PGA (g)	Depth to Groundwater (m)	S_T (mm)	S_{V1D} (mm)	$S_{E,L}$ (mm)
Sep-10	7.1	0.18	2.8	14±75	3±20	11±78
Feb-11	6.2	0.44	2.8	179±25	85±50	94±56
Jun-11	6.2	0.21	2.8	30±25	5±25	25±35
Dec-11	6.1	0.36	2.5	66±50	58±50	8±71

Notes: S_T = Total settlement (Table 6); S_{V1D} = Average vertical settlement due to volumetric compression using Boulanger and Idriss (2014) (BI-2014), Zhang et al. (2002) (ZRB-2002) procedures and de Greef and Lengkeek (2018) thin-layer correction; $S_{E,L}$ = Ejecta-induced settlement as the difference between the LiDAR-based S_T and S_{V1D}.

Table 8b: Ejecta-induced settlement for the top 20-m of the soil profile for Patch B within the 50-m buffer for the 50th %ile PGA and P_L=50% using BI-2014, ZRB-2002, C_{FC} = 0.13, and I_C cutoff of 2.6.

Earthquake Event(s)	M_W	PGA (g)	Depth to Groundwater (m)	S_T (mm)	S_{V1D} (mm)	$S_{E,L}$ (mm)
Sep-10	7.1	0.18	2.8	1±100	7±20	-6±102
Feb-11	6.2	0.44	2.8	193±50	121±50	72±71
Jun-11	6.2	0.21	2.8	15±50	8±25	7±56
Dec-11	6.1	0.36	2.5	26±50	81±50	-55±71

Notes: S_T = Total settlement (Table 6); S_{V1D} = Average vertical settlement due to volumetric compression using Boulanger and Idriss (2014) (BI-2014), Zhang et al. (2002) (ZRB-2002) procedures and de Greef and Lengkeek (2018) thin-layer correction; $S_{E,L}$ = Ejecta-induced settlement as the difference between the LiDAR-based S_T and S_{V1D}.

Table 8c: Ejecta-induced settlement for the top 20-m of the soil profile for Patch C for the 50th %ile PGA and P_L=50% using BI-2014, ZRB-2002, C_{FC} = 0.13, and I_C cutoff of 2.6.

Earthquake Event(s)	M_W	PGA (g)	Depth to Groundwater (m)	S_T (mm)	S_{V1D} (mm)	$S_{E,L}$ (mm)
Sep-10	7.1	0.18	2.8	-60±NA	9±20	-69±NA
Feb-11	6.2	0.44	2.8	127±NA	83±50	44±NA
Jun-11	6.2	0.21	2.8	-11±NA	10±25	-21±NA
Dec-11	6.1	0.36	2.5	24±NA	64±50	-40±NA

Notes: S_T = Total settlement (Table 6); S_{V1D} = Average vertical settlement due to volumetric compression using Boulanger and Idriss (2014) (BI-2014), Zhang et al. (2002) (ZRB-2002) procedures and de Greef and Lengkeek (2018) thin-layer correction; $S_{E,L}$ = Ejecta-induced settlement as the difference between the LiDAR-based S_T and S_{V1D}.

Table 8d: Ejecta-induced settlement for the top 20-m of the soil profile for Road within the 10-m buffer for the 50th %ile PGA and P_L=50% using BI-2014, ZRB-2002, C_{FC} = 0.13, and I_C cutoff of 2.6.

Earthquake Event(s)	M_W	PGA (g)	Depth to Groundwater (m)	S_T (mm)	S_{V1D} (mm)	$S_{E,L}$ (mm)
Sep-10	7.1	0.18	2.8	NA±75	5±20	NA
Feb-11	6.2	0.44	2.8	159±25	103±50	56±56
Jun-11	6.2	0.21	2.8	43±25	7±25	36±35
Dec-11	6.1	0.36	2.5	61±50	70±50	-9±71

Notes: S_T = Total settlement (Table 6); S_{V1D} = Average vertical settlement due to volumetric compression using Boulanger and Idriss (2014) (BI-2014), Zhang et al. (2002) (ZRB-2002) procedures and de Greef and Lengkeek (2018) thin-layer correction; $S_{E,L}$ = Ejecta-induced settlement as the difference between the LiDAR-based S_T and S_{V1D}.

Table 8e: Ejecta-induced settlement for the top 20-m of the soil profile for Road within the 20-m buffer for the 50th %ile PGA and P_L=50% using BI-2014, ZRB-2002, C_{FC} = 0.13, and I_C cutoff of 2.6.

Earthquake Event(s)	M_W	PGA (g)	Depth to Groundwater (m)	S_T (mm)	S_{V1D} (mm)	$S_{E,L}$ (mm)
Sep-10	7.1	0.18	2.8	6±75	5±20	1±78
Feb-11	6.2	0.44	2.8	178±25	103±50	75±56
Jun-11	6.2	0.21	2.8	44±25	7±25	37±35
Dec-11	6.1	0.36	2.5	51±50	70±50	-19±71

Notes: S_T = Total settlement (Table 6); S_{V1D} = Average vertical settlement due to volumetric compression using Boulanger and Idriss (2014) (BI-2014), Zhang et al. (2002) (ZRB-2002) procedures and de Greef and Lengkeek (2018) thin-layer correction; $S_{E,L}$ = Ejecta-induced settlement as the difference between the LiDAR-based S_T and S_{V1D}.

Table 8f: Ejecta-induced settlement for the top 20-m of the soil profile for Road within the 50-m buffer for the 50th %ile PGA and P_L=50% using BI-2014, ZRB-2002, C_{FC} = 0.13, and I_c cutoff of 2.6.

Earthquake Event(s)	M_W	PGA (g)	Depth to Groundwater (m)	S_T (mm)	S_{V1D} (mm)	$S_{E.L}$ (mm)
Sep-10	7.1	0.18	2.8	-19±75	5±20	-24±78
Feb-11	6.2	0.44	2.8	190±25	103±50	87±56
Jun-11	6.2	0.21	2.8	71±25	7±25	64±35
Dec-11	6.1	0.36	2.5	41±50	70±50	-29±71

Notes: S_T = Total settlement (Table 6); S_{V1D} = Average vertical settlement due to volumetric compression using Boulanger and Idriss (2014) (BI-2014), Zhang et al. (2002) (ZRB-2002) procedures and de Greef and Lengkeek (2018) thin-layer correction; $S_{E,L}$ = Ejecta-induced settlement as the difference between the LiDAR-based S_T and S_{V1D}.

Note 3: The uncertainty for volumetric settlement was derived based on the sensitivity of volumetric settlement to PGA, C_{FC}, and P_L for each earthquake event for VsVp 57203 *Shirley Intermediate School* and CC LIQ 1 – CPT 5586 – *Vivian St* sites. Taking the 50th percentile as the baseline case, the minimum and maximum values corresponding to the difference between the 25th percentile and the 50th percentile and the 75th percentile and the 50th percentile were determined. The arithmetic mean of the range of the minimum and maximum difference was evaluated for each patch at the two sites. The maximum arithmetic mean for each earthquake event was rounded to the nearest five and used as the uncertainty value. Accordingly, the 1-D volumetric settlement uncertainties of ±20, ±50, ±25, and ±50 mm for the Sep-10, Feb-11, Jun-11, and Dec-11 earthquake events, respectively, were used for all sites in this study.

Table 9a: Coverage area and height of ejecta estimates for Patch A using photographs.

Earthquake Event	$A_{E,cone}$ (m^2)	$H_{E,cone}$ (mm)	$A_{E,thin}$ (m^2)	$H_{E,thin}$ (mm)	A_T (m^2)
Sep-10	0	0	0	0	20
Feb-11	0	0	6.9	40-60	20
Jun-11	0.93	50-100	0	0	20
Dec-11	0	0	0	0	20

Notes: $A_{E,thick/thin}$ = Coverage area of thick/thin ejecta layers; $H_{E,thick/thin}$ = Lower-upper estimate of height of thick/thin ejecta layers; A_T = Total assessment area of a buffer being considered; Thin and thick layers correspond to light gray and dark gray colors of ejecta observed in aerial photographs.

Table 9b: Coverage area and height of ejecta estimates for Patch B using photographs.

Earthquake Event	$A_{E,thick}$ (m^2)	$H_{E,thick}$ (m)	$A_{E,thin}$ (m^2)	$H_{E,thin}$ (m)	A_T (m^2)
Sep-10	0	0	0	0	13
Feb-11	0	0	7.6	10-30	13
Jun-11	0	0	0	0	13
Dec-11	0	0	0	0	13

Notes: $A_{E,thick/thin}$ =Coverage area of thick/thin ejecta layers; $H_{E,thick/thin}$ = Lower-upper estimate of height of thick/thin ejecta layers; A_T= Total assessment area of a buffer being considered; Thin and thick layers correspond to light gray and dark gray colors of ejecta observed in aerial photographs.

Table 9c: Coverage area and height of ejecta estimates for Patch C using photographs.

Earthquake Event	Sep-10	Feb-11	Jun-11	Dec-11*
$d_{E,sinkhole1}$ (mm)	0	750-1500	NA	0
$A_{E,sinkhole1}$ (m^2)	0	4.6	NA	0
$d_{E,sinkhole2}$ (mm)	0	300-500	NA	0
$A_{E,sinkhole2}$ (m^2)	0	1.9	NA	0
$H_{E,cone}$ (mm)	0	100-150	NA	100-200
$A_{E,cone}$ (m^2)	0	2.8	NA	10.55
$H_{E,thick1}$ (mm)	0	250-350	NA	70-150
$A_{E,thick1}$ (m^2)	0	17	NA	46.8
$H_{E,thin1}$ (mm)	0	70-140	NA	0
$A_{E,thin1}$ (m^2)	0	15	NA	0
$H_{E,thin2}$ (mm)	0	50-100	NA	0
$A_{E,thin2}$ (m^2)	0	8.8	NA	0
A_T (m^2)	47	47	47	47

Notes: $A_{E,sinkhole}$ = Coverage area of sinkhole; $d_{E,sinkhole}$ = Lower-upper estimate of depth of sinkhole; $A_{E,cone}$ = Coverage area of conically shaped ejecta layers; $H_{E,cone}$ = Lower-upper estimate of height of conically shaped ejecta layers; $A_{E,thick/thin}$ =Coverage area of thick/thin ejecta layers; $H_{E,thick/thin}$ = Lower-upper estimate of height of thick/thin ejecta layers; A_T= Total assessment area of a buffer being considered; Thin and thick layers correspond to light gray and dark gray colors of ejecta observed in aerial photographs; NA = Not available due to the poor quality of the aerial photographs so the estimate was made based on the claimant's reporting of two times lesser volume of ejecta for the Jun-11 EQ than for the Feb-11 EQ; * indicates uncertainty in the assumption that the site was remediated (e.g., filling of sinkholes and leveling) according to the inspection report from 28-10-2011.

Table 9d: Coverage area and height of ejecta estimates for Road within the 20-m buffer using photographs.

EQ Event	$H_{E,thin}$ (mm)	$A_{E,thin}$ (m^2)	$H_{E,thick}$ (mm)	$A_{E,thick}$ (m^2)	$H_{E,prism/pyr}$ (mm)	$V_{E,prism+pyr}$ (m^3)	$H_{E,cc}$ (mm)	$V_{E,cc}^*$ (m^3)	A_T (m^2)
Sep-10	0	0	0	0	0	0	0	0	266
Feb-11	10-20	8.4	0	0	12-250	2.7-3.7	0	0	256
Jun-11	0	0	20-40	10	23-210	0.786-1.04	358-797	4.17	215
Dec-11	0	0	20-40	6.8	16-200	0.761-1.17	0	0	266

Notes: $A_{E,thick/thin}$ = Coverage area of thick/thin ejecta layers; $H_{E,thick/thin}$ = Lower-upper estimate of height of thick/thin ejecta layers; $H_{E,prism/pyr}$ = Lower-upper estimate of ejecta height near the curb based on 2-4% cross slope of normal crown; $V_{E,prism}$ = Lower-upper estimate of total volume of prismatic-shape ejecta; $V_{E,pyr}$ = Lower-upper estimate of total volume of pyramidal-shape ejecta; $V_{E,cc}$ = Volume of conically shaped ejecta pile components; $H_{E,cc}$ = Lower-upper estimate of height of conically shaped ejecta pile components (based on the repose angle of 30°); A_T= Total assessment area of a buffer being considered; * indicates uncertainty in the place of origin of the ejected material (backyard vs. road).

Table 9e: Coverage area and height of ejecta estimates for Road within the 50-m buffer (without the 20-m buffer) using photographs.

EQ Event	$H_{E,thin}$ (mm)	$A_{E,thin}$ (m^2)	$H_{E,thick}$ (mm)	$A_{E,thick}$ (m^2)	$H_{E,prism/pyr}$ (mm)	$V_{E,prism/pyr}$ (m^3)	$H_{E,cc/pile}$ (mm)	$V_{E,cc/pile}^*$ (m^3)	A_T (m^2)
Sep-10	0	0	0	0	0	0	0	0	1617
Feb-11	10-20	110	20-40	9.9	10-250	1.2-1.5	0	0	1593
Jun-11	10-20	38	20-40	1.5	7-70	0.221-0.441	260-629	1.29	1492
Dec-11	0	0	20-40	72	12-200	0.955-1.20	450-476	1.57-1.68	1595

Notes: $A_{E,thick/thin}$ = Coverage area of thick/thin ejecta layers; $H_{E,thick/thin}$ = Lower-upper estimate of height of thick/thin ejecta layers; $H_{E,prism/pyr}$ = Lower-upper estimate of ejecta height near the curb based on 2-4% cross slope of normal crown; $V_{E,prism}$ = Lower-upper estimate of total volume of prismatic-shape ejecta; $V_{E,pyr}$ = Lower-upper estimate of total volume of pyramidal-shape ejecta; $V_{E,cc}$ = Volume of conically shaped ejecta pile components; $H_{E,cc}$ = Lower-upper estimate of height of conically shaped ejecta pile components (based on the repose angle of 30°); $V_{E,pile}$ = Volume of piles for Dec-11 EQ; $H_{E,pile}$ = Lower-upper estimate of height of pile for Dec-11 EQ; A_T= Total assessment area of a buffer being considered; * indicates uncertainty in the place of origin of the ejected material (backyard vs. road).

Note 4: The values in Table 9 correspond to the coverage area of ejecta outlined in aerial photographs (Figures 86-89) and the lower and upper estimates of ejecta height based on geometry, ground photographs (Figures 91, 93-96), and EQC LDAT property inspection notes (Figures 90 and 92) and reports (the claimant reported 40 m^3 and 20 m^3 of ejecta being removed from the property with Patches B and C as a result of the Feb-11 EQ and the Jun-11 EQ, respectively; ejected material was up to 500 mm high; the depth of the biggest sinkhole was about 1.5 m; an approximate settlement at rear was 300 mm, while the front lawn settled about 100 mm). The ejecta-induced settlement using photographs and engineering judgment, $S_{E,P}$, is estimated as

$$S_{E,P} = \frac{\sum_{i=1}^{a} A_{E,thick,i} * H_{E,thick,i} + \sum_{j=1}^{b} A_{E,thin,j} * H_{E,thin,j} + \frac{1}{3}\sum_{k=1}^{c} A_{E,pile,k} * R_{E,pile,k} * tan30°}{A_T} + \frac{\sum_{l=1}^{d}\left(\frac{1}{3}(A_{E,conical\ end\ 1,l} + A_{E,conical\ end\ 2,l}) * H_{E,pile,l} + \frac{1}{2} A_{E,prismatic\ middle,l} * H_{E,pile,l}\right)}{A_T} + \frac{\frac{1}{3}\sum_{m=1}^{e} A_{E,cone,m} * H_{E,cone,m} + \frac{1}{2}\sum_{n=1}^{f} W_{E,prism,n} * H_{E,prism,n} * L_{E,prism,n}}{A_T} + \frac{\frac{1}{3}\sum_{p=1}^{g} W_{E,pyramid,p} * H_{E,pyramid} * L_{E,pyramid} + \frac{1}{3}\sum_{r=1}^{h} A_{E,sinkhole,r} * H_{E,sinkhole,r}}{A_T} = \frac{\sum_{i=1}^{a} V_{E,thick,i} + \sum_{j=1}^{b} V_{E,thin,j} + \sum_{k=1}^{c} V_{E,conical\ component,k} + \sum_{l=1}^{d} V_{E,pile,l}}{A_T} + \frac{\sum_{m=1}^{e} V_{E,cone,m} + \sum_{n=1}^{f} V_{E,prism,n} + \sum_{p=1}^{g} V_{E,pyramid,p} + \sum_{r=1}^{h} V_{E,sinkhole,r}}{A_T}$$

where

- $A_{E,thick,i}$ and $H_{E,thick,i}$ are the area and the height of a thick ejecta layer, respectively;
- $A_{E,thin,j}$ and $H_{E,thin,j}$ are the area and the height of a thin ejecta layer, respectively;
- $A_{E,pile,k}$ and $R_{E,pile,k}$ are the area and the radius of an ejecta pile component, respectively, shaped as a cone with the repose angle of 30°;
- $A_{E,conical\ end\ 1/2,l}$ and $A_{E,prismatic\ middle,l}$ are the areas of half-cone ends of an ejecta pile and the area of a middle of an ejecta pile shaped as a triangular prism, respectively, while $H_{E,pile,l}$ is the height of an ejecta pile;
- $A_{E,cone,m}$ and $H_{E,cone,m}$ are the area and the height of a conically shaped ejecta, respectively;
- $W_{E,prism,n}$ and $L_{E,prism,n}$ are the width and the length of the coverage area of a prismatically shaped ejecta layer, respectively, and $H_{E,prism,n}$ is the height of a prism-like ejecta layer;
- $W_{E,pyr,p}$ and $L_{E,pyr,p}$ are the width and the length of the coverage area of a pyramid-like ejecta layer, respectively, and $H_{E,pyr,p}$ is the height of a pyramid-like ejecta layer;
- A_T is the total assessment area for a buffer being considered (Figure 1).

Table 10a: Ejecta-induced settlement estimates for Patches A, B, and C based on photographs.

Earthquake Event	Patch A		Patch B (50-m buffer)		Patch C	
	$S_{E,P,lower}$ (mm)	$S_{E,P,upper}$ (mm)	$S_{E,P,lower}$ (mm)	$S_{E,P,upper}$ (mm)	$S_{E,P,lower}$ (mm)	$S_{E,P,upper}$ (mm)
Sep-10	0	0	0	0	0	0
Feb-11	14	21	6	18	153	249
Jun-11	1	2	0	0	77*	125*
Dec-11	0	0	0	0	78**	165**

Note: $S_{E,P,lower}$ and $S_{E,P,upper}$ correspond to lower and upper estimates of $S_{E,P}$, respectively; * indicates the estimates based on the claimant's story; ** indicates uncertainty due to the possibility of site remediation prior to the event.

Table 10b: Ejecta-induced settlement estimates for Road based on photographs.

Earthquake Event	Road (20-m buffer)		Road (50-m buffer)	
	$S_{E,P,lower}$ (mm)	$S_{E,P,upper}$ (mm)	$S_{E,P,lower}$ (mm)	$S_{E,P,upper}$ (mm)
Sep-10	0	0	0	0
Feb-11	11	15	3	5
Jun-11	5-24	7-27	1-6	2-7
Dec-11	3	5	3	4

Note: $S_{E,P,lower}$ and $S_{E,P,upper}$ correspond to lower and upper estimates of $S_{E,P}$, respectively.

Table 11a: Best final estimates of ejecta-induced settlement for Patches A, B, and C.

EQ Event	Patch A			Patch B			Patch C		
	$S_{E,L}$ (mm)	$S_{E,P}$ (mm)	$S_{E,final}$ (mm)	$S_{E,L}$ (mm)	$S_{E,P}$ (mm)	$S_{E,final}$ (mm)	$S_{E,L}$ (mm)	$S_{E,P}$ (mm)	$S_{E,final}$ (mm)
Sep-10	11±78	0	0	-6±102	0	0	-69±NA	0	0
Feb-11	94±56	17.5±3.5	25±5	72±71	12±6	20±10	44±NA	201±48	200±50
Jun-11	25±35	1.5±0.5	5±5	7±56	0	0	-21±NA	101±24	100±25
Dec-11	8±71	0	0	-55±71	0	0	-40±NA	122±44*	120±45*

Notes: $S_{E,L}$ = Ejecta-induced settlement based on LiDAR data reported in Table 8; $S_{E,P}$ = Median ejecta-induced settlement for the range of values reported in Table 10; $S_{E,final}$ = Best final estimate of ejecta-induced settlement rounded to the nearest 5; Final plus/minus values are also rounded to the nearest 5; * indicates uncertainty due to the possible site remediation.

Table 11b: Best final estimates of ejecta-induced settlement for Road.

EQ Event	Road (20-m buffer)			Road (50-m buffer)		
	$S_{E,L}$ (mm)	$S_{E,P}$ (mm)	$S_{E,final}$ (mm)	$S_{E,L}$ (mm)	$S_{E,P}$ (mm)	$S_{E,final}$ (mm)
Sep-10	1±78	0	0	-24±78	0	0
Feb-11	75±56	13±2	20±5	87±56	4±1	10±5
Jun-11	37±35	*16±7	20±5	64±35	*4±2	10±5
Dec-11	-19±71	4±1	5±5	-29±71	*3.5±0.5	5±5

Notes: $S_{E,L}$ = Ejecta-induced settlement based on LiDAR data reported in Table 8; $S_{E,P}$ = Median ejecta-induced settlement for the range of values reported in Table 10; $S_{E,final}$ = Best final estimate of ejecta-induced settlement rounded to the nearest 5; Final plus/minus values are also rounded to the nearest 5; indicates uncertainty due to the unknown origin of ejecta.

Note 5:

- For Patch A, $S_{E,final}$ for the Sep-10 and Dec-11 EQs is based solely on $S_{E,P}$, while $S_{E,final}$ for the Feb-11 and Jun-11 EQs is a weighted average of $S_{E,L}$ and $S_{E,P}$ with the weight coefficients of 0.1 and 0.9, respectively.
- For Patch B, $S_{E,final}$ for the Sep-10, Jun-11, and Dec-11 EQs is based on $S_{E,P}$ only, whereas $S_{E,final}$ is based on the weighted average of $S_{E,L}$ and $S_{E,P}$ with the weights of 0.1 and 0.9, respectively.
- For Patch C, $S_{E,final}$ is based solely on $S_{E,P}$ for all earthquake events.

- For Road, $S_{E,final}$ is equal to $S_{E,P}$ for the Sep-10 and Dec-11 EQs, whereas $S_{E,final}$ for the Feb-11 and Jun-11 EQs is a weighted average of $S_{E,L}$ and $S_{E,P}$ with the weight coefficients of 0.1 and 0.9, respectively.
- The $S_{E,final}$ uncertainties are also a weighted average of uncertainties associated with $S_{E,L}$ and $S_{E,P}$ with the same weights used for the mean $S_{E,L}$ and $S_{E,P}$ estimates.
- The weights are based on the LiDAR error bands, density of LiDAR points, LPI prediction error (Maurer et al. 2014[3]), presence of ejecta at the site at the time of LiDAR surveys, discrepancy between $S_{E,L}$ and $S_{E,P}$, and completeness of visual evidence (i.e., ground and aerial photographs and EQC LDAT property inspection reports for the site). The Pinewood Ave site is in the apparent zone of higher ground surface subsidence for the Sep-10 EQ and the apparent zone of lower ground surface subsidence for the Feb-11 EQ (i.e., the underestimate of the ground surface elevation by the Sep-10 LiDAR survey). The site is in the zone of accurate LPI prediction of liquefaction severity for the Sep-10 EQ, but in the zone of slight to moderate LPI overprediction of liquefaction severity for the Feb-11 EQ. The LDAT property inspection reports are available for Patches A, B, and C. There are no ground photographs of the road.

Summary:

- **The best estimate of the ejecta-induced free-field ground settlement at the Pinewood Ave site for the SEP 2010, FEB 2011, JUN 2011, and DEC 2011 earthquake is 0 mm, 25±5 mm, 5±5 mm, and 0 mm, respectively. During the FEB 2011 earthquake, approximately 5% of the unobstructed area of the site settled 200±50 mm due to ejecta. Similarly, about 5% of the unobstructed area of the site underwent 100±25 mm and 120±45 mm of ejecta-induced ground settlement during the JUN 2011 and DEC 2011 earthquake, respectively.**
- **The best estimate of the ejecta-induced free-field ground settlement of the road at the Pinewood Ave site for the SEP 2010, FEB 2011, JUN 2011, and DEC 2011 earthquake is 0 mm, 10±5 mm, 10±5 mm, and 5±5 mm, respectively.**
- **Patch C represents an interesting case study because the removal of vegetation within it likely weakened the soil profile structure and resulted in the sinkhole formation and severe quantities of the ejected material.**

Note 6: CC LIQ 5 was later renamed as CPT 61991.

Note 7: The initial outline of Patch C was changed hence the old outline in many figures.

[3] Maurer, B. W., Green, R. A., Cubrinovski, M., & Bradley, B. A. (2014). Evaluation of the Liquefaction Potential Index for Assessing Liquefaction Hazard in Christchurch, New Zealand. *Journal of Geotechnical and Geoenvironmental Engineering*, 140(7), 04014032-1-11. doi:10.1061/(asce)gt.1943-5606.0001117

Figure 9: Location of the site.

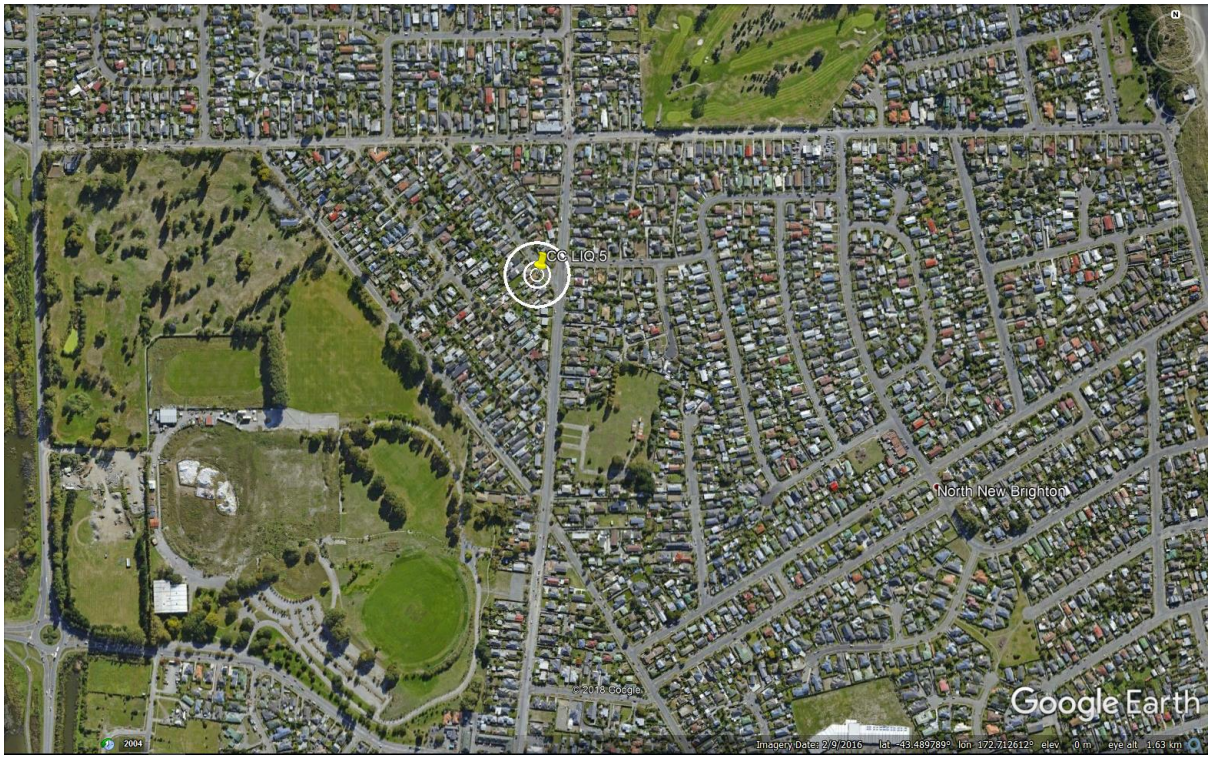

Figure 10: Position of the site relative to nearby buildings, vegetation, and free-face features.

Figure 11: Street view of the site showing flat land.

Figure 12: Satellite image of the site taken in Dec 2004.

Figure 13: Satellite image of the site taken in Mar 2009.

Figure 14: Satellite image of the site taken in Apr 2012.

Figure 15: Satellite image of the site taken in Sep 2013.

Figure 16: Satellite image of the site taken in Feb 2014.

Figure 17: Satellite image of the site taken in Aug 2014.

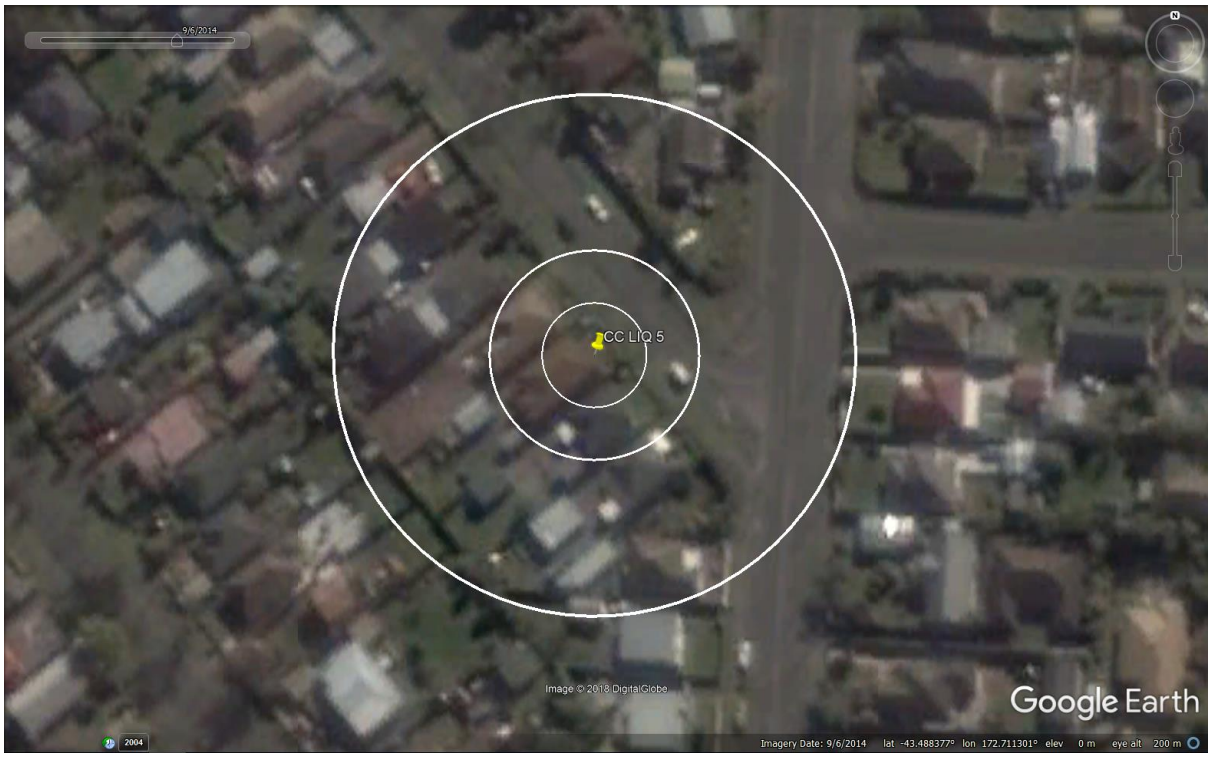

Figure 18: Satellite image of the site taken in Sep 2014.

Figure 19: Satellite image of the site taken in Jan 2015.

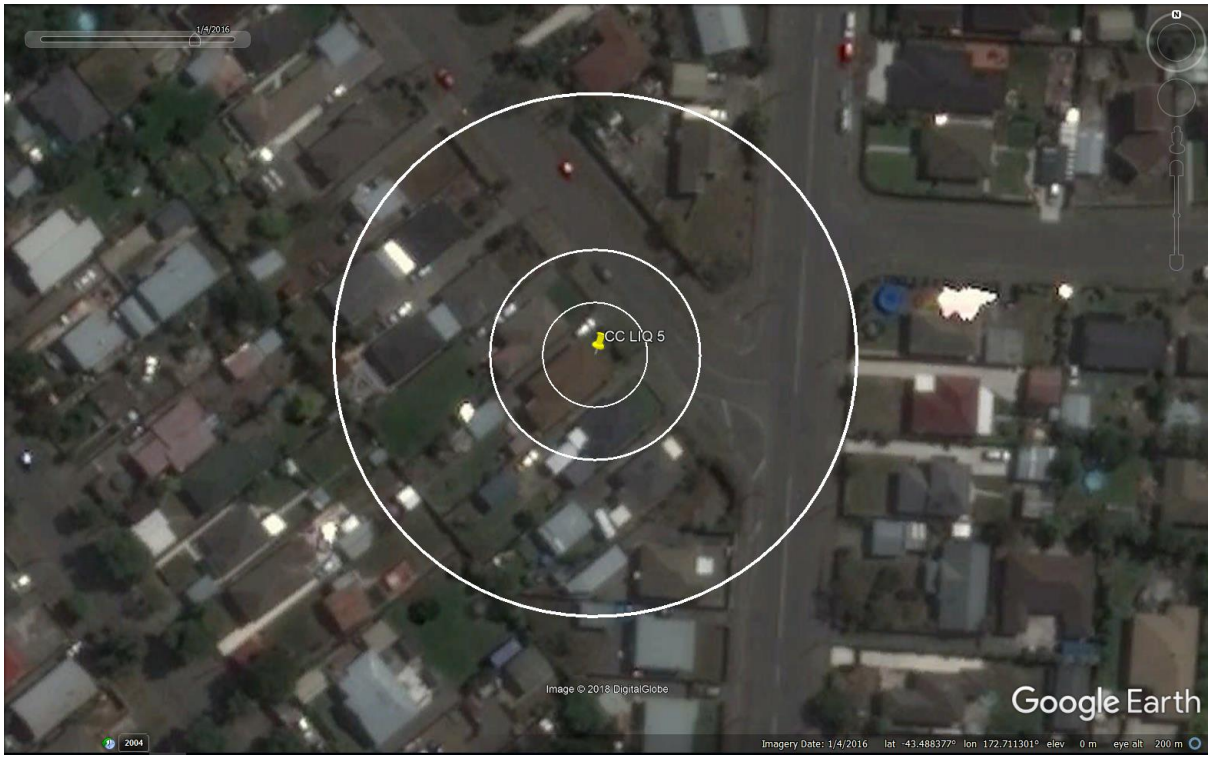

Figure 20: Satellite image of the site taken in Jan 2016.

Figure 21: Aerial photograph of the site taken on Sep 4, 2010.

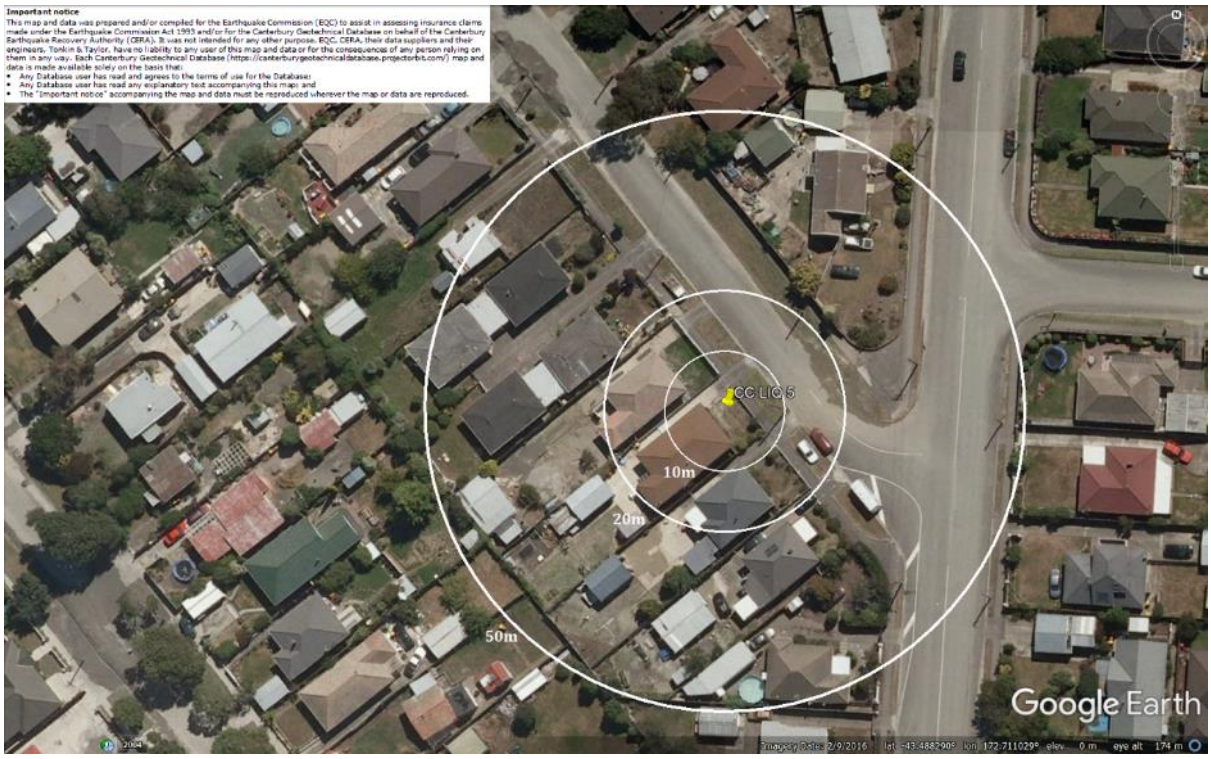

Figure 22: Aerial photograph of the site taken on Feb 24, 2011.

Figure 23: Aerial photograph of the site taken on June 14-15, 2011.

Figure 24: Aerial photograph of the site taken on Dec 24, 2011.

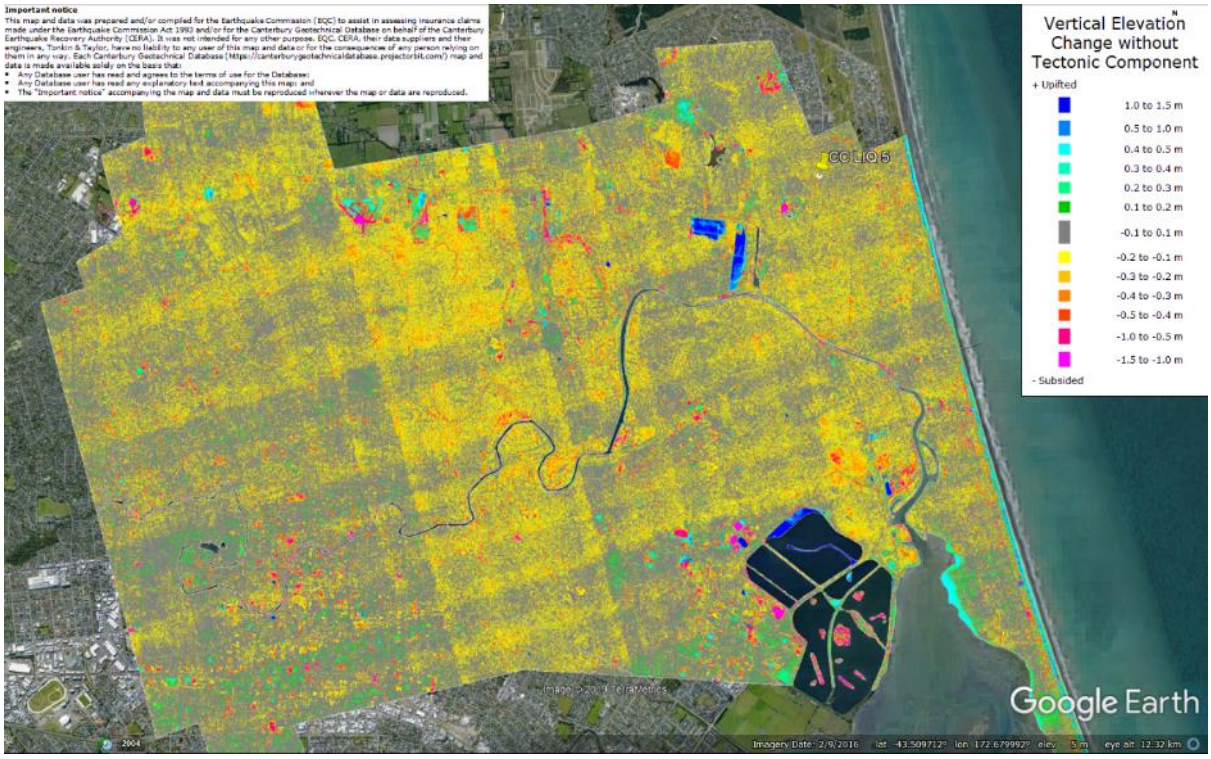

Figure 25: Vertical Ground Movements (Surface – Tectonic) for Sep 2010 Earthquake – the site is in the apparent zone of overestimated ground surface subsidence (i.e., Sep 2010 flight band error).

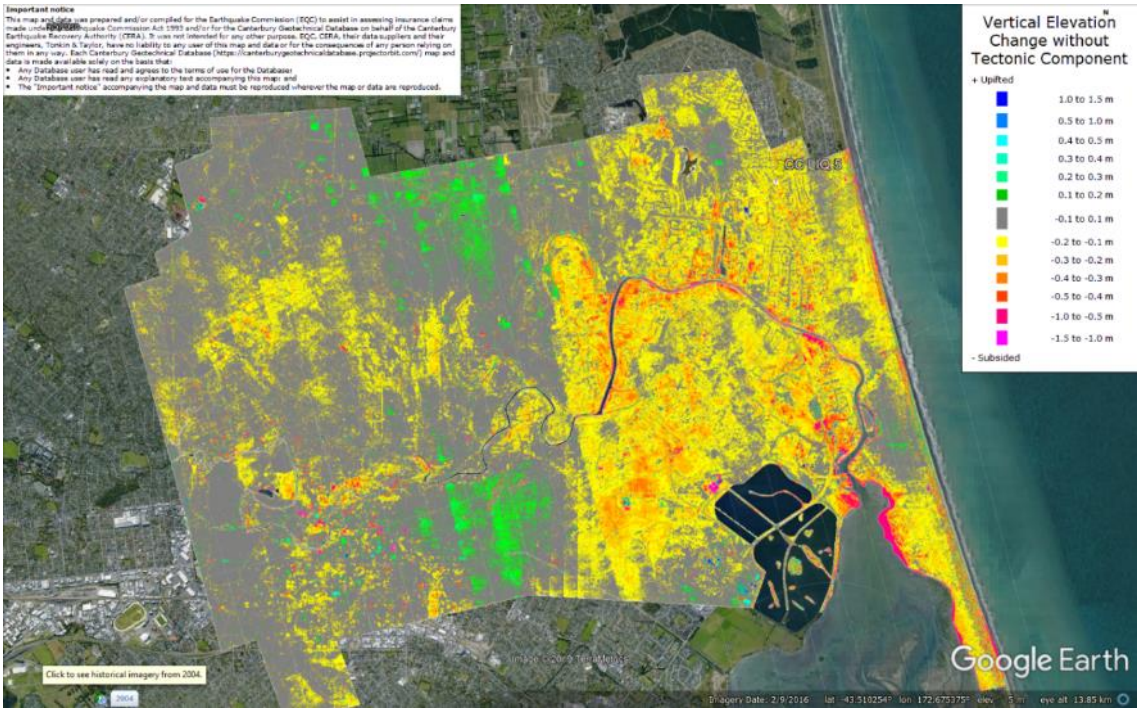

Figure 26: Vertical Ground Movements (Surface – Tectonic) for Feb 2011 Earthquake – the site is in the apparent zone of underestimated ground surface subsidence (i.e., Sep 2010 flight band error).

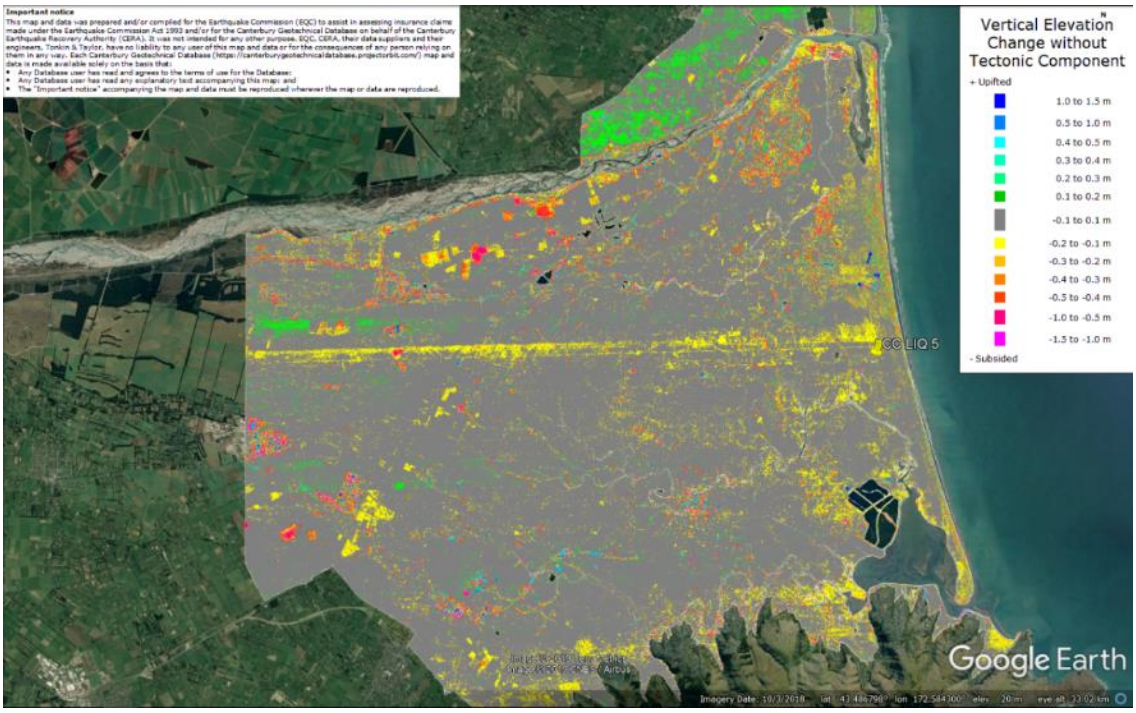

Figure 27: Vertical Ground Movements (Surface – Tectonic) for June 2011 Earthquake – the site is not in the apparent zone of overestimated or underestimated ground surface subsidence.

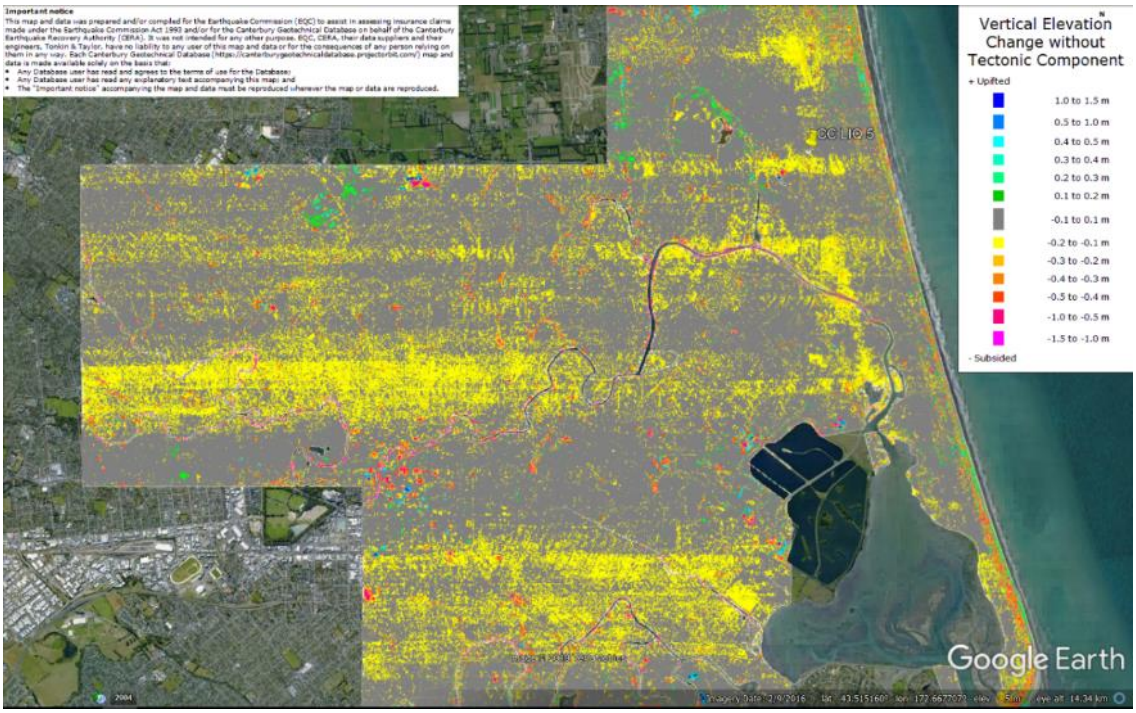

Figure 28: Vertical Ground Movements (Surface – Tectonic) for Dec 2011 Earthquake – the site is not in the apparent zone of overestimated or underestimated ground surface subsidence.

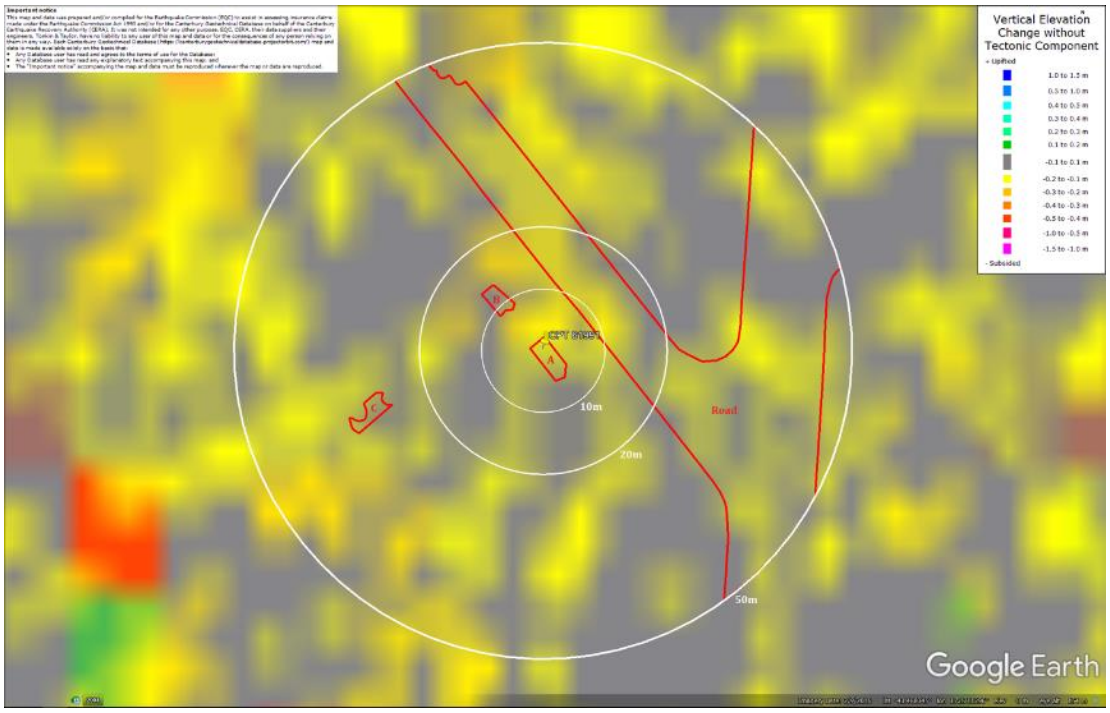

Figure 29: Ground surface subsidence without tectonic component for Sep 2010 Earthquake according to the LiDAR DEM.

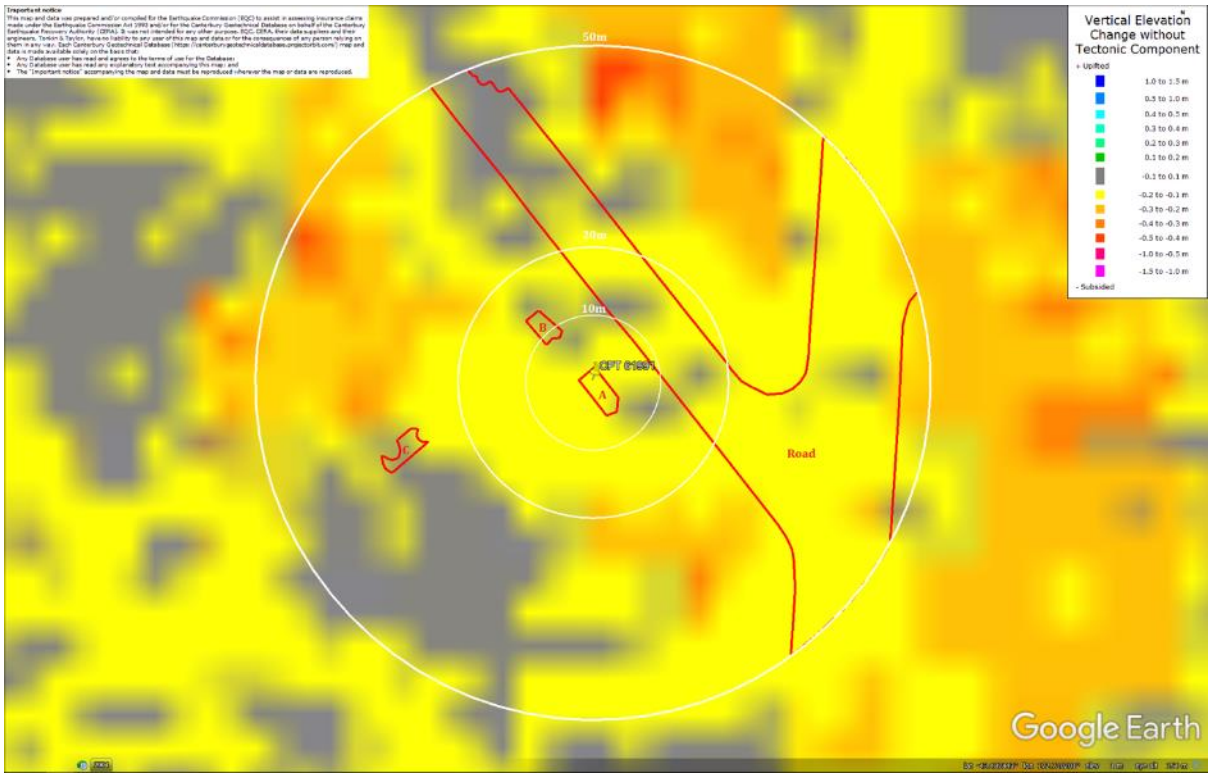

Figure 30: Ground surface subsidence without tectonic component for Feb 2011 Earthquake according to the LiDAR DEM.

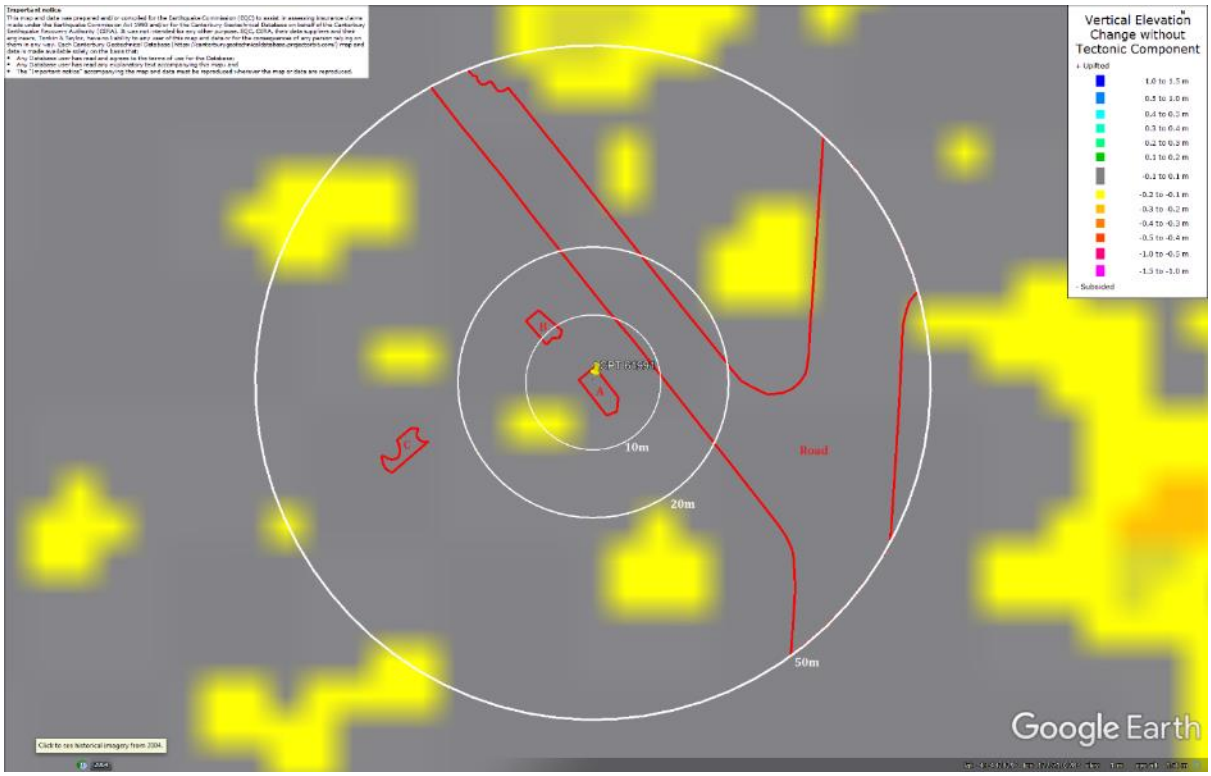

Figure 31: Ground surface subsidence without tectonic component for Jun 2011 Earthquake according to the LiDAR DEM.

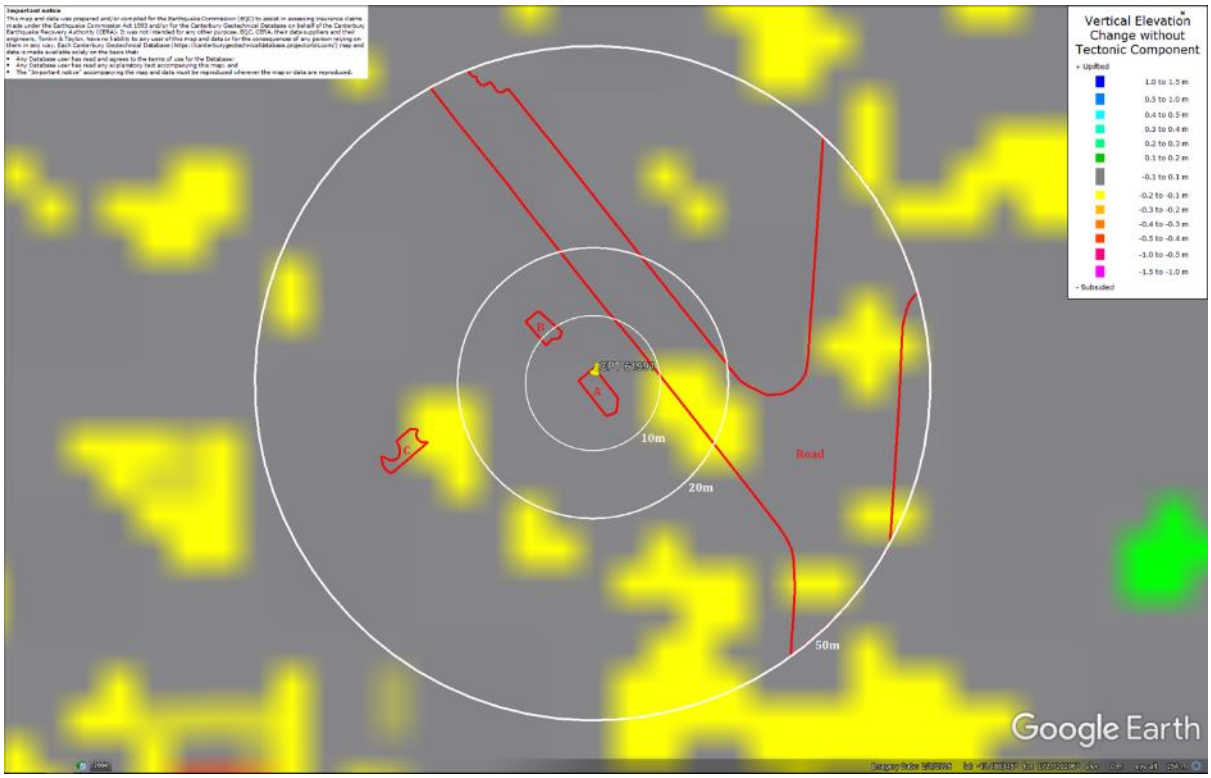

Figure 32: Ground surface subsidence without tectonic component for Dec 2011 Earthquake according to the LiDAR DEM.

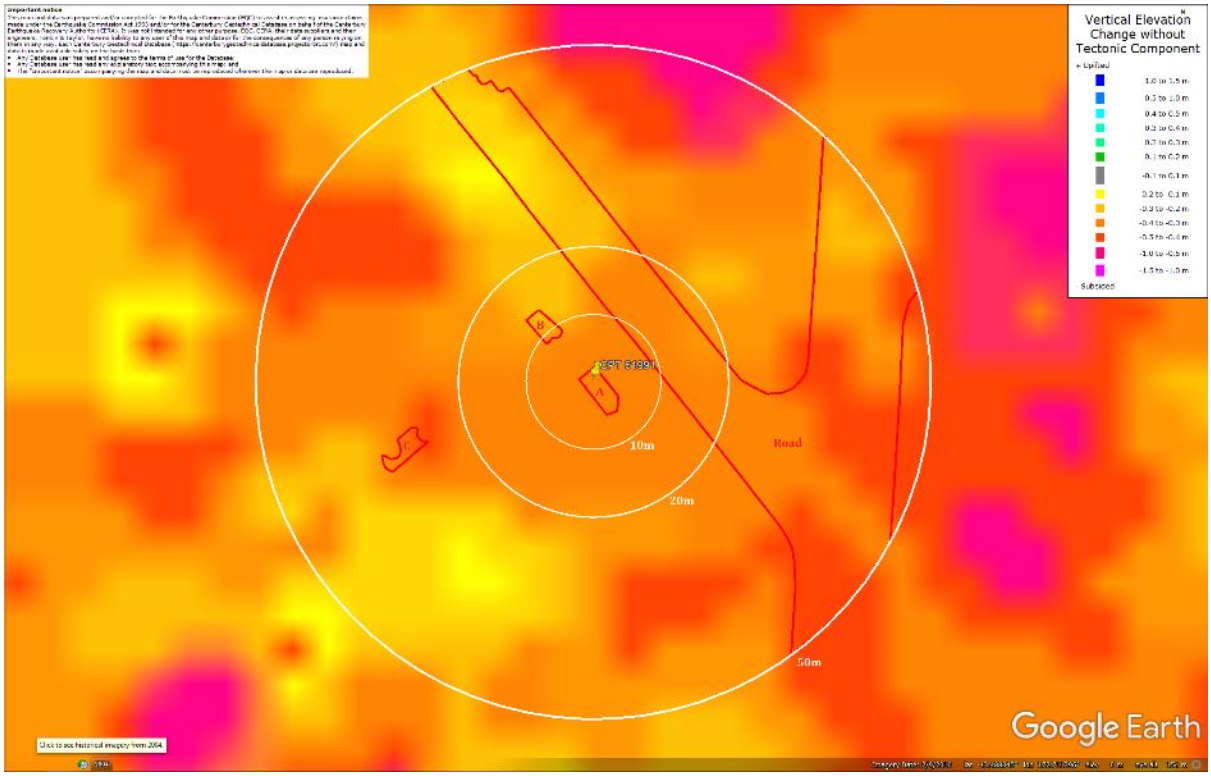

Figure 33: Ground surface subsidence without tectonic component for Canterbury Earthquake Sequence according to the LiDAR DEM.

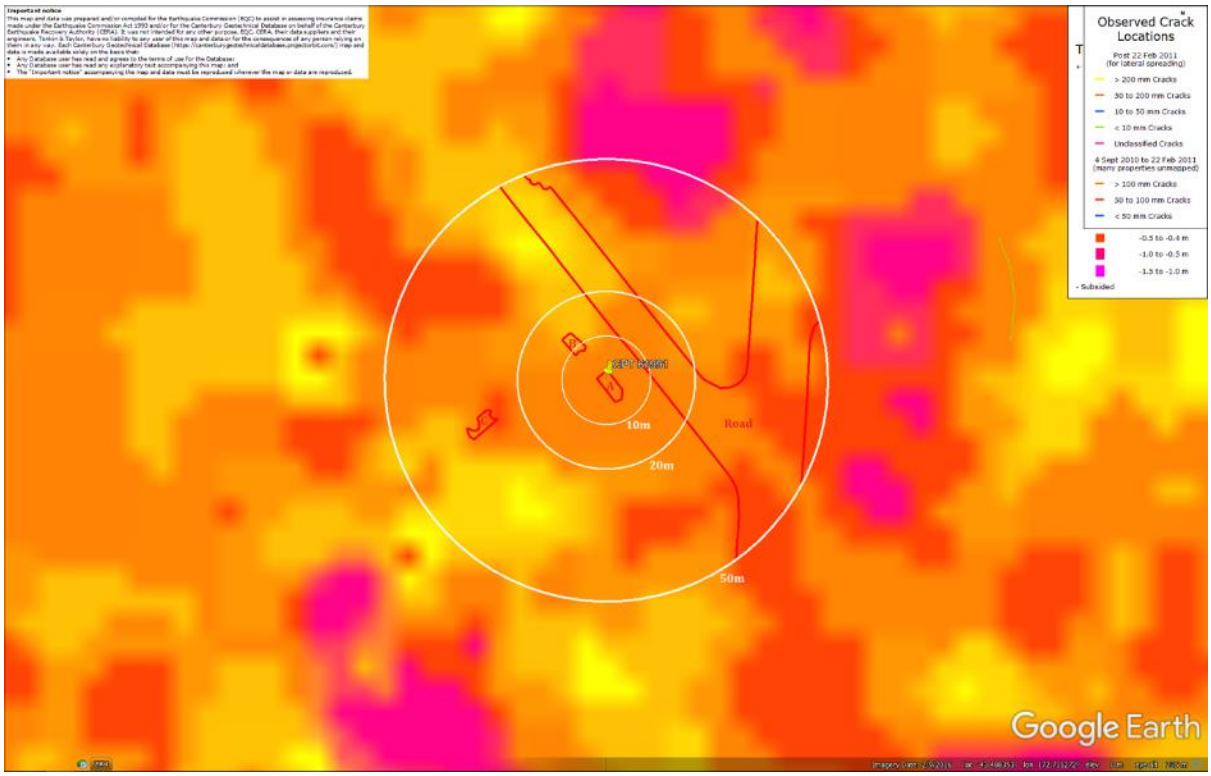

Figure 34: Absence of ground cracks indicates no lateral spreading for Canterbury Earthquake Sequence.

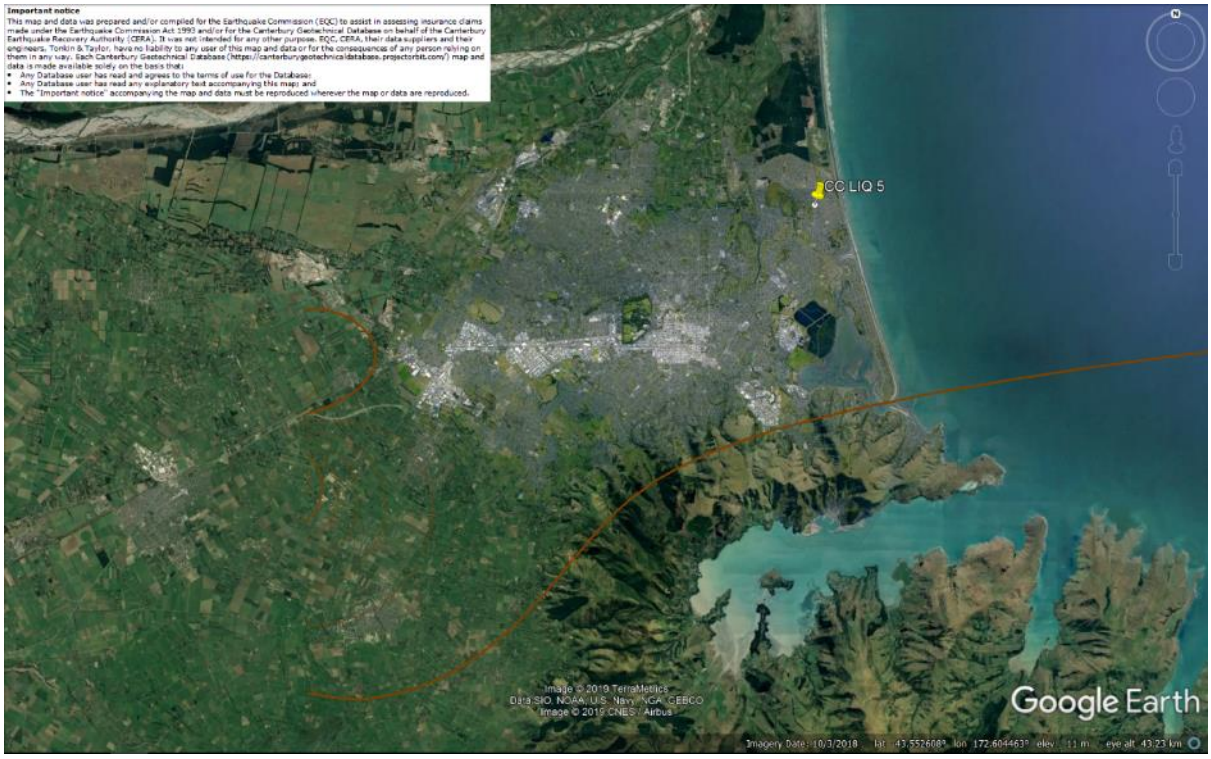

Figure 35: Vertical tectonic movements for Sep 2010 Earthquake.

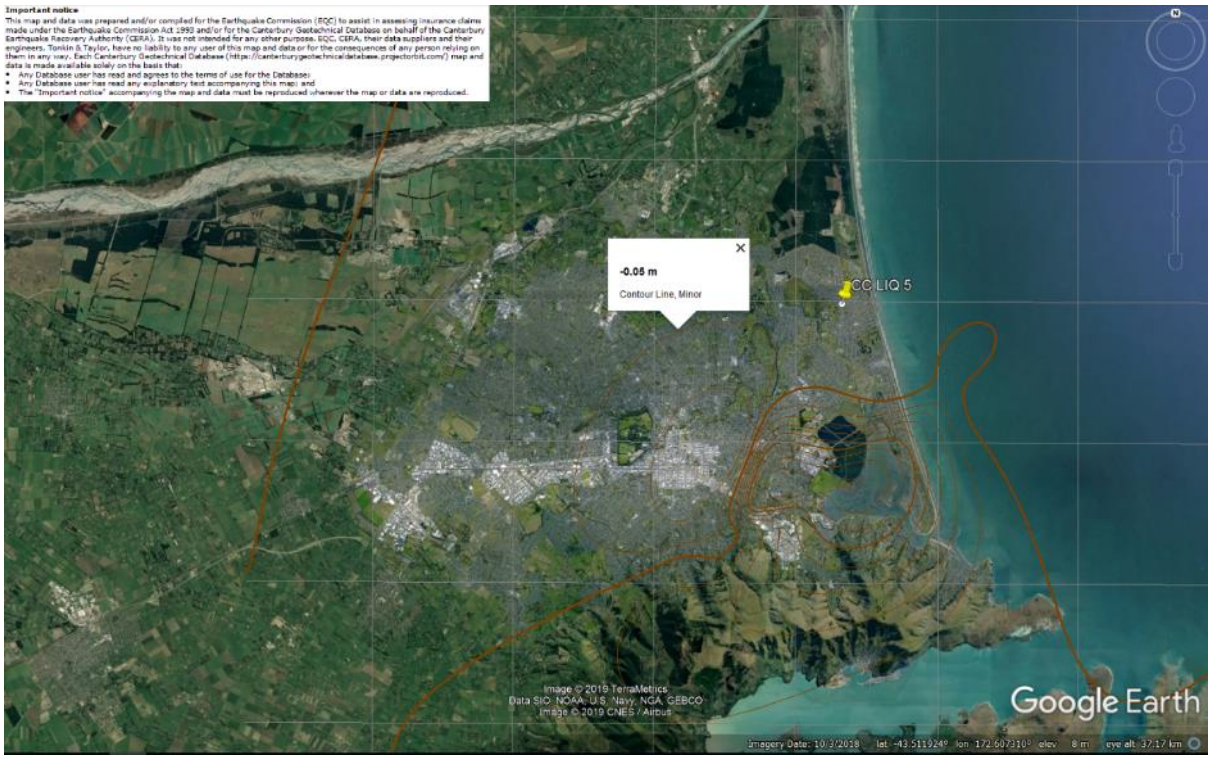

Figure 36: Vertical tectonic movements for Feb 2011 Earthquake.

Figure 37: Vertical tectonic movements for June 2011 Earthquake.

Figure 38: Vertical tectonic movements for Dec 2011 Earthquake.

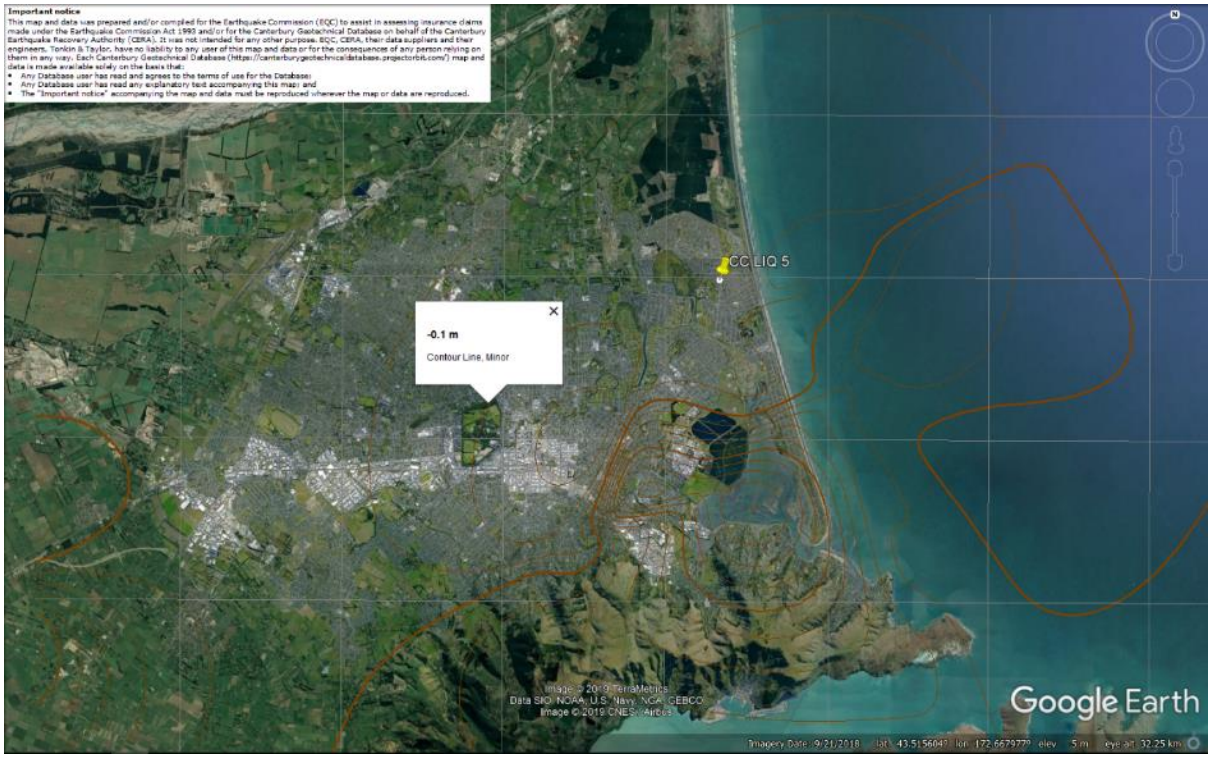

Figure 39: Vertical tectonic movements for Canterbury Earthquake Sequence.

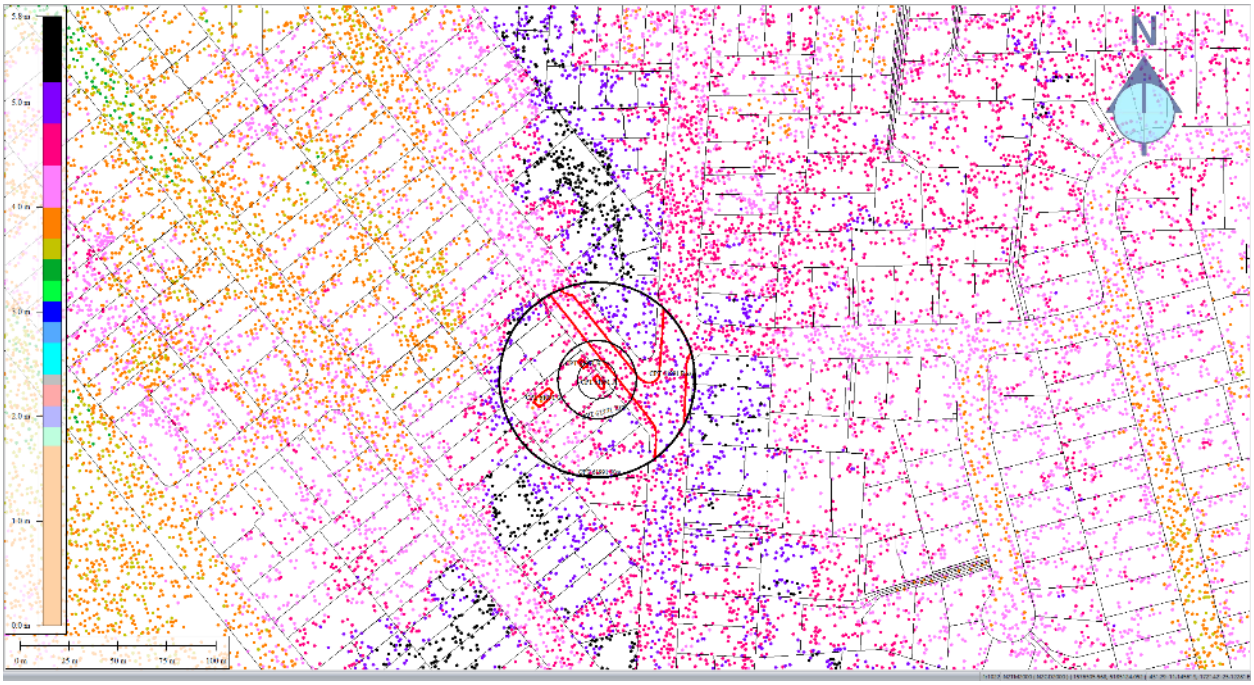

Figure 40: Jul 2003 LiDAR survey.

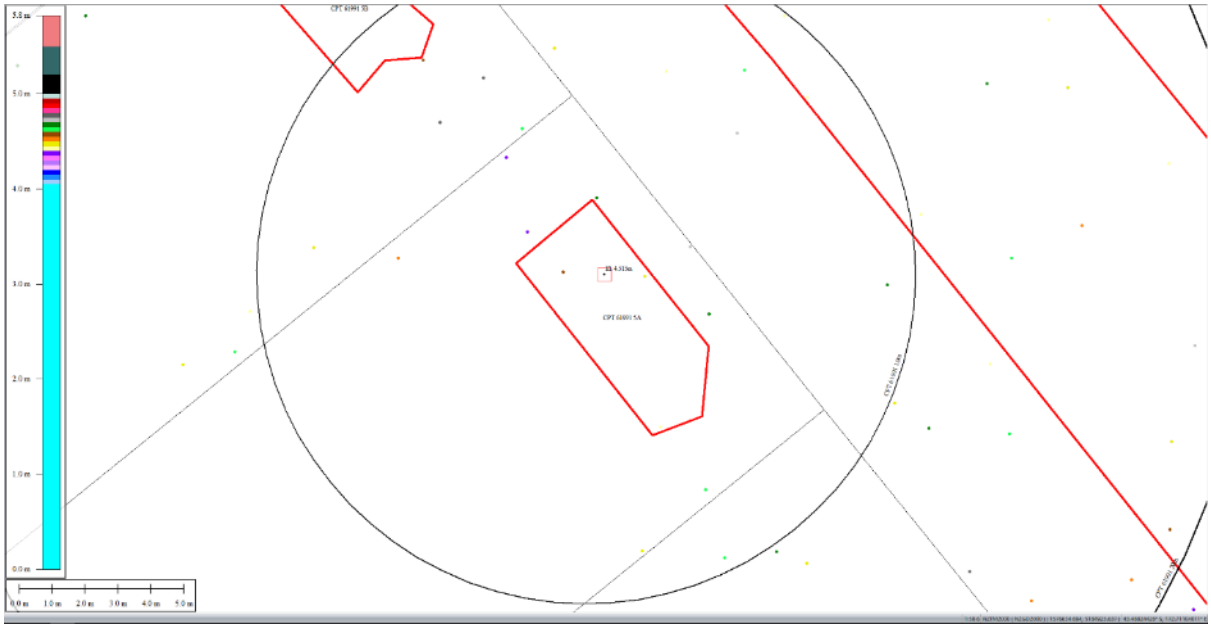

Figure 41: Ground surface elevation for Patch A for Jul 2003 LiDAR survey.

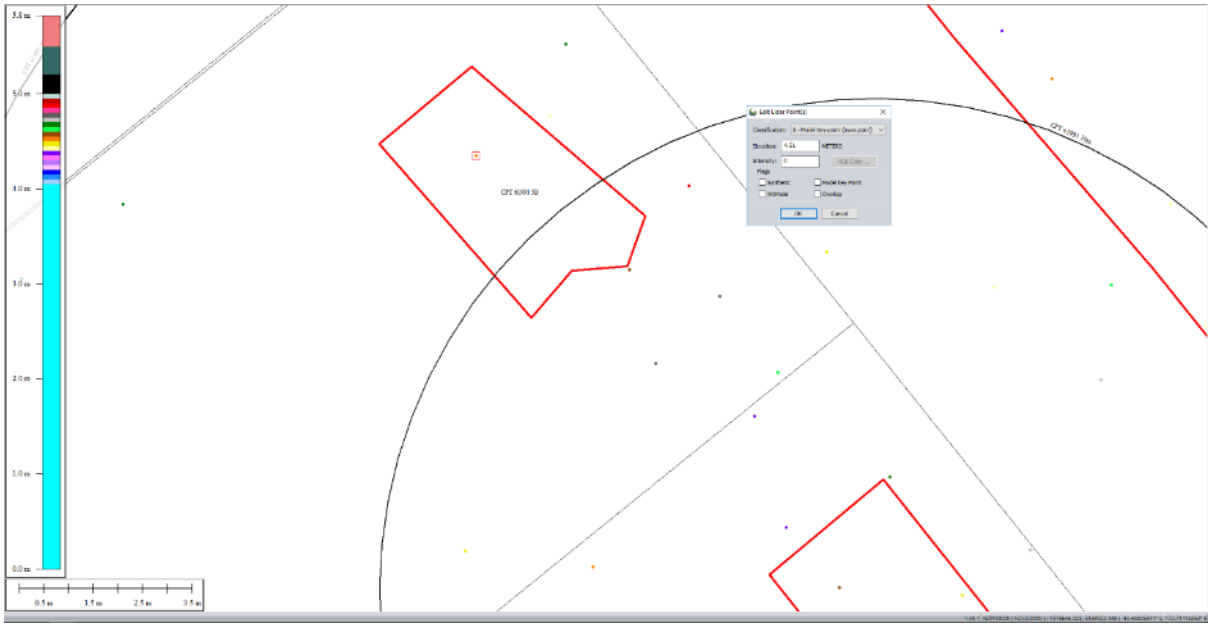

Figure 42: Ground surface elevation for Patch B for the 10-m and 20-m buffers for Jul 2003 LiDAR survey.

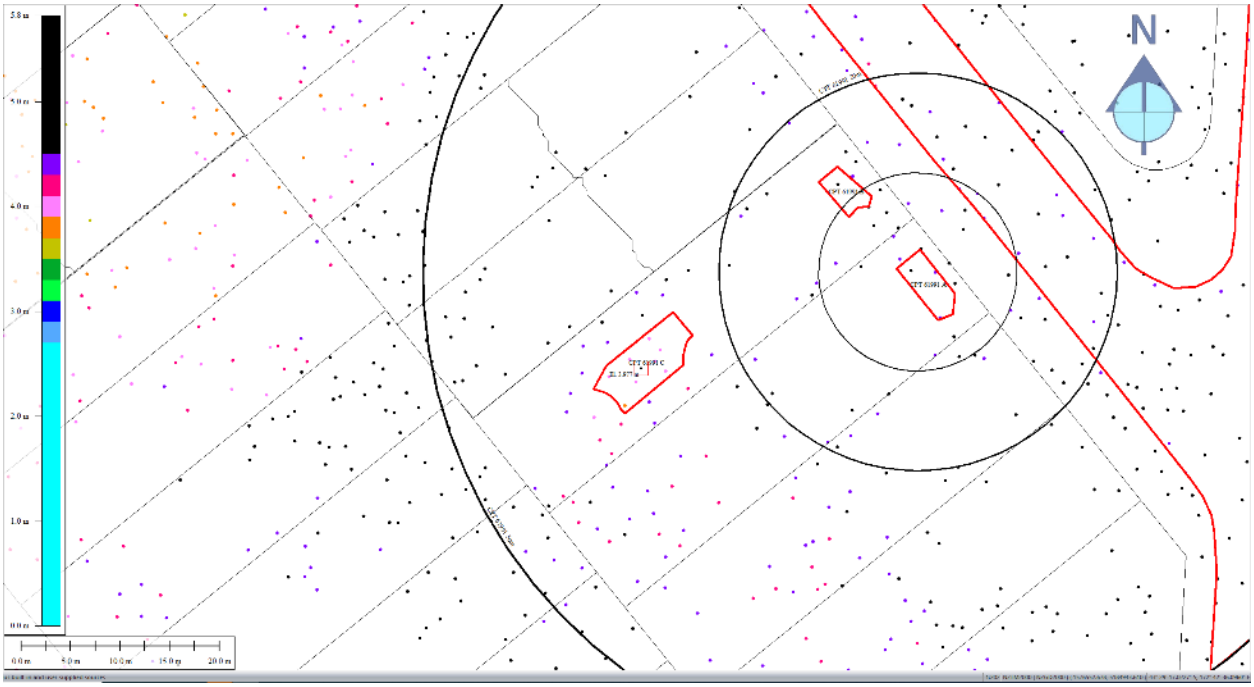

Figure 43: Ground surface elevation for Patch C for Jul 2003 LiDAR survey.

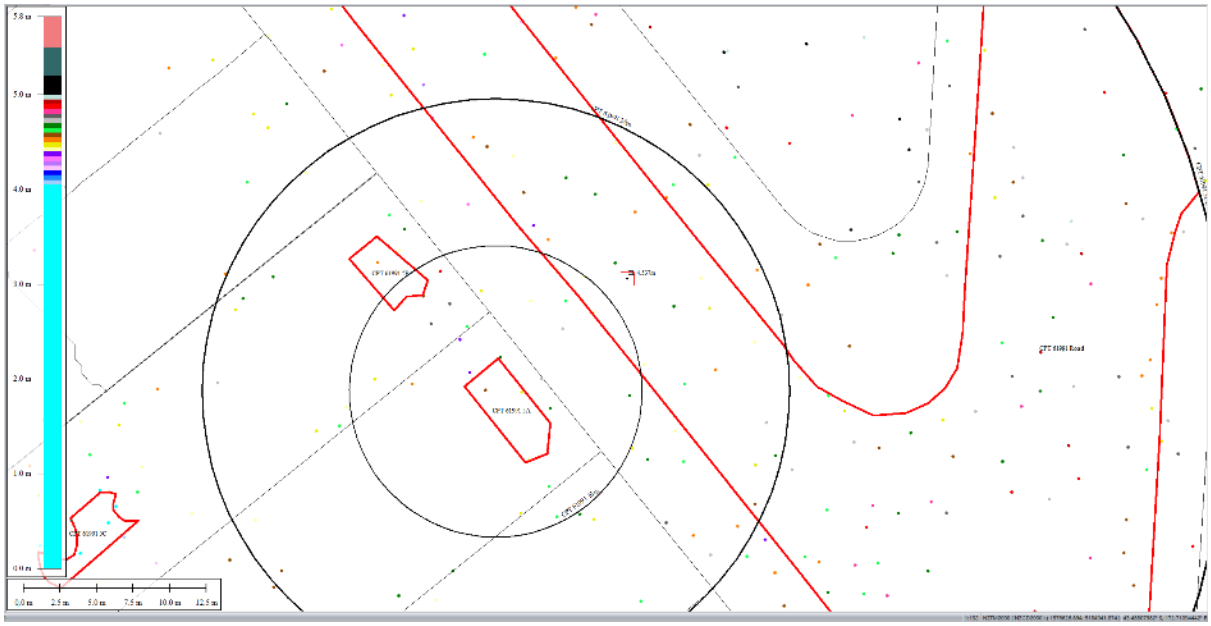

Figure 44: Ground surface elevation for Road averaged over the 20-m buffer for Jul 2003 LiDAR survey.

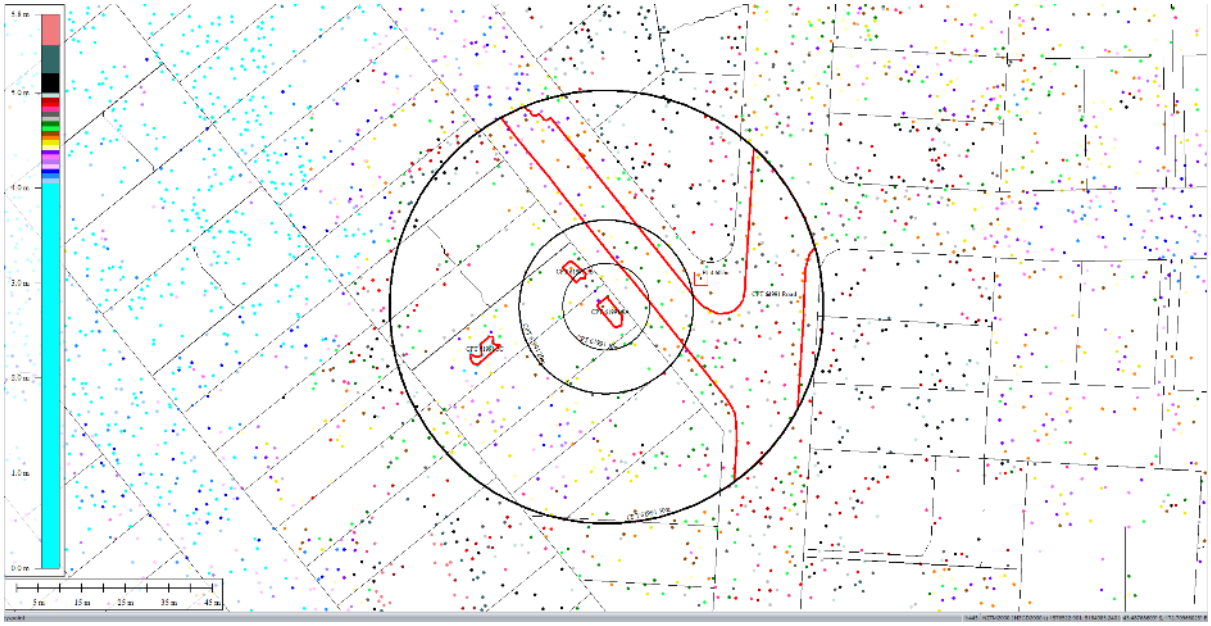

Figure 45: Ground surface elevation for Road averaged over the 50-m buffer for Jul 2003 LiDAR survey.

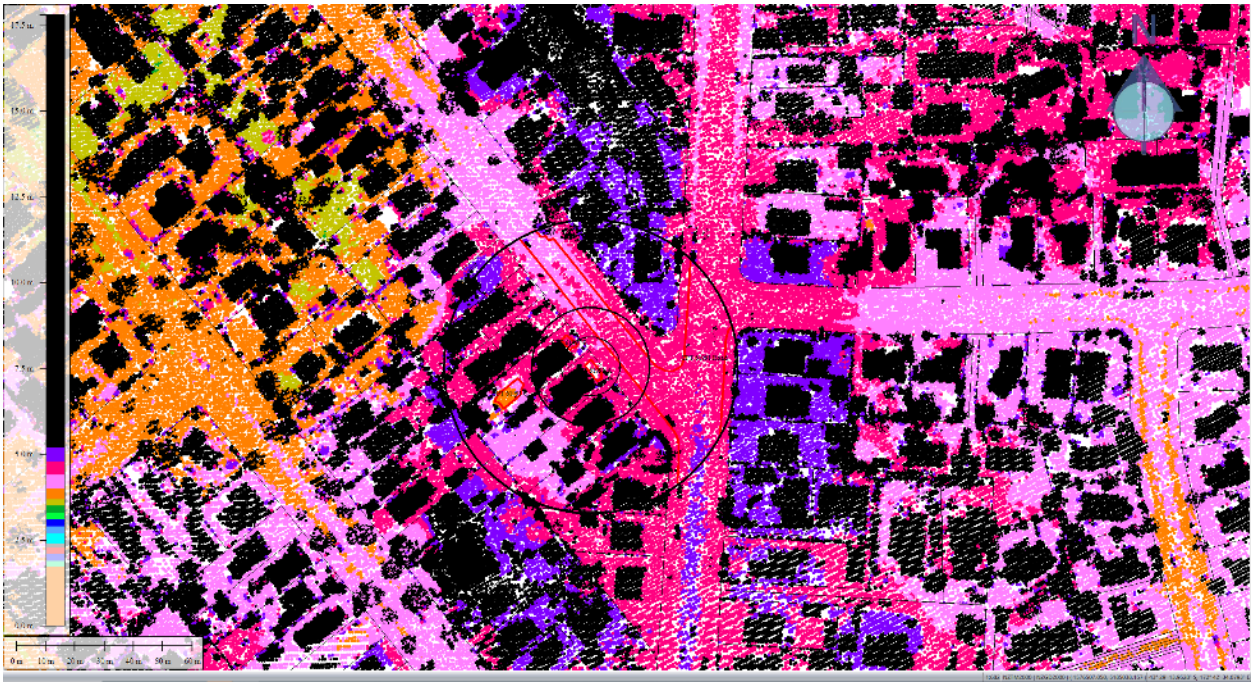

Figure 46: Sep 5, 2010 LiDAR survey.

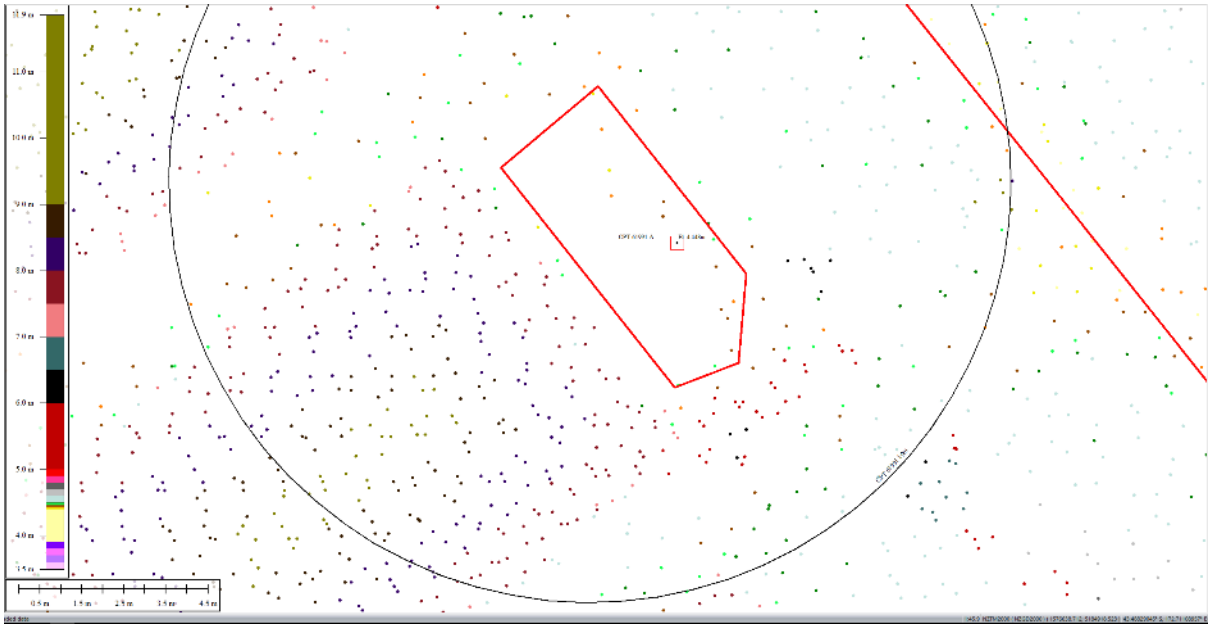

Figure 47: Ground surface elevation for Patch A for Sep 5, 2010 LiDAR survey.

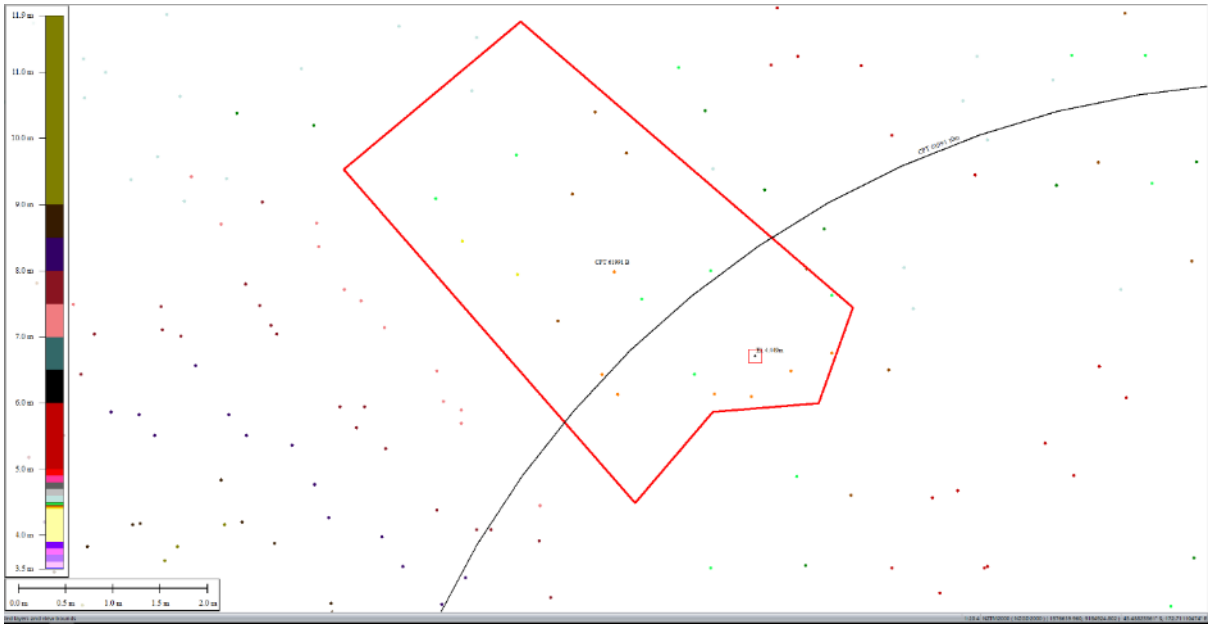

Figure 48: Ground surface elevation for Patch B averaged over the 10-m buffer for Sep 5, 2010 LiDAR survey.

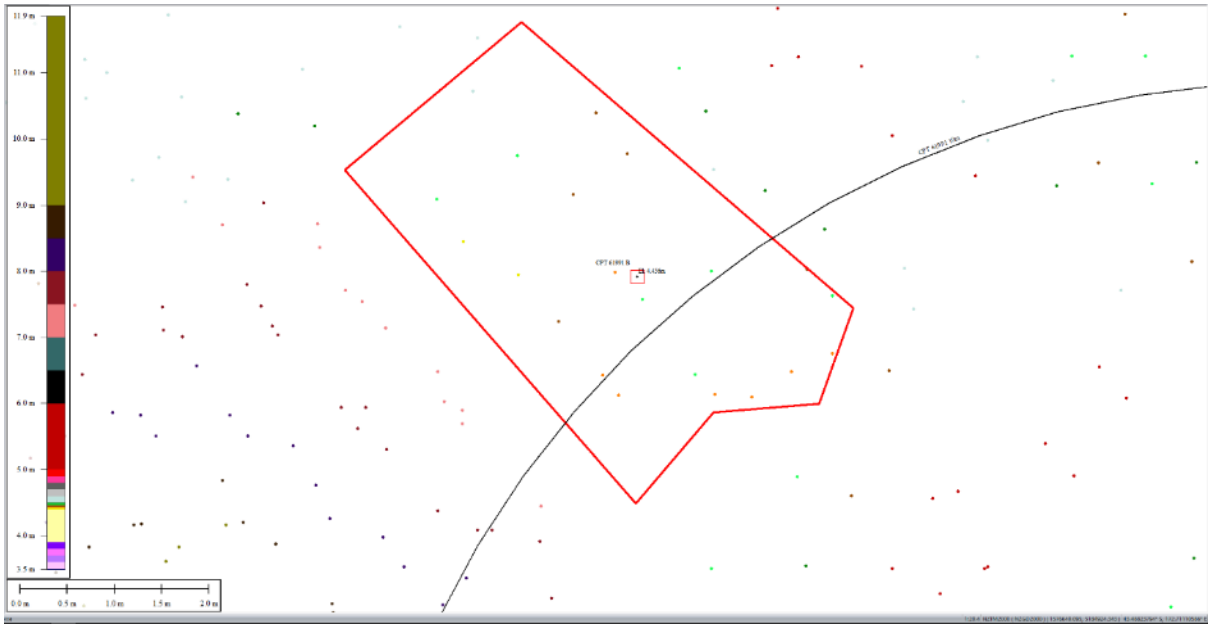

Figure 49: Ground surface elevation for Patch B averaged over the 20-m buffer for Sep 5, 2010 LiDAR survey.

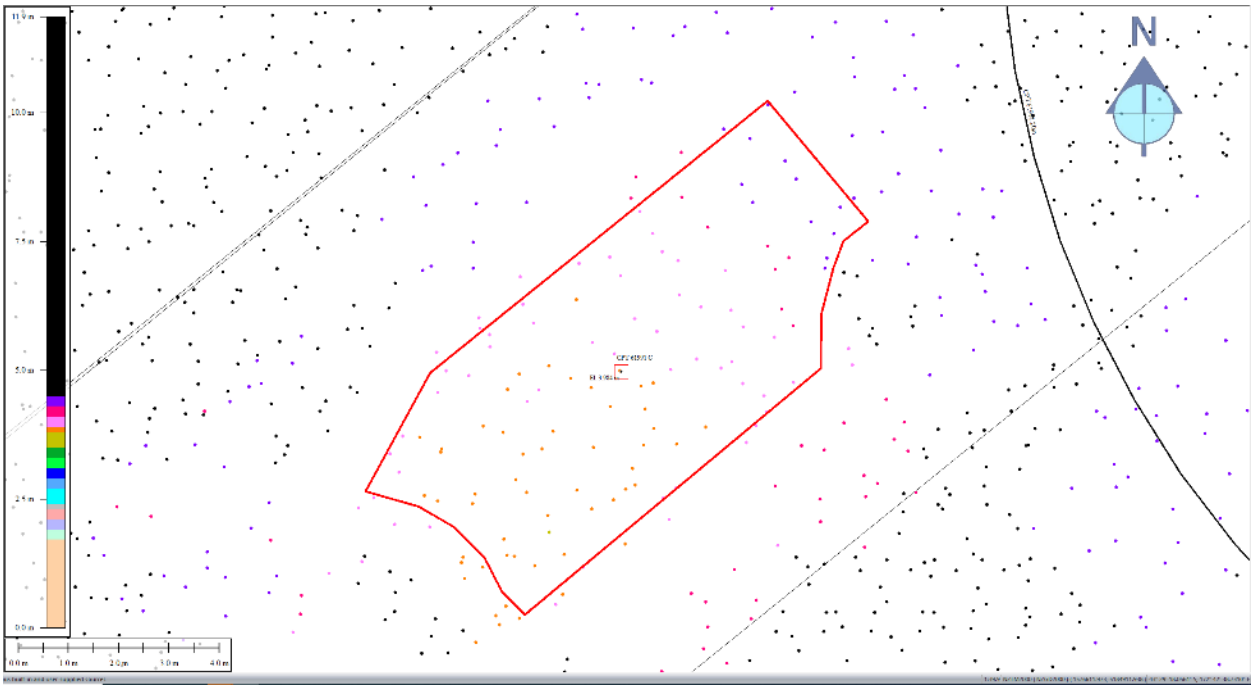

Figure 50: Ground surface elevation for Patch C for Sep 5, 2010 LiDAR survey.

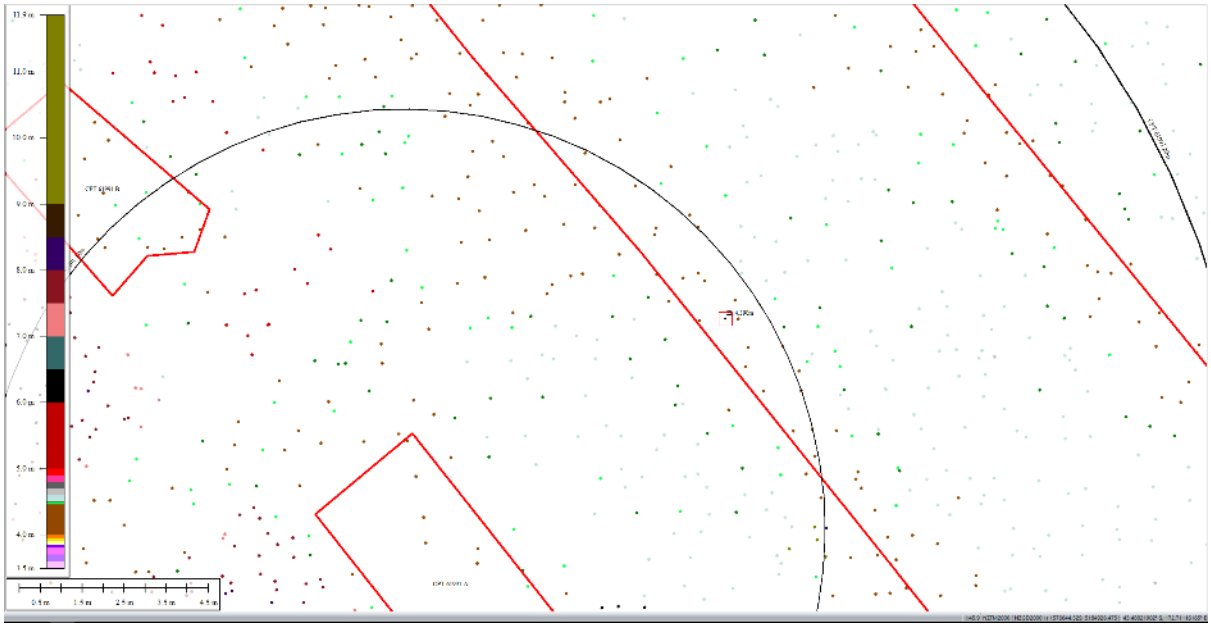

Figure 51: Ground surface elevation for Road averaged over the 10-m buffer for Sep 5, 2010 LiDAR survey.

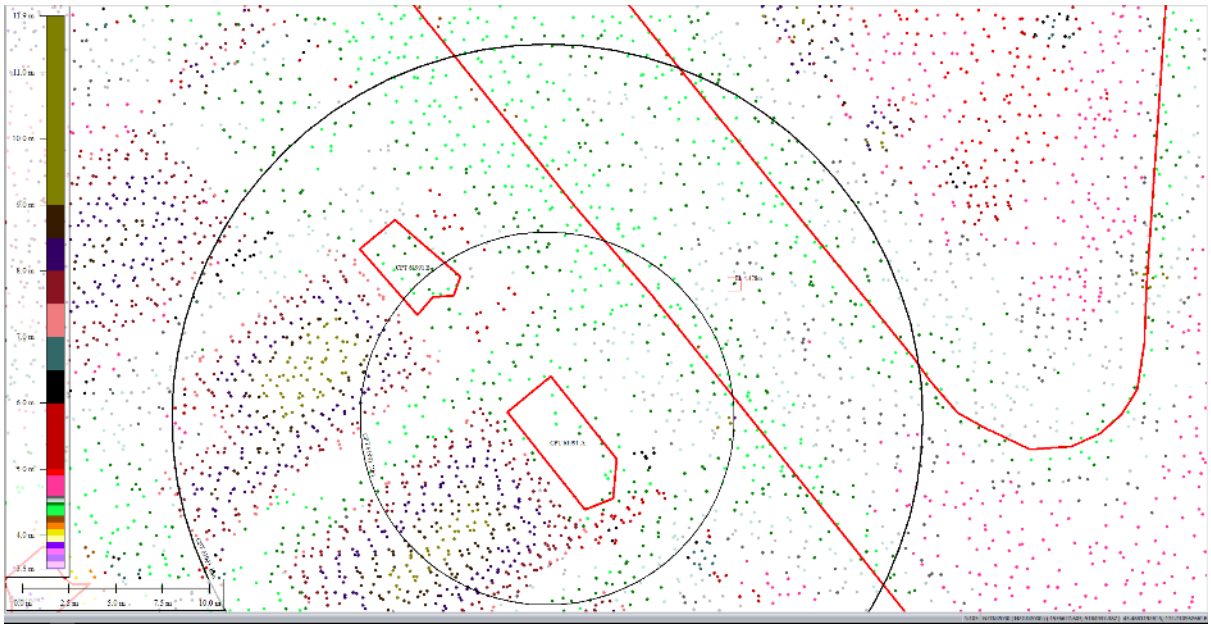

Figure 52: Ground surface elevation for Road averaged over the 20-m buffer for Sep 5, 2010 LiDAR survey.

Figure 53: Ground surface elevation for Road averaged over the 50-m buffer for Sep 5, 2010 LiDAR survey.

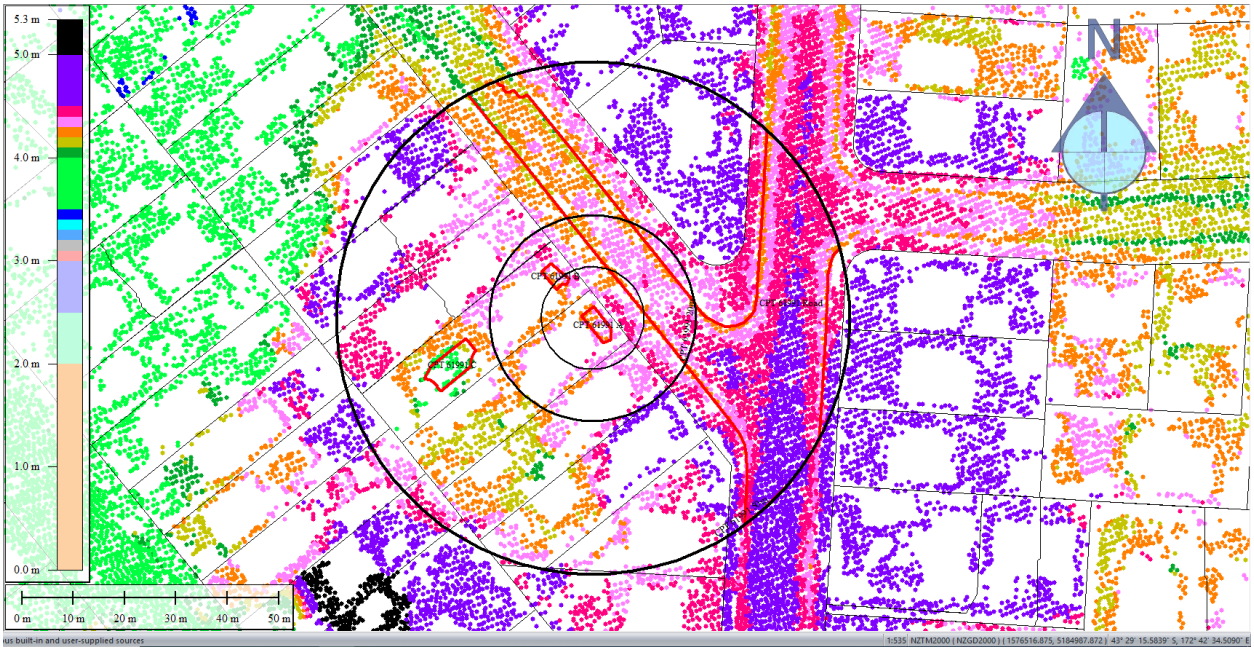

Figure 54: May 2011 LiDAR survey.

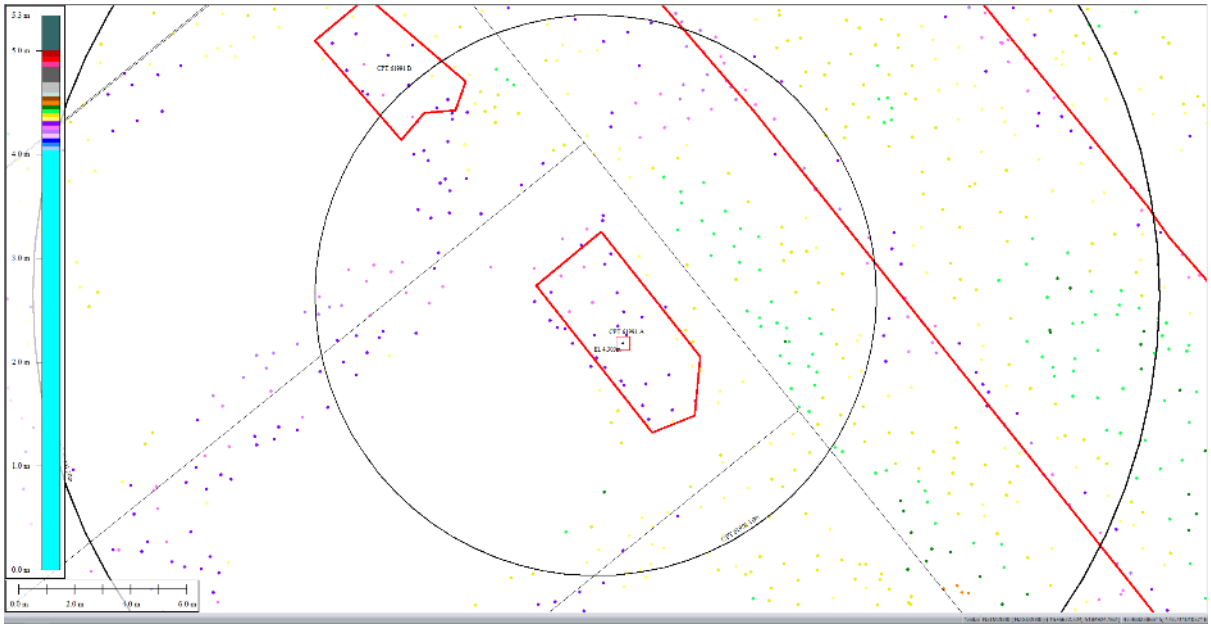

Figure 55: Ground surface elevation for Patch A for May 2011 LiDAR survey.

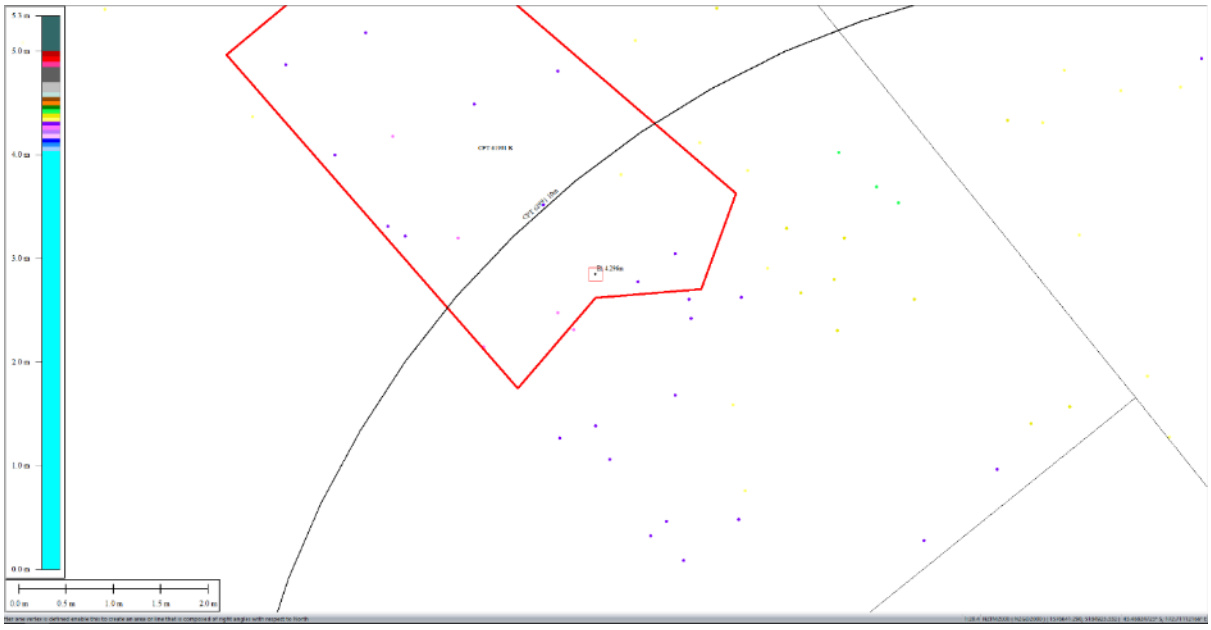

Figure 56: Ground surface elevation for Patch B averaged over the 10-m buffer for May 2011 LiDAR survey.

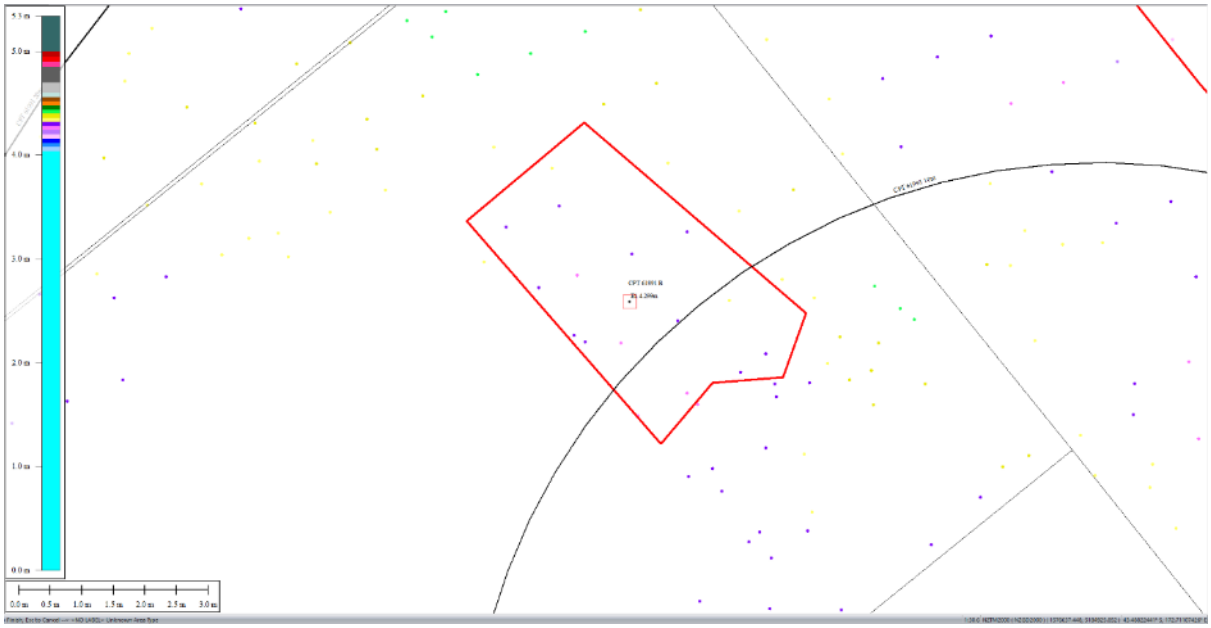

Figure 57: Ground surface elevation for Patch B averaged over the 20-m buffer for May 2011 LiDAR survey.

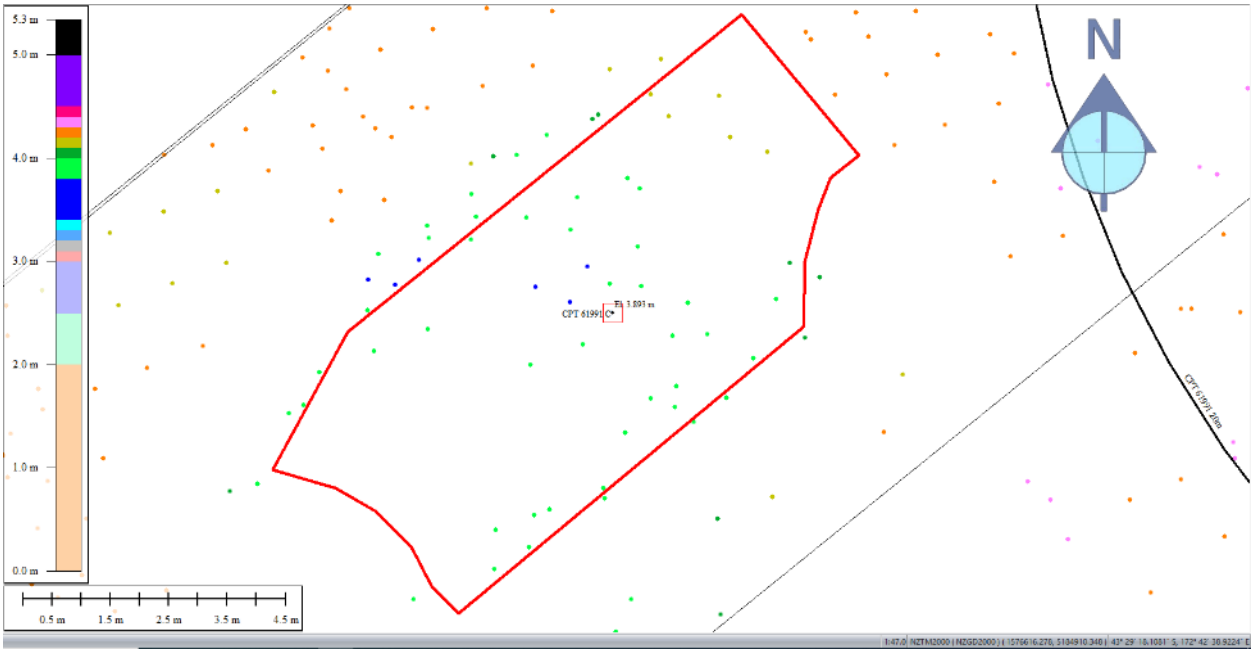

Figure 58: Ground surface elevation for Patch C for May 2011 LiDAR survey.

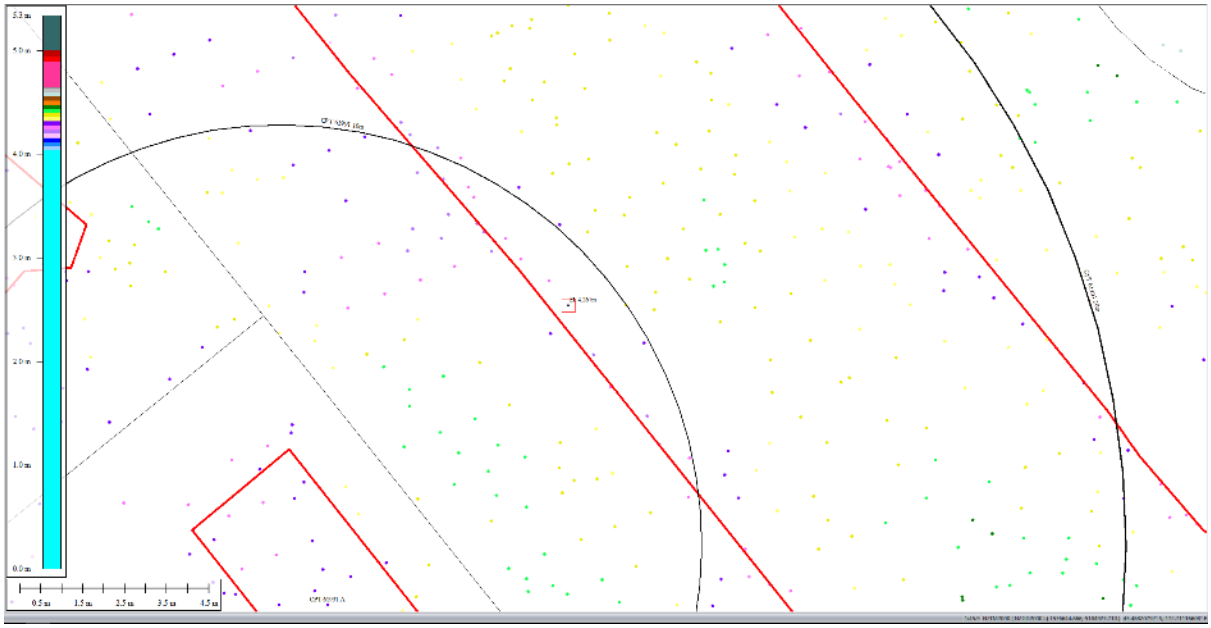

Figure 59: Ground surface elevation for Road averaged over the 10-m buffer for May 2011 LiDAR survey.

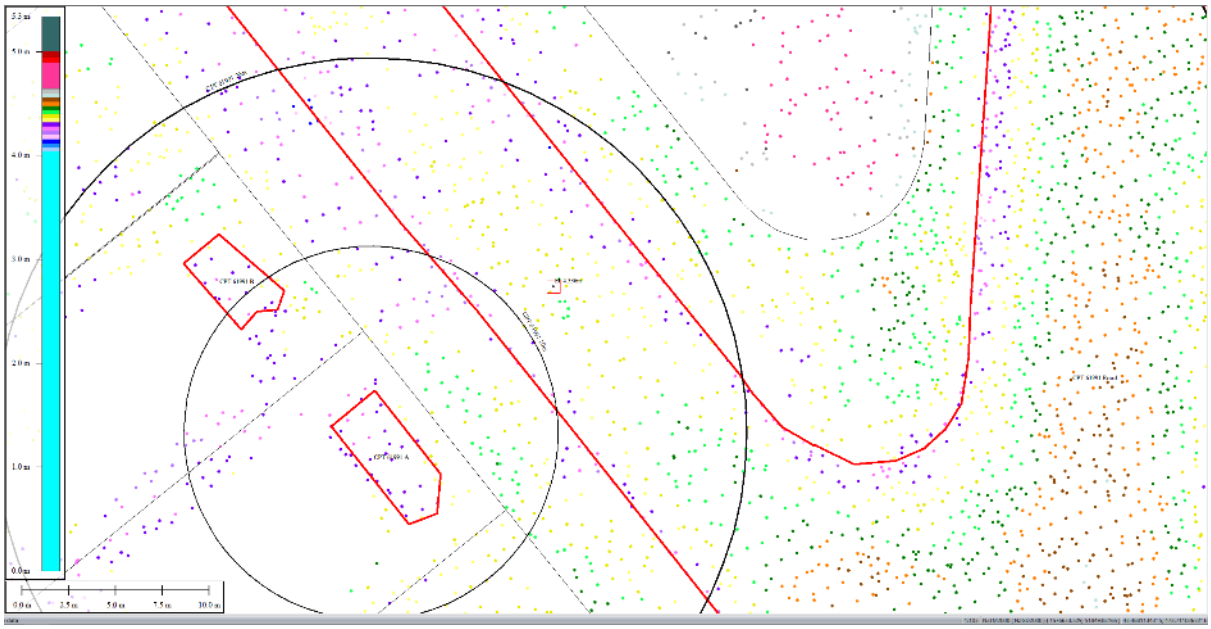

Figure 60: Ground surface elevation for Road averaged over the 20-m buffer for May 2011 LiDAR survey.

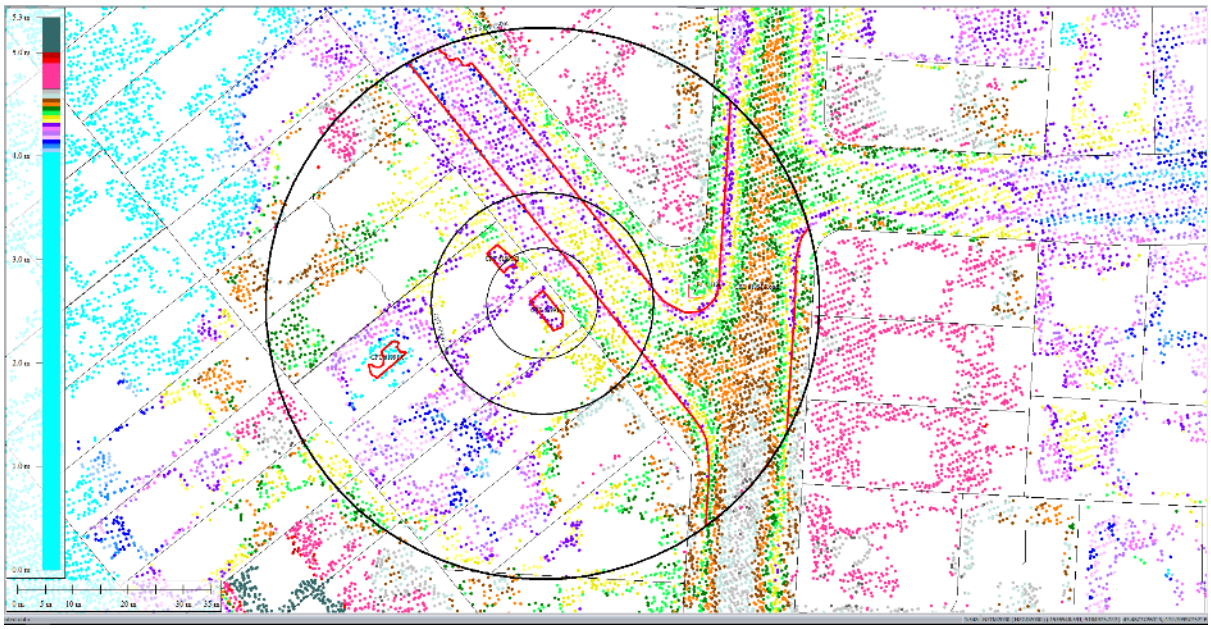

Figure 61: Ground surface elevation for Road averaged over the 50-m buffer for May 2011 LiDAR survey.

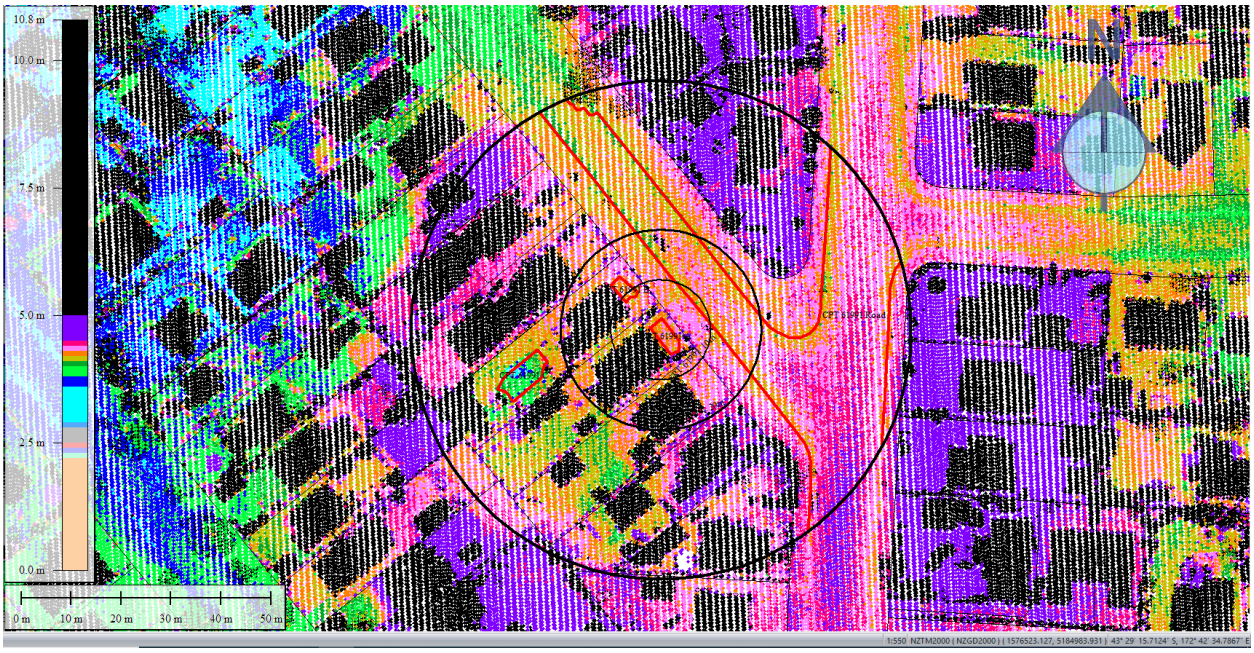

Figure 62: Sep 2011 LiDAR survey.

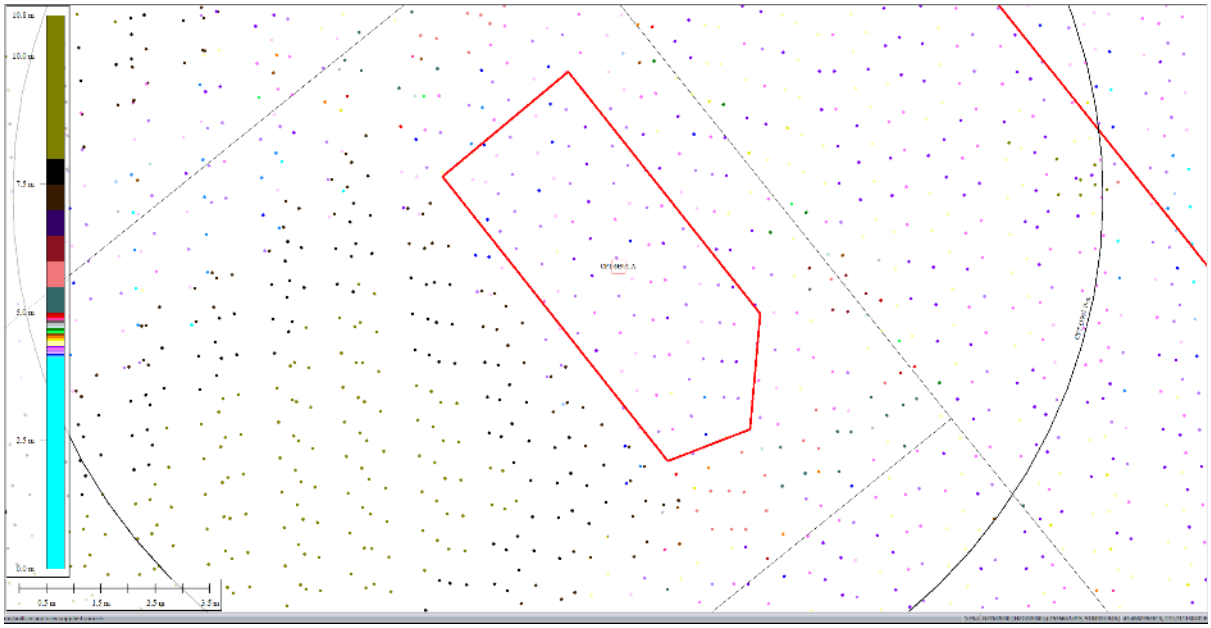

Figure 63: Ground surface elevation for Patch A for Sep 2011 LiDAR survey.

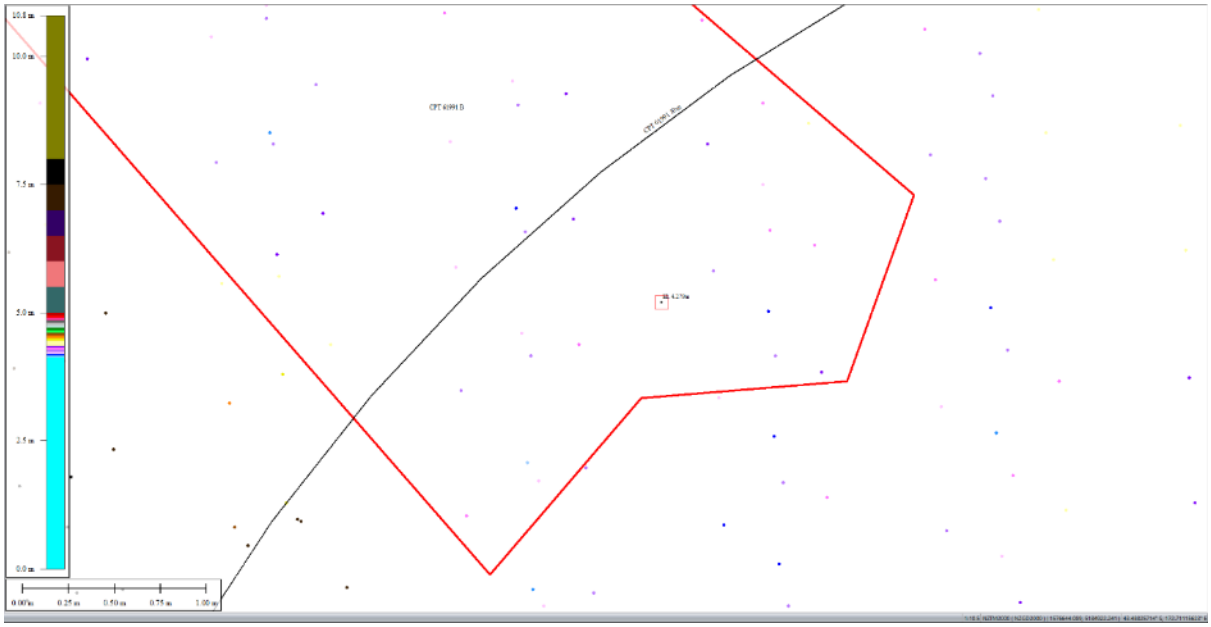

Figure 64: Ground surface elevation for Patch B averaged over the 10-m buffer for Sep 2011 LiDAR survey.

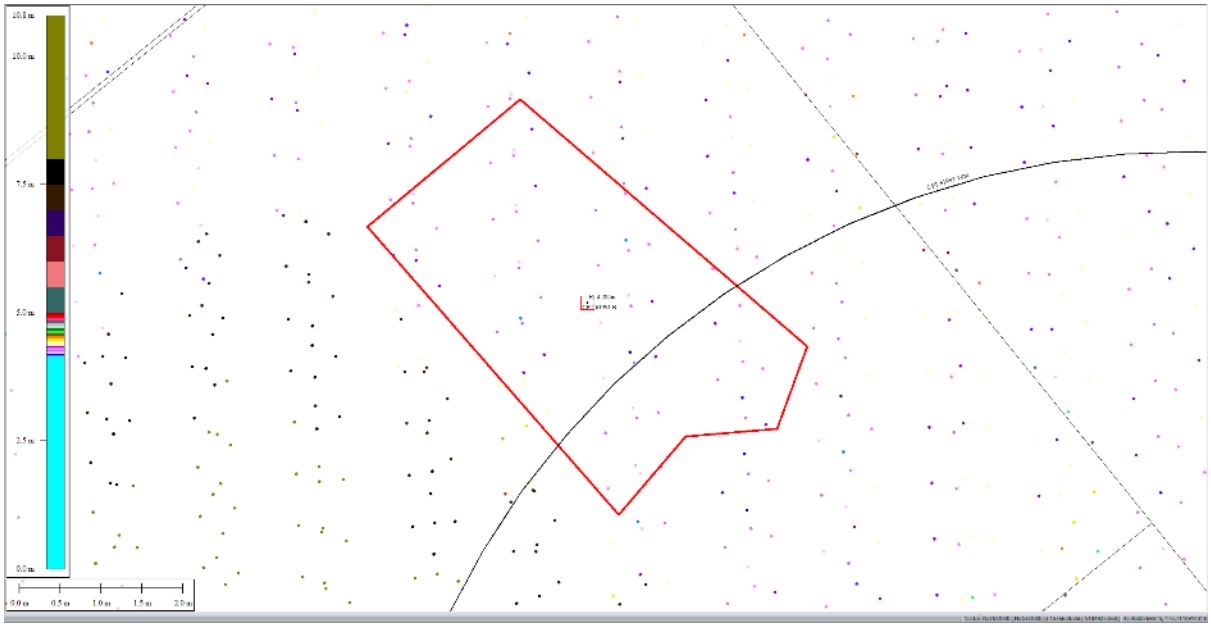

Figure 65: Ground surface elevation for Patch B averaged over the 20-m buffer for Sep 2011 LiDAR survey.

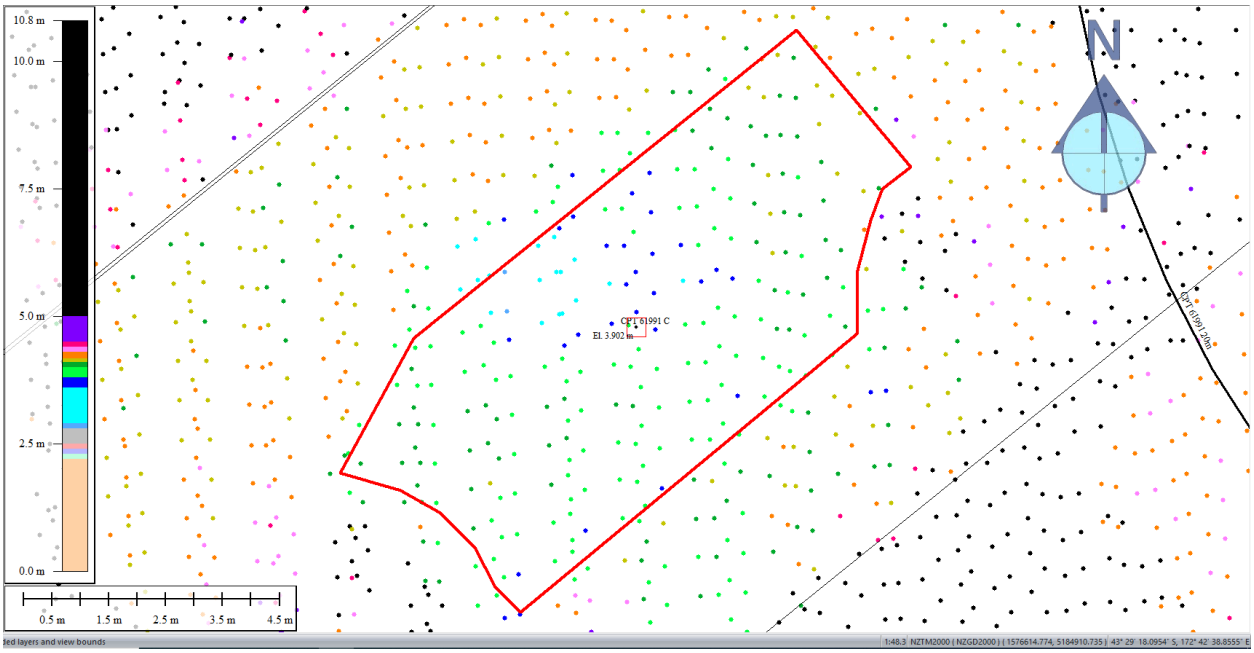

Figure 66: Ground surface elevation for Patch C for Sep 2011 LiDAR survey.

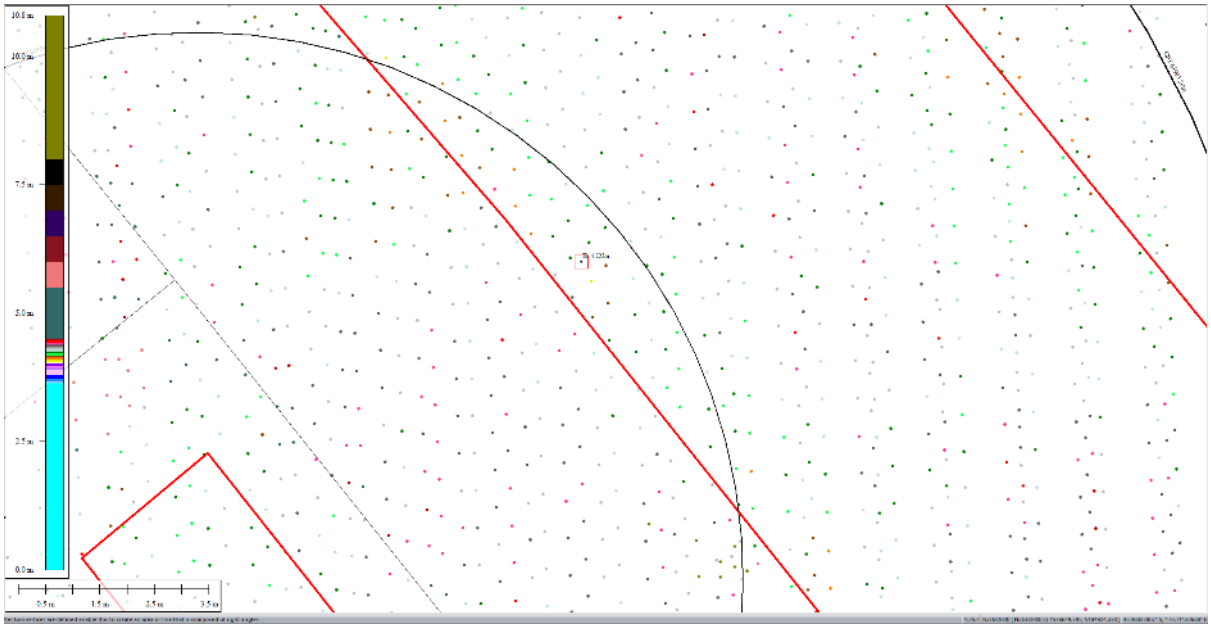

Figure 67: Ground surface elevation for Road averaged over the 10-m buffer for Sep 2011 LiDAR survey.

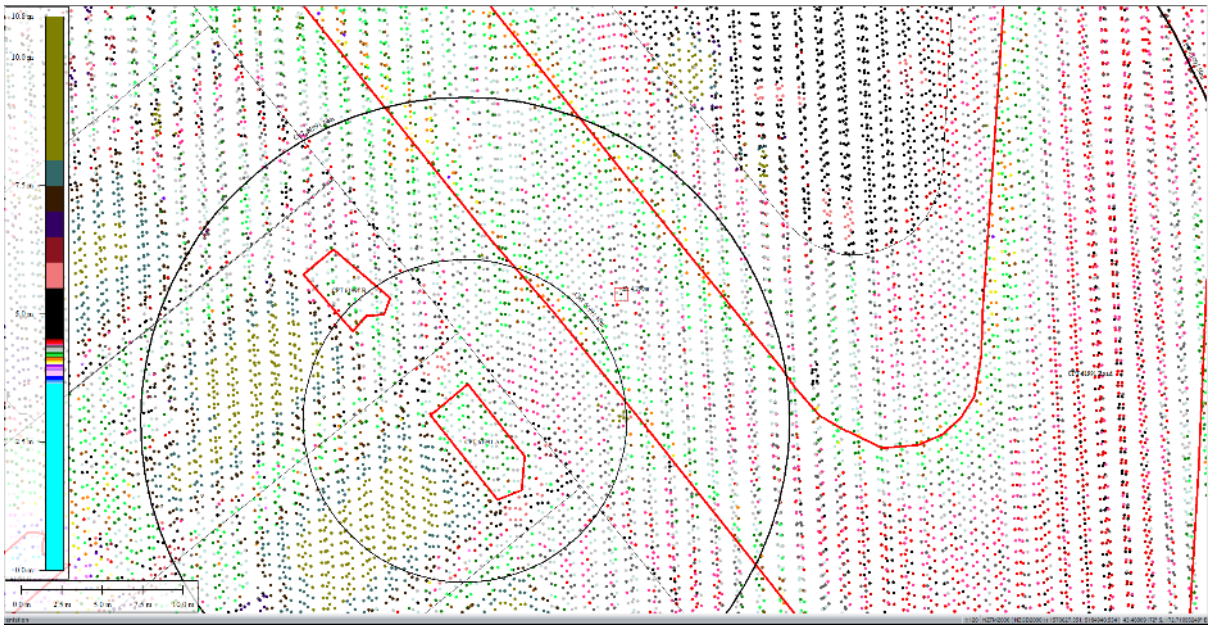

Figure 68: Ground surface elevation for Road averaged over the 20-m buffer for Sep 2011 LiDAR survey.

Figure 69: Ground surface elevation for Road averaged over the 50-m buffer for Sep 2011 LiDAR survey.

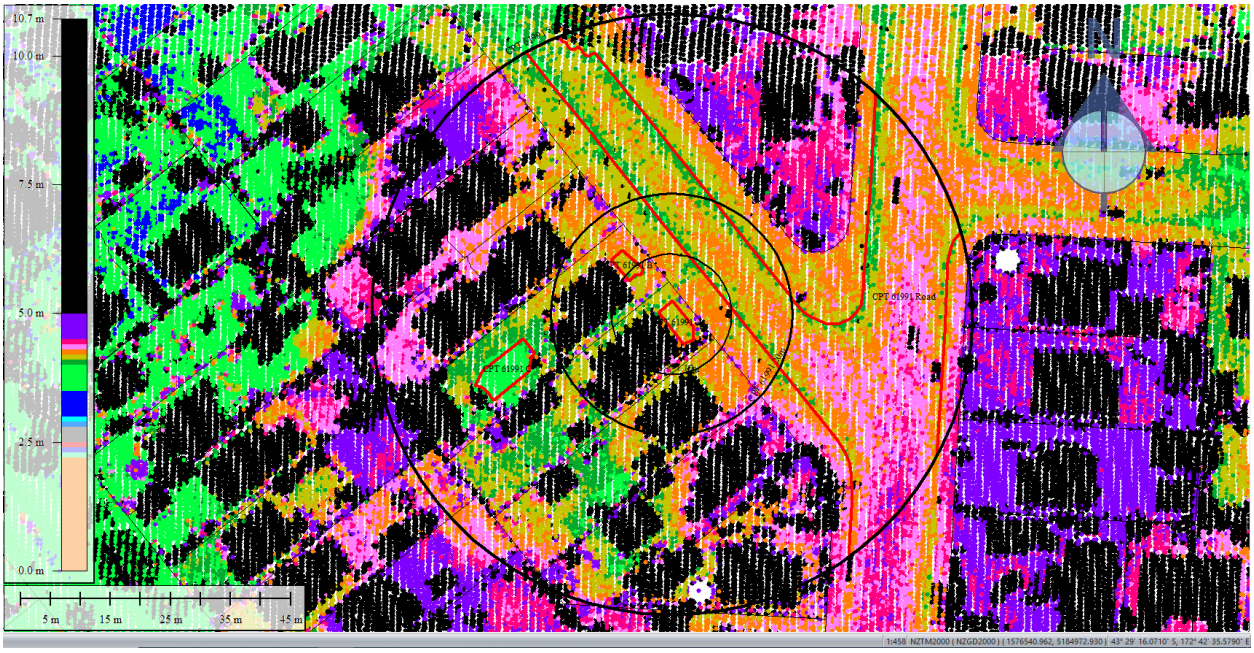

Figure 70: Feb 2012 LiDAR survey.

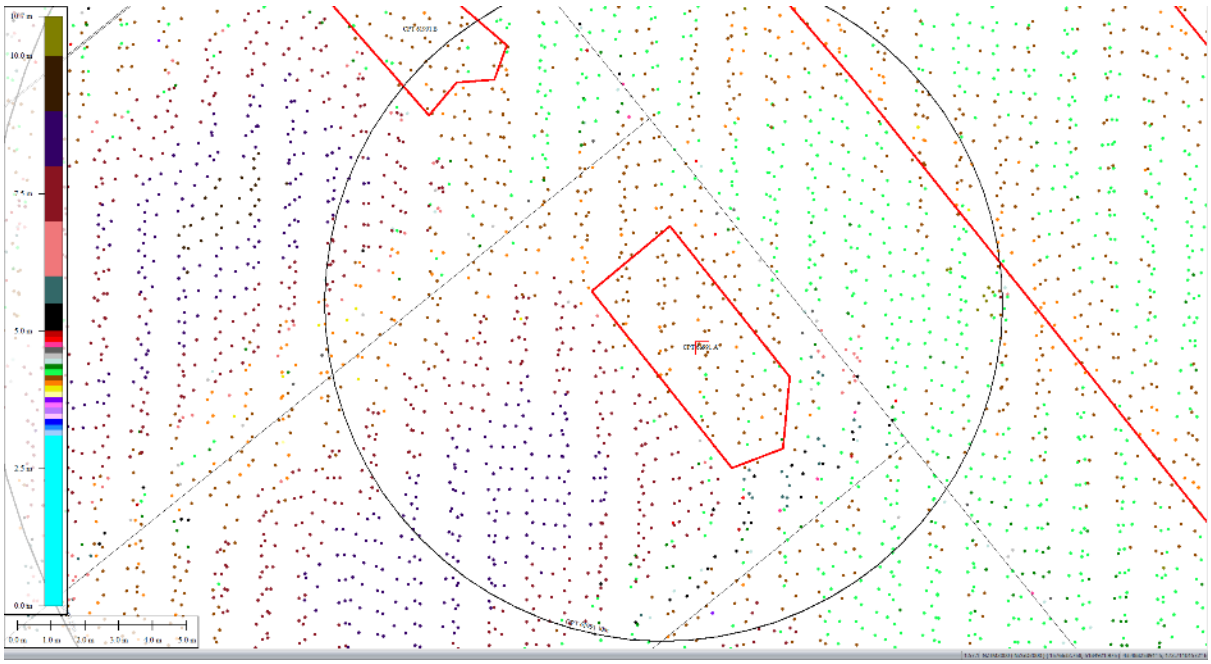

Figure 71: Ground surface elevation for Patch A for Feb 2012 LiDAR survey.

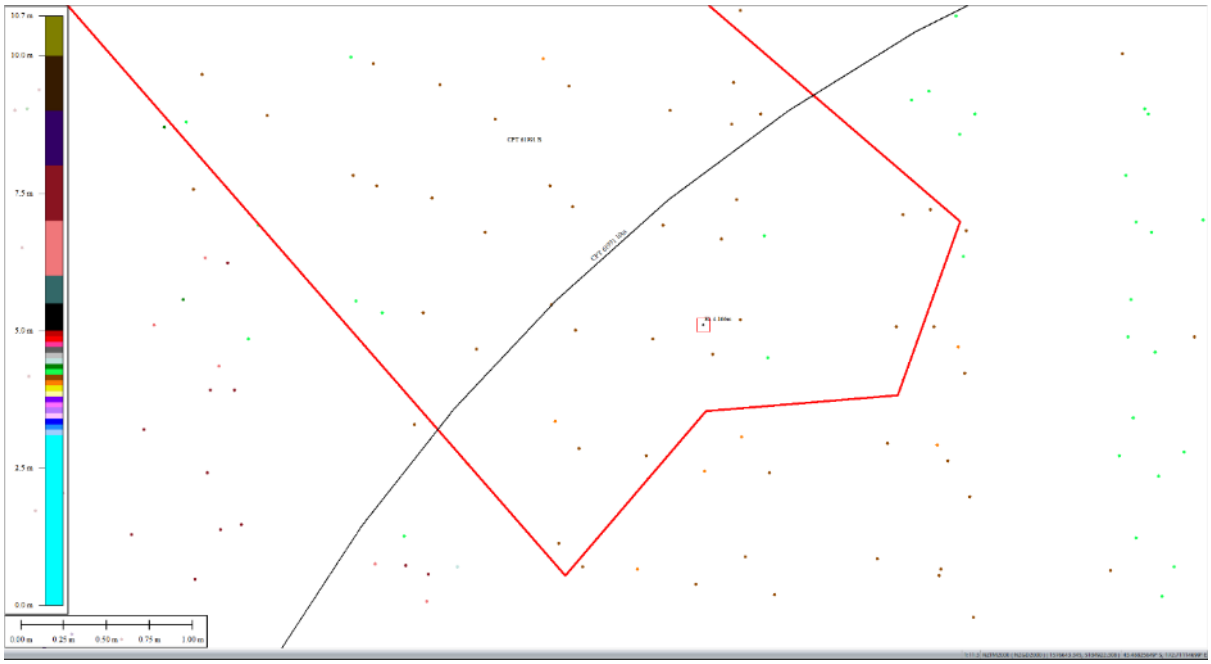

Figure 72: Ground surface elevation for Patch B averaged over the 10-m buffer for Feb 2012 LiDAR survey.

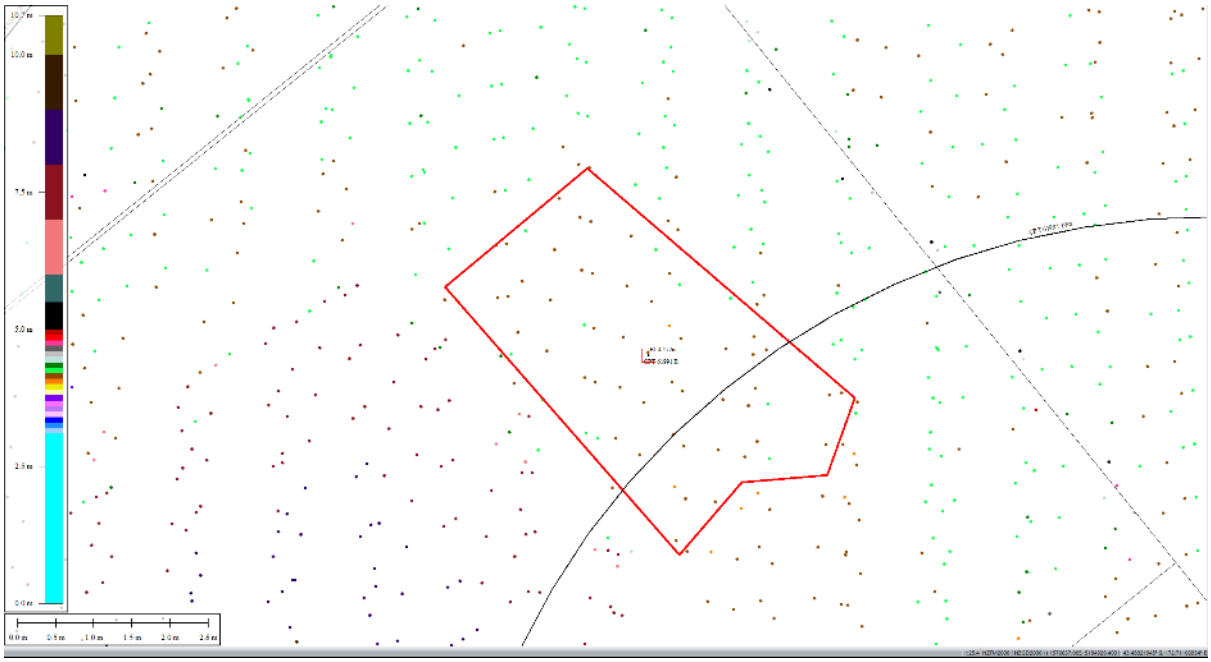

Figure 73: Ground surface elevation for Patch B averaged over the 20-m buffer for Feb 2012 LiDAR survey.

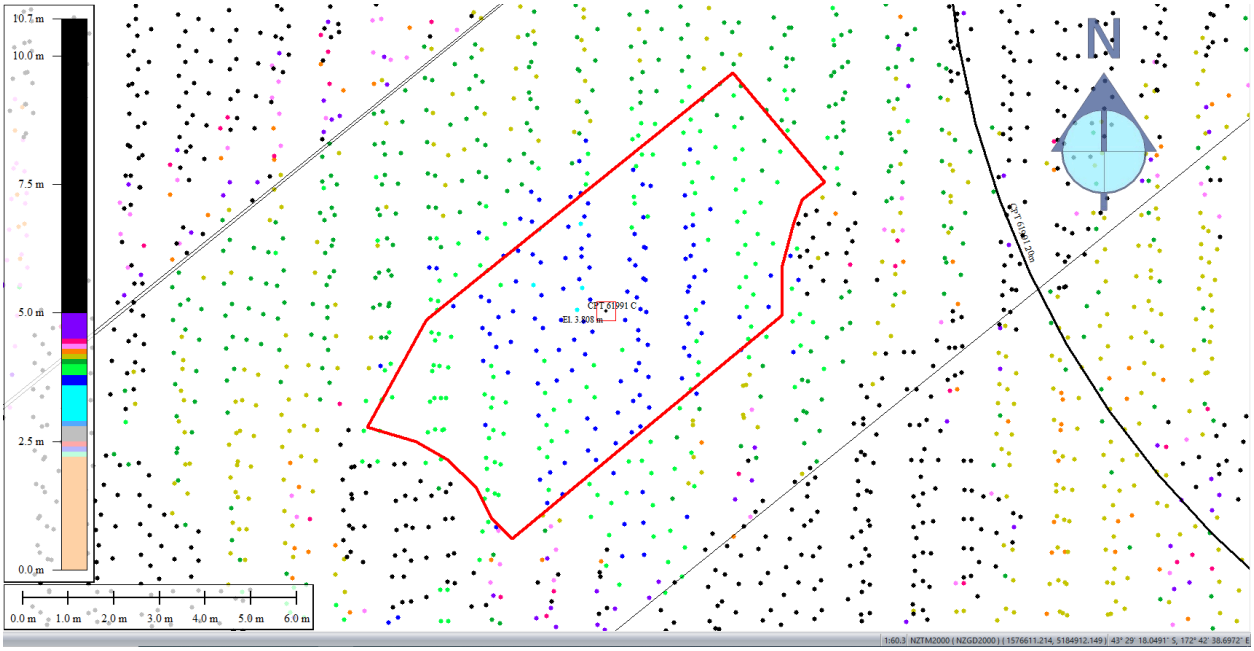

Figure 74: Ground surface elevation for Patch C for Feb 2012 LiDAR survey.

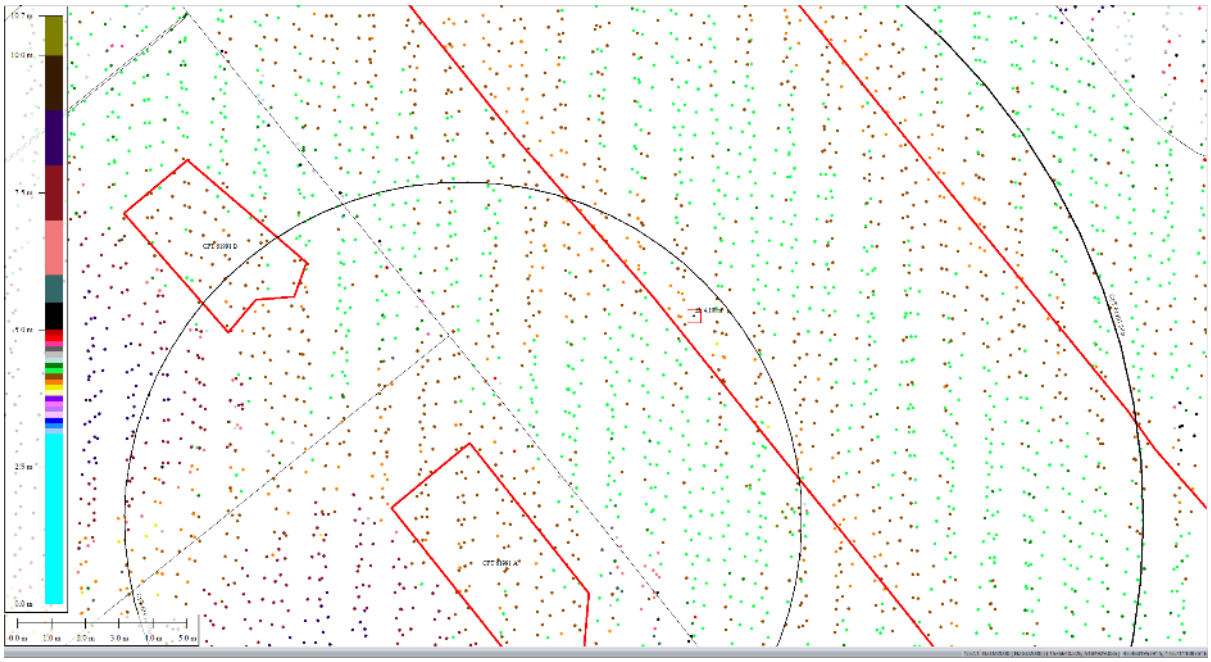

Figure 75: Ground surface elevation for Road averaged over the 10-m buffer for Feb 2012 LiDAR survey.

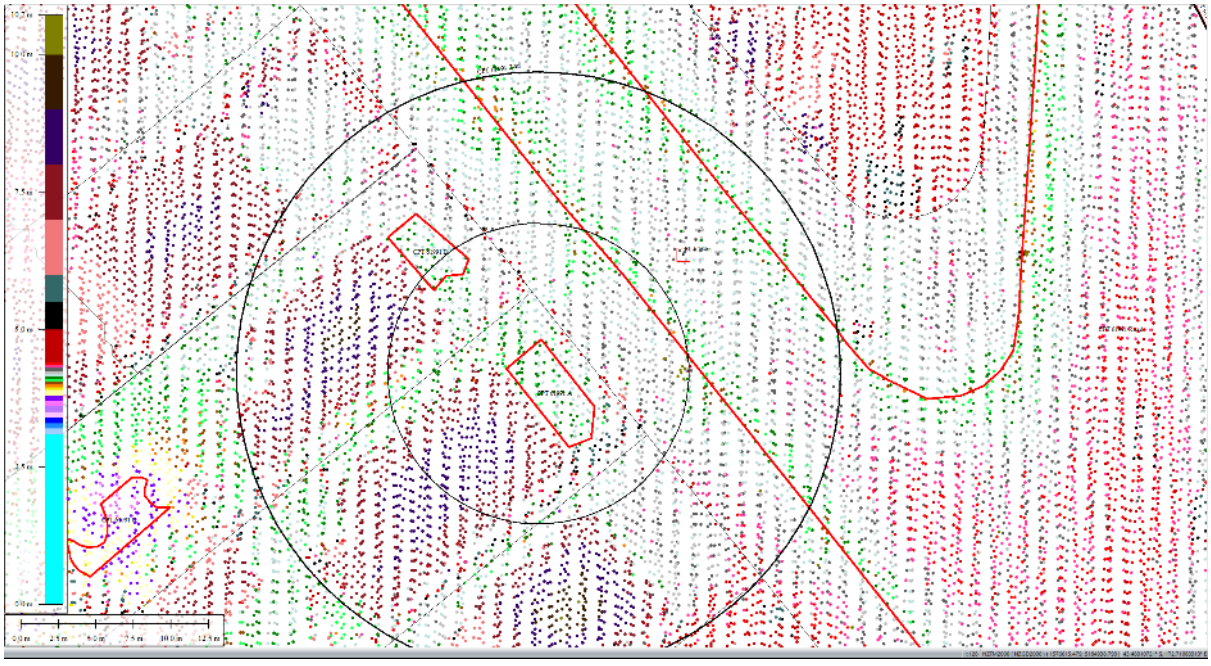

Figure 76: Ground surface elevation for Road averaged over the 20-m buffer for Feb 2012 LiDAR survey.

Figure 77: Ground surface elevation for Road averaged over the 50-m buffer for Feb 2012 LiDAR survey.

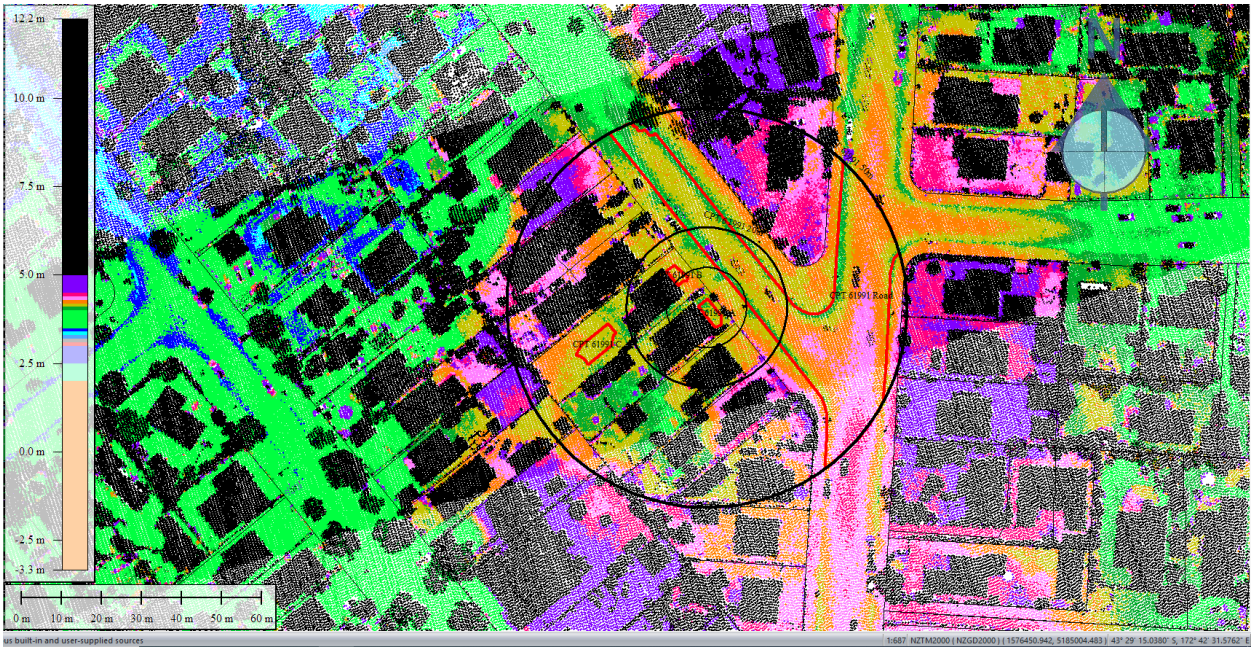

Figure 78: Oct 2015 LiDAR survey.

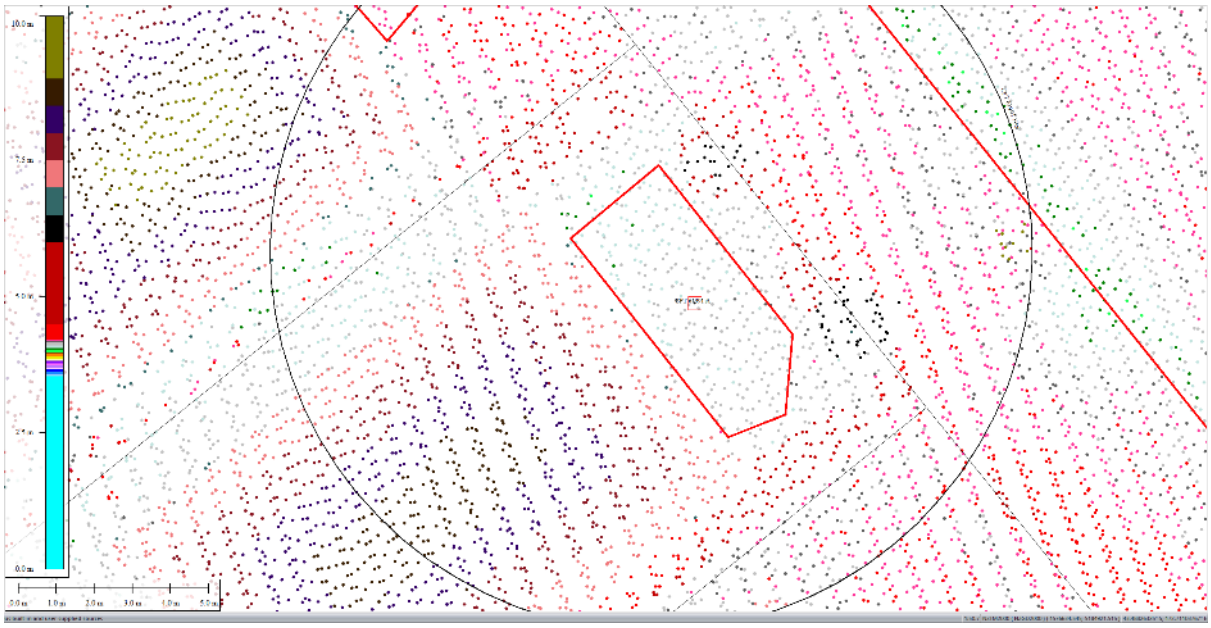

Figure 79: Ground surface elevation for Patch A for Oct 2015 LiDAR survey.

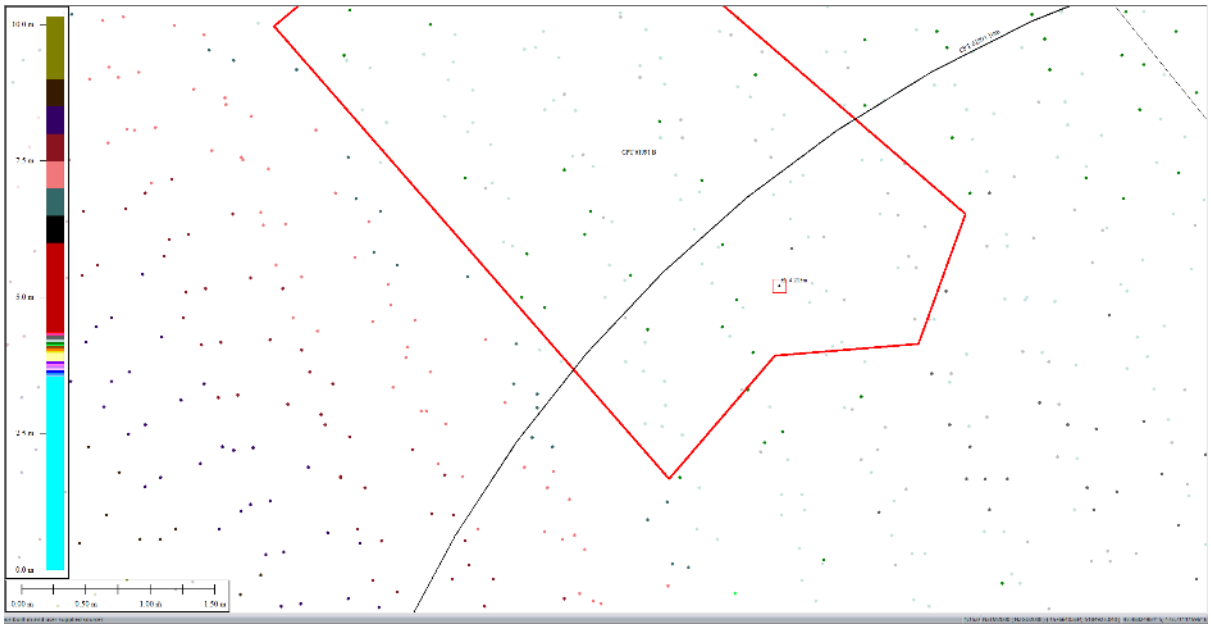

Figure 80: Ground surface elevation for Patch B averaged over the 10-m buffer for Oct 2015 LiDAR survey.

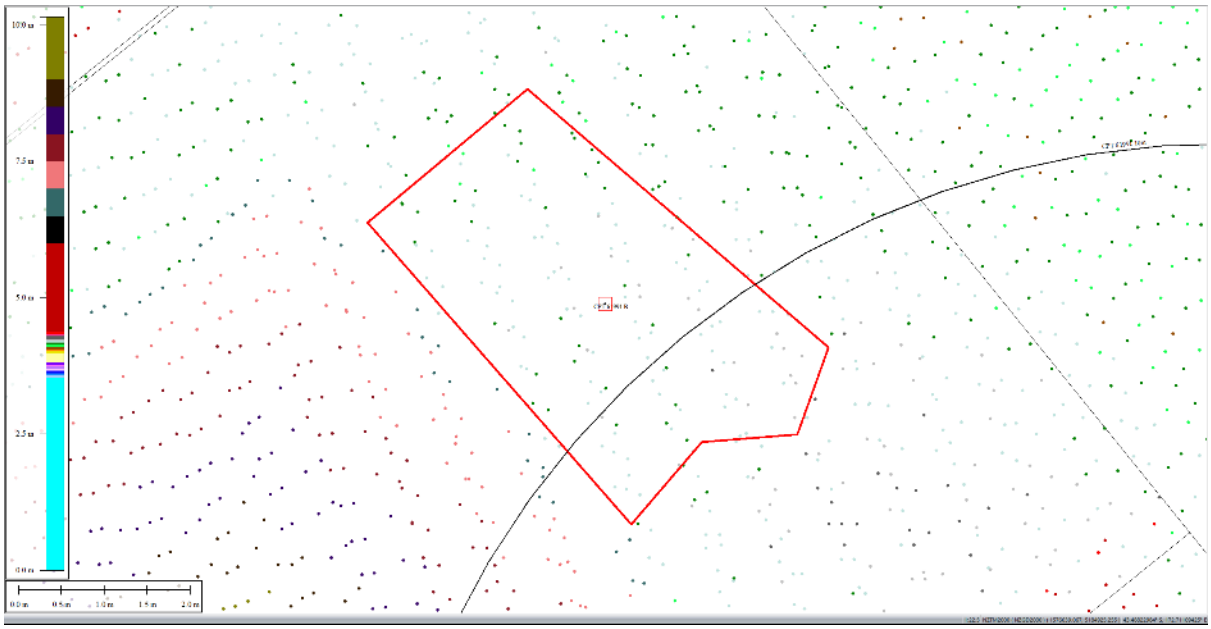

Figure 81: Ground surface elevation for Patch B averaged over the 20-m buffer for Oct 2015 LiDAR survey.

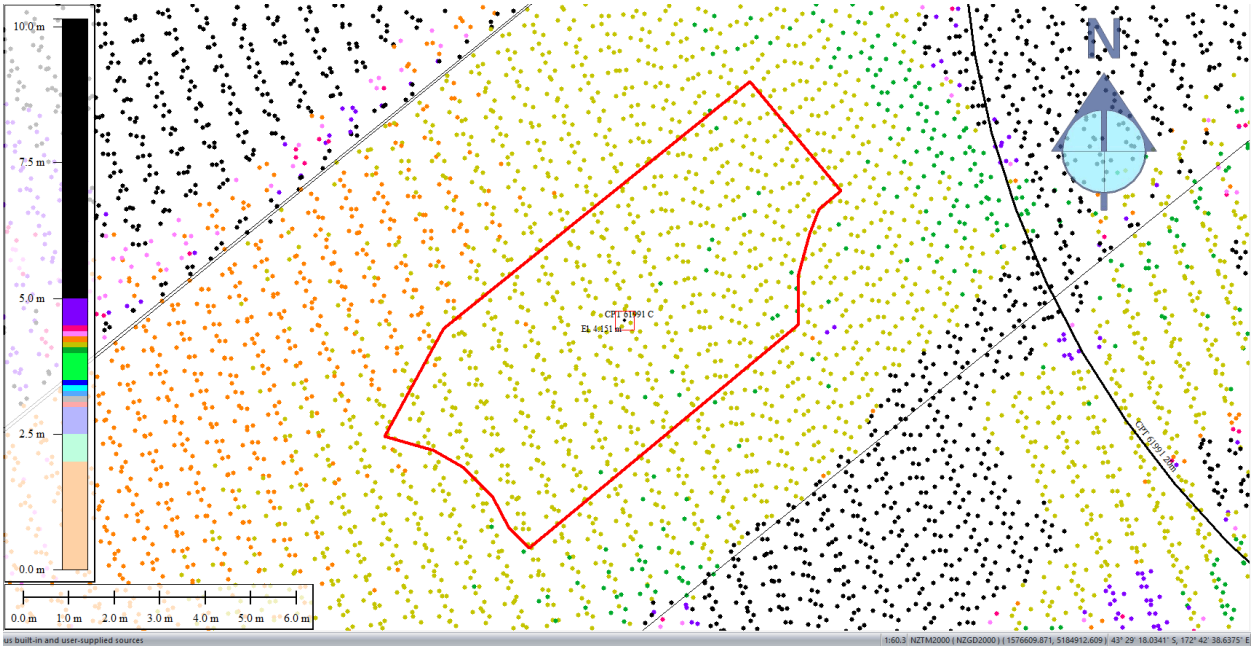

Figure 82: Ground surface elevation for Patch C for Oct 2015 LiDAR survey.

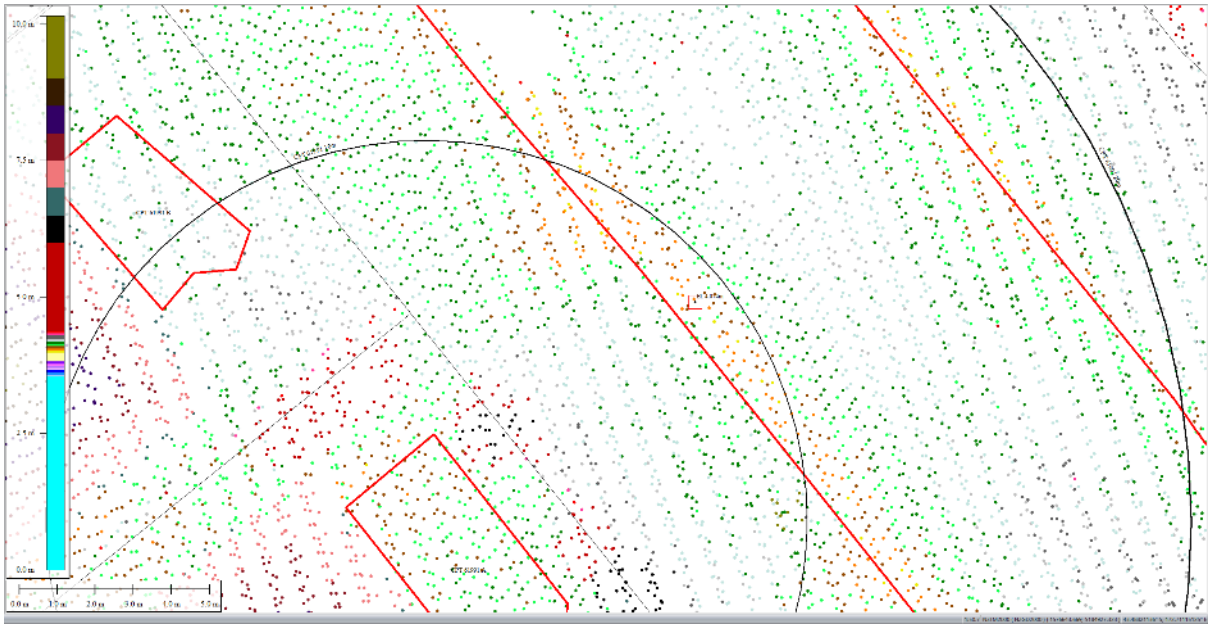

Figure 83: Ground surface elevation for Road averaged over the 10-m buffer for Oct 2015 LiDAR survey.

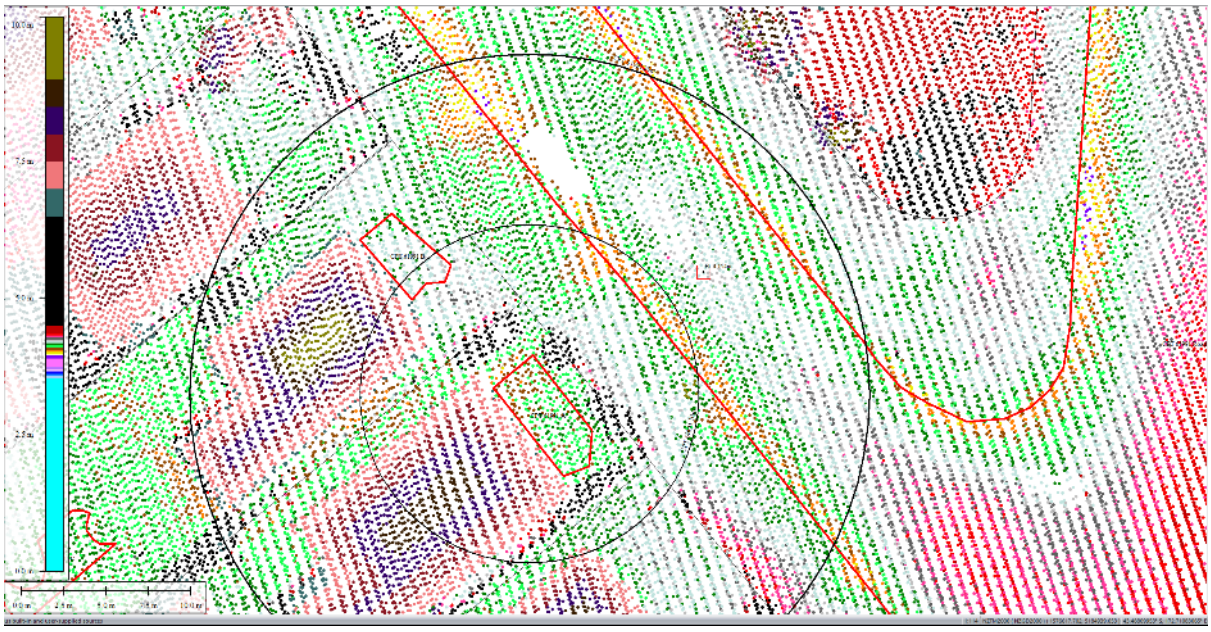

Figure 84: Ground surface elevation for Road averaged over the 20-m buffer for Oct 2015 LiDAR survey.

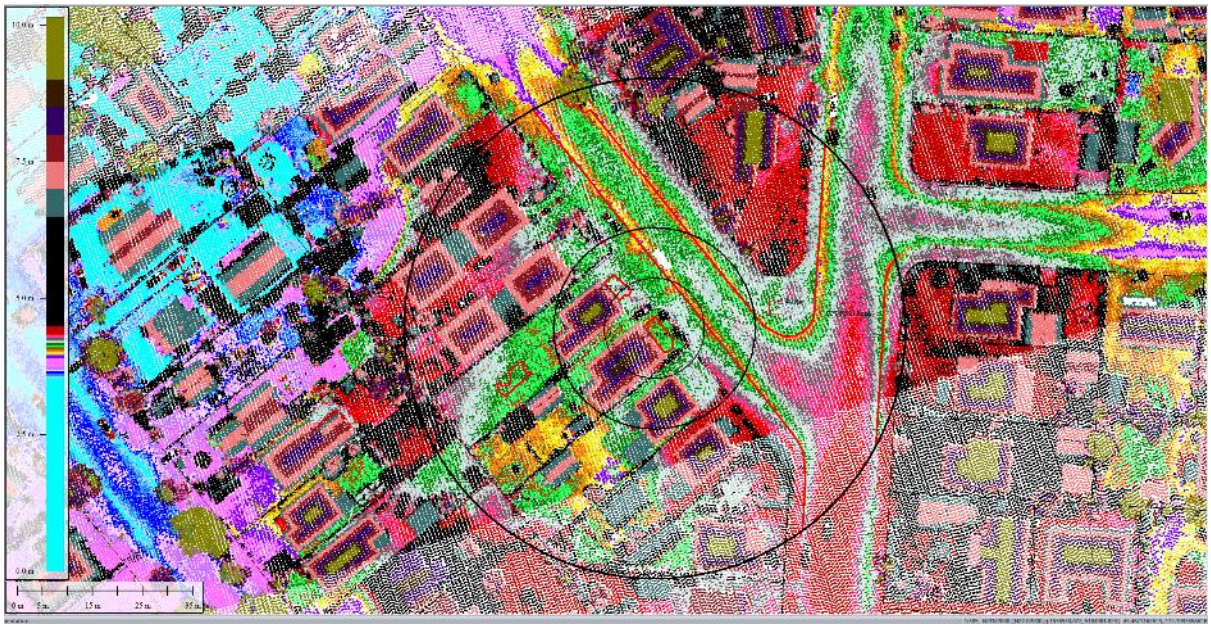

Figure 85: Ground surface elevation for Road averaged over the 50-m buffer for Oct 2015 LiDAR survey.

Figure 86: Absence of ejecta at the site for Sep-10 EQ.

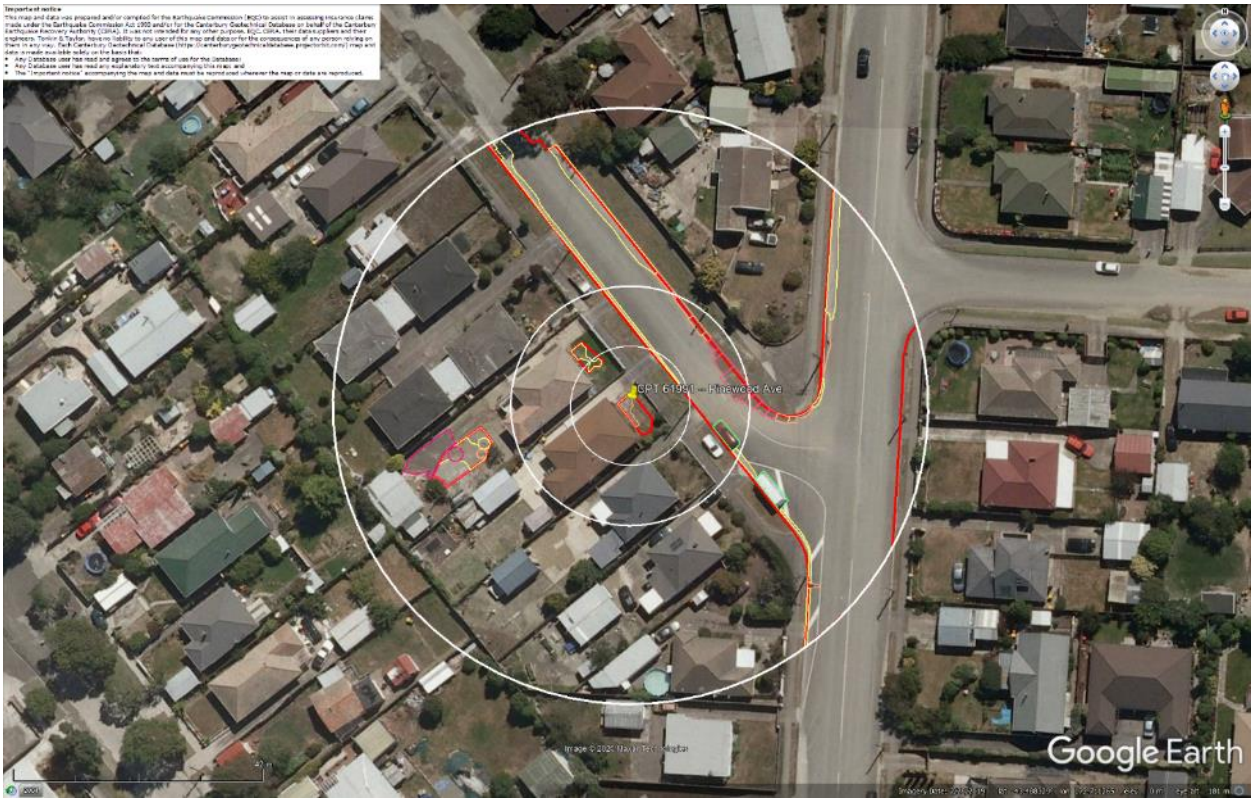

Figure 87: Ejecta outline for Feb-11 EQ.

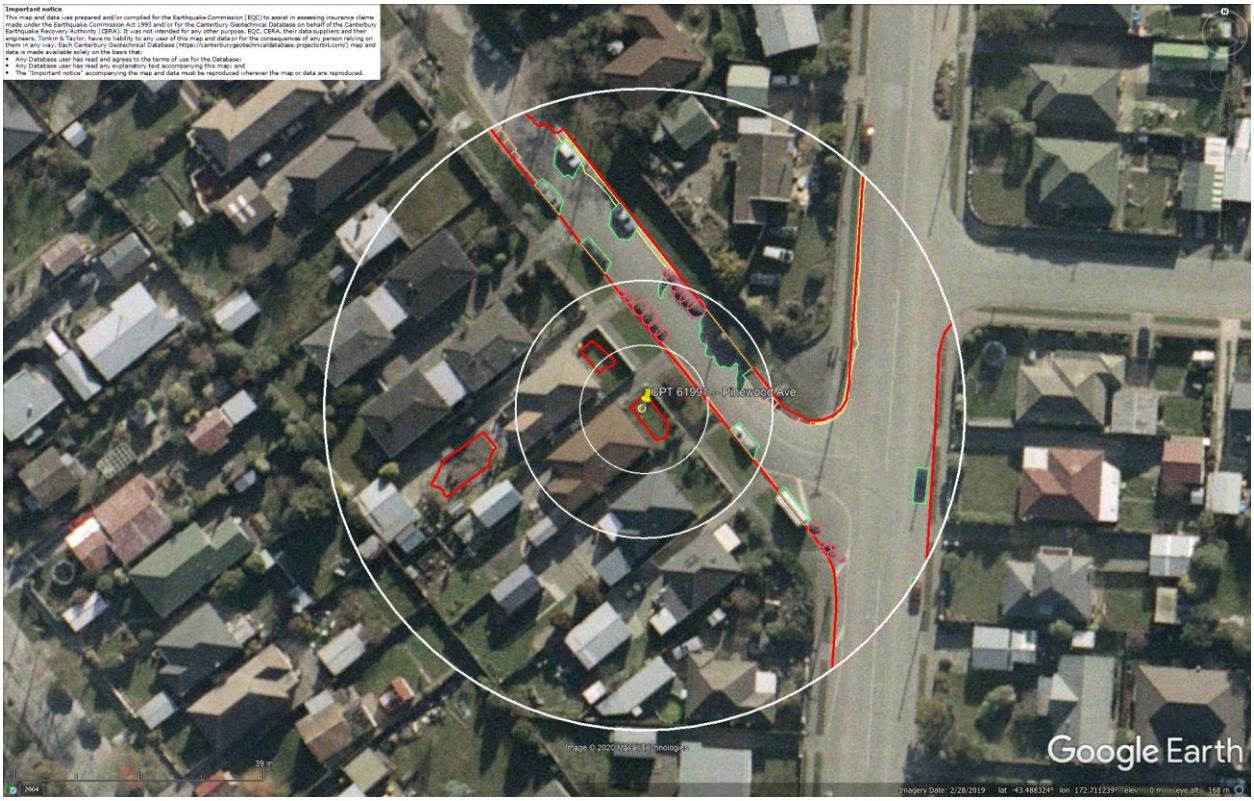

Figure 88: Ejecta outline for Jun-11 EQ.

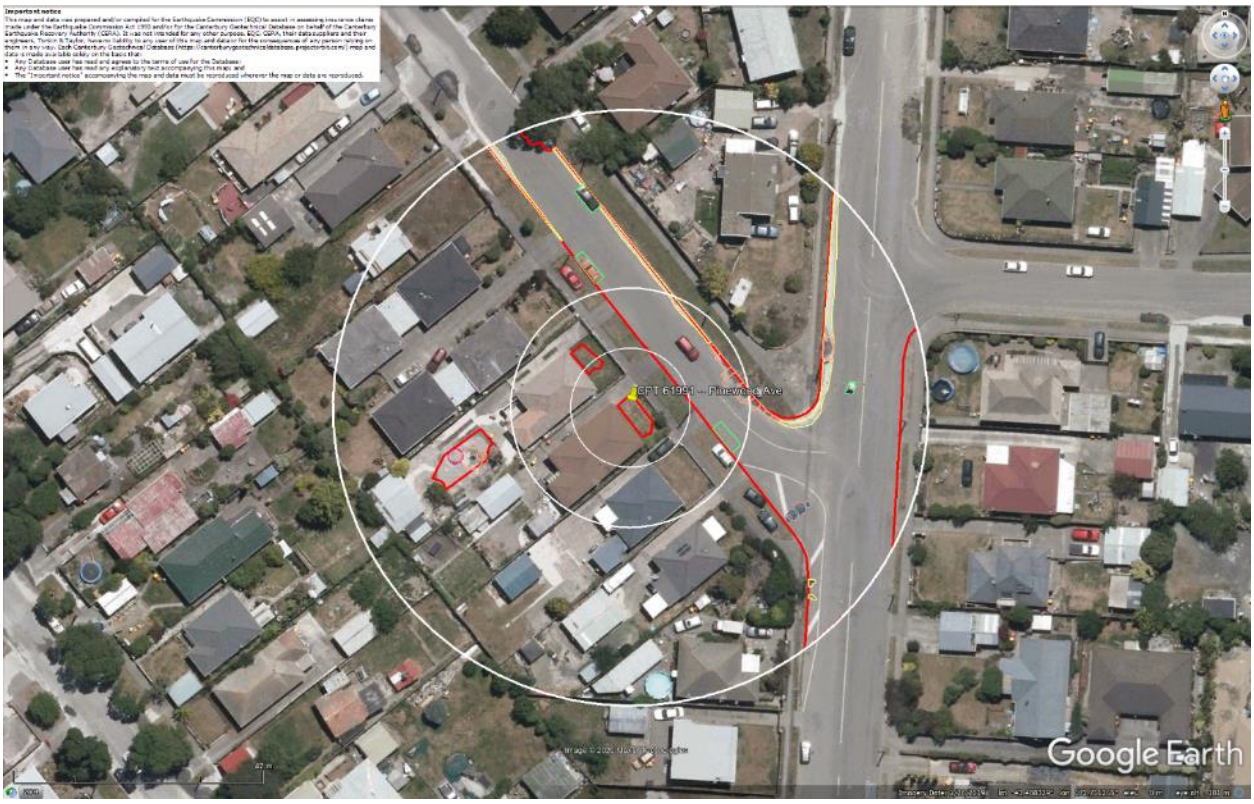

Figure 89: Ejecta outline for Dec-11 EQ.

Contents of this figure cannot be shared as doing so is restricted by a Non-Disclosure Agreement.

Figure 90: Inspection report for Patch A.

Figure 91: Ground photograph of Patch A.

Contents of this figure cannot be shared as doing so is restricted by a Non-Disclosure Agreement.

Figure 92: Inspection report for Patches B and C.

Figure 93: Ground photographs of Patch B.

Figure 94: Ground photographs of the sinkhole within Patch C.

Figure 95: Ground photographs of the ejected material within Patch C.

Figure 96: Cracks in the driveway next to Patch C.

Figure 97: PGA for Sep-10 EQ (st. dev. = 0.300-0.325 ln units).

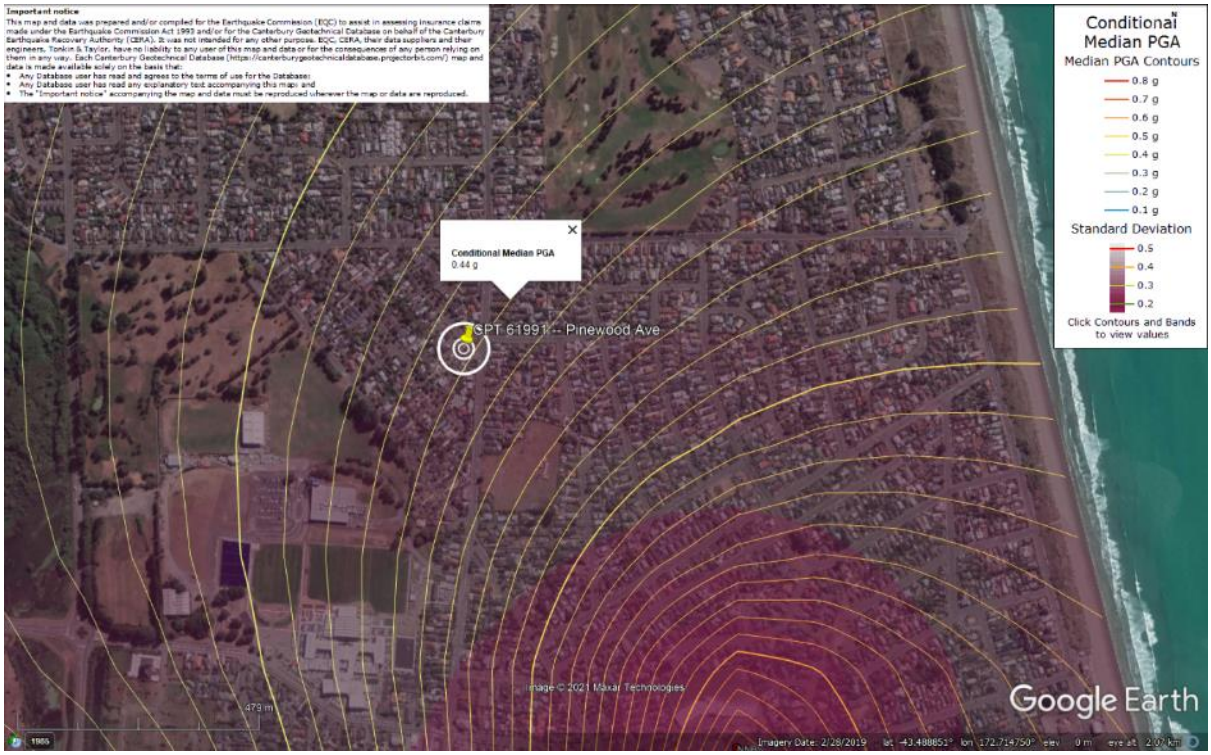

Figure 98: PGA for Feb-11 EQ (st. dev. = 0.325-0.350 ln units).

Figure 99: PGA for Jun-11 EQ (st. dev. = 0.325-0.350 ln units).

Figure 100: PGA for Dec-11 EQ (st. dev. = 0.375-0.425 ln units).

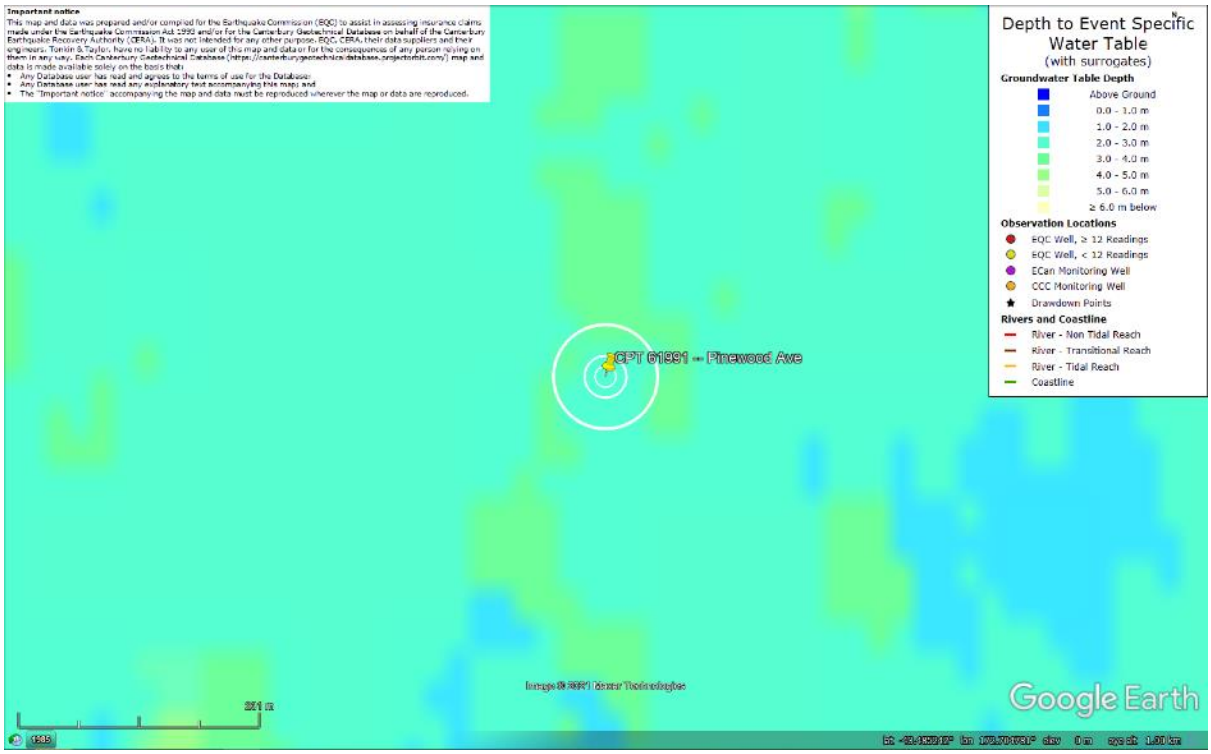

Figure 101: Depth to groundwater table for Sep-10 EQ.

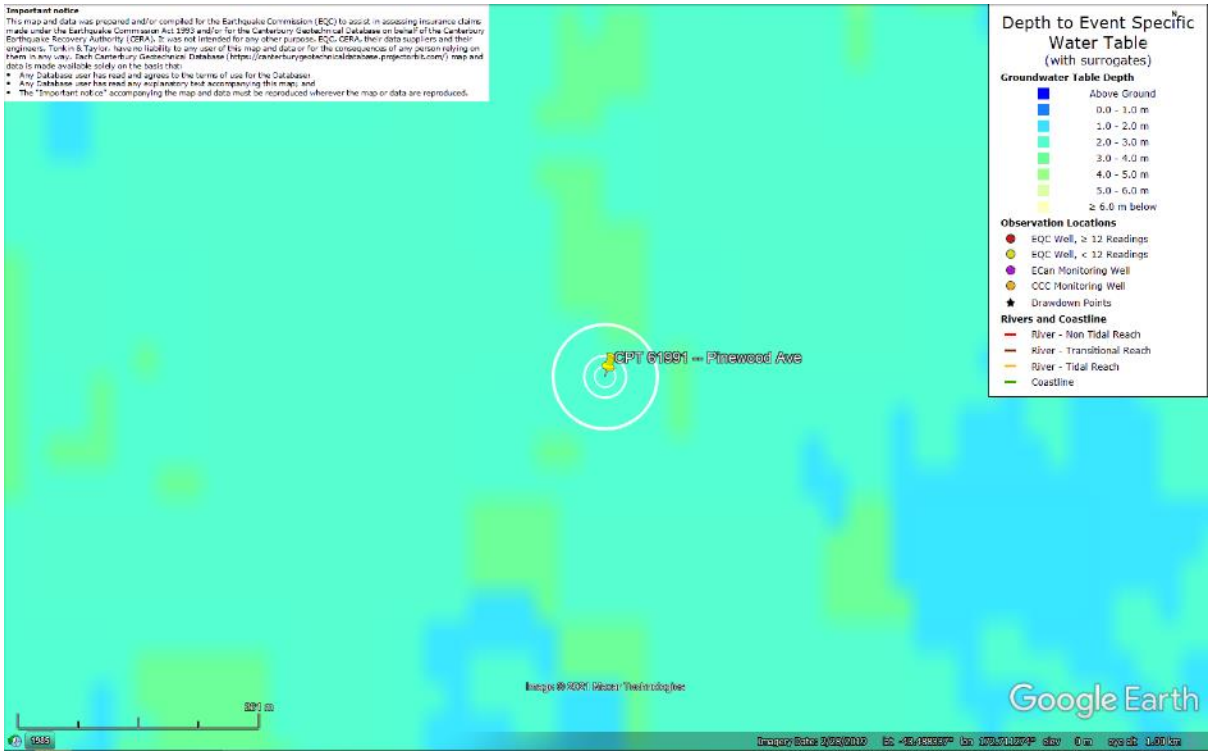

Figure 102: Depth to groundwater table for Feb-11 EQ.

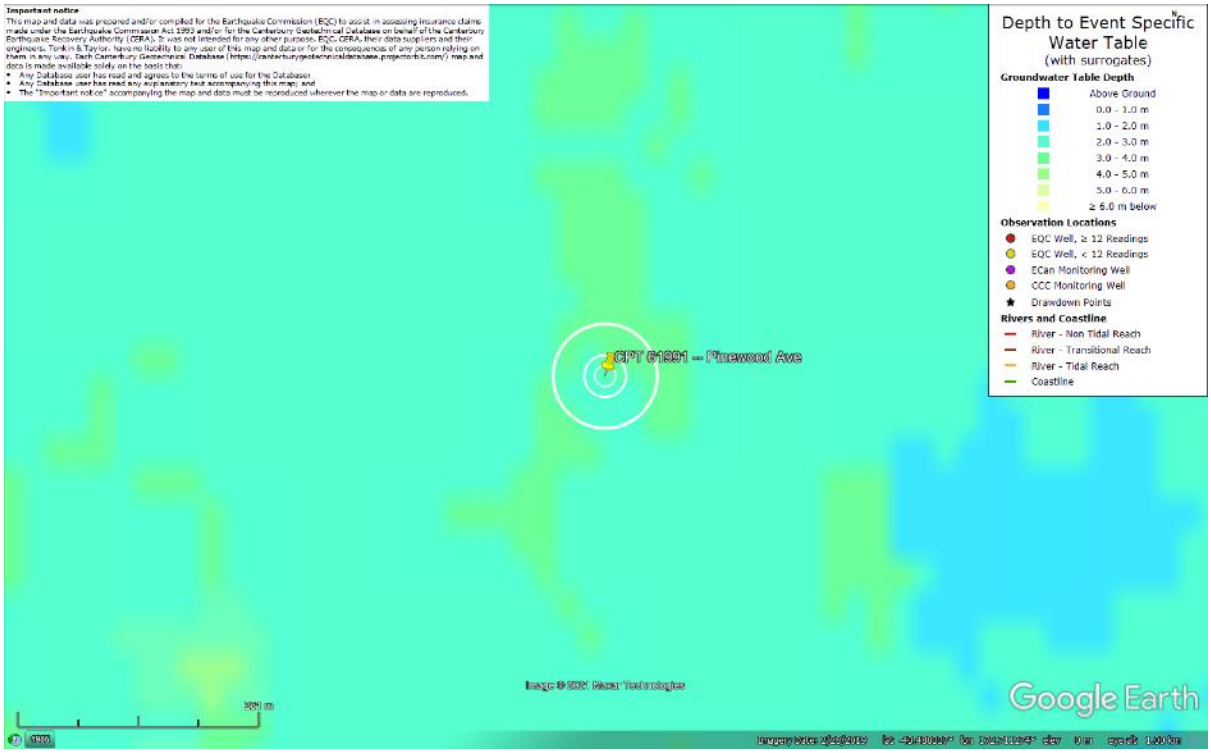

Figure 103: Depth to groundwater table for Jun-11 EQ.

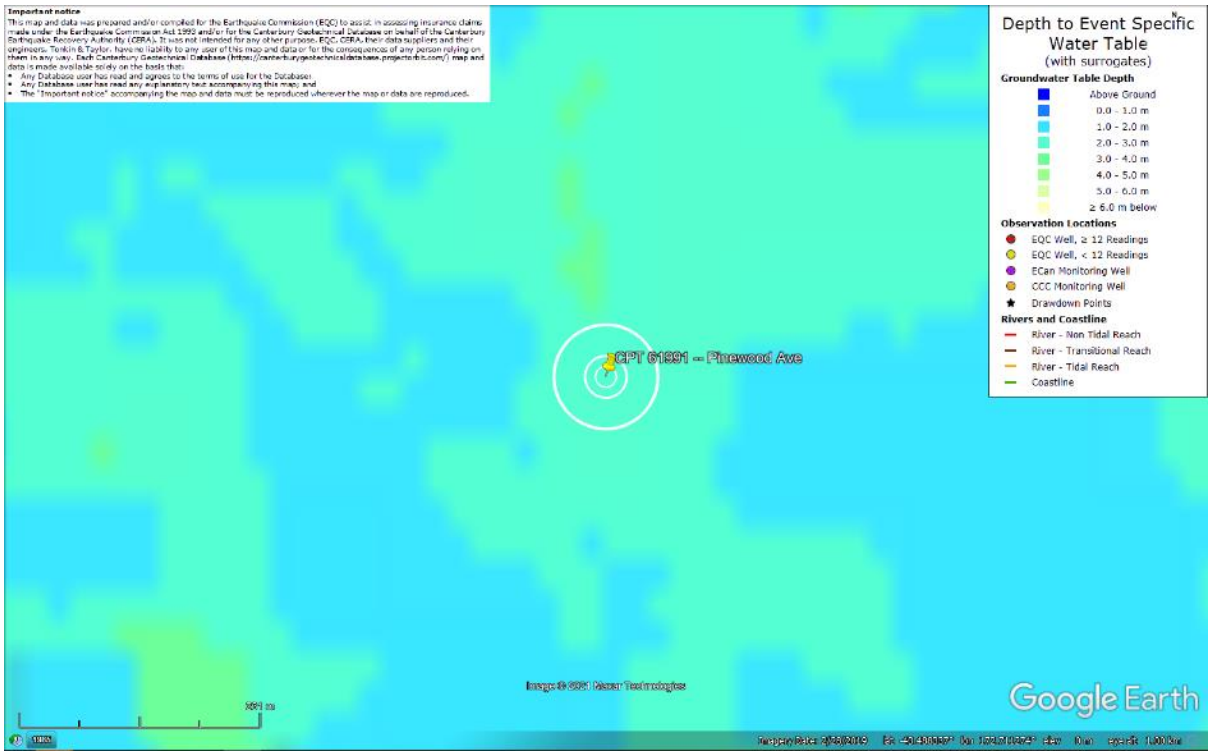

Figure 104: Depth to groundwater table for Dec-11 EQ.

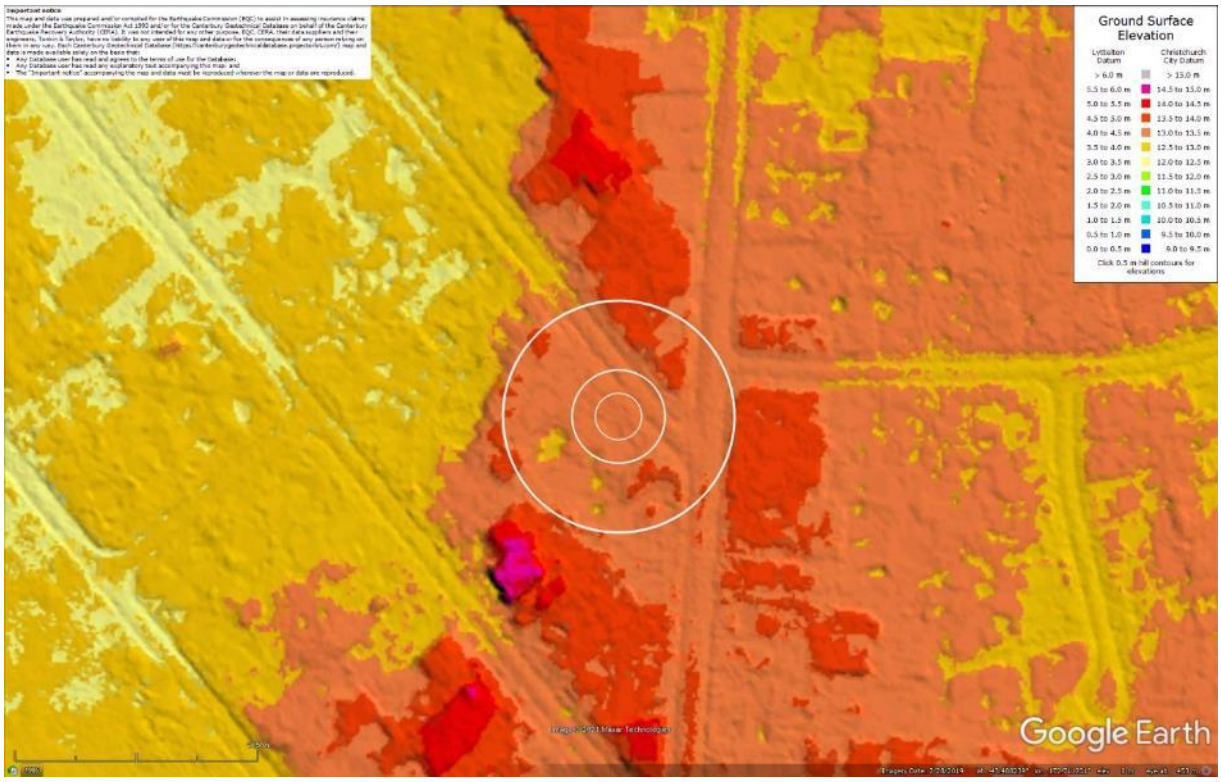

Figure 105: Ground surface elevation according to the Sep-11 LiDAR survey.

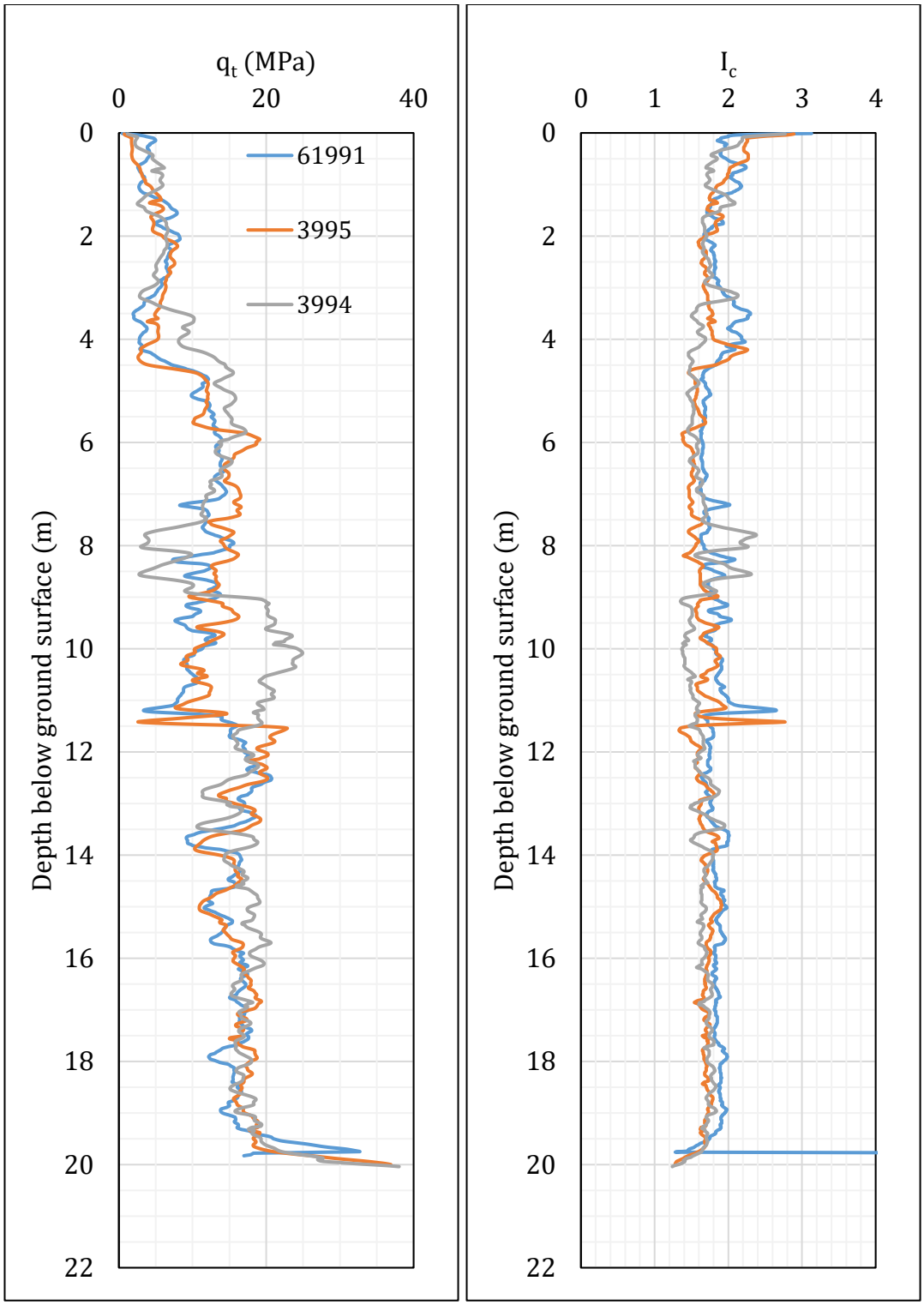

Figure 106: q_t and I_c profiles.

Note 8: The selection of CPTs for the area considered for settlement assessment (Figure 1) is based on the proximity of the CPTs to the considered areas. In accordance with that, the following table shows CPTs that were used for the volumetric settlement analysis in *Cliq v.3.0.3.2*, a CPT soil liquefaction software developed by GeoLogismiki. (The average volumetric settlements were reported in Table 8.)

Table 12: CPT profiles used in volumetric settlement analysis for areas selected for settlement assessment.

CPT ID No.	Patch A	Patch B	Patch C	Road
61991	✓			✓
3995		✓		✓
3994			✓	

Table 13: CPT-based results.

		CPT ID		
EQ Event	Parameter	61991	3995	3994
Sep-10	S_{V1D} (mm)	3	7	9
	LSN	1	1	1
	LPI	0	0	0
	LPI_{ish}	0	0	0
	$D_{FS<1}$ (m)	undet.	undet.	undet.
Feb-11	S_{V1D} (mm)	85	121	83
	LSN	15	19	13
	LPI	7	9	7
	LPI_{ish}	3	7	5
	$D_{FS<1}$ (m)	2.85	2.82	2.82
Jun-11	S_{V1D} (mm)	5	8	10
	LSN	1	2	1
	LPI	0	0	0
	LPI_{ish}	0	0	0
	$D_{FS<1}$ (m)	undet.	undet.	undet.
Dec-11	S_{V1D} (mm)	58	81	64
	LSN	11	15	12
	LPI	4	5	5
	LPI_{ish}	1	4	3
	$D_{FS<1}$ (m)	3.15	2.86	2.52

Notes: $D_{FS<1}$ = Depth to the first liquefiable layer ($FS_L<1$) that is at least 200-mm thick, as determined by the Boulanger and Idriss (2016) liquefaction-triggering procedure (P_L=50%, C_{FC}=0.13, and $I_{c,cutoff}$ =2.6), and exported from *Cliq v.3.0.3.2*; undet. = the specified soil layer was not detected.

Note 9: Based on the borehole log (BH 2958, Figure 1), the groundwater table is at a depth of 3.45 m below the ground surface. The ground subsurface profile consists of (1) asphalt and gravelly fill to a depth of 0.3 m and (2) fine to medium sand, SP, of the Christchurch formation to a depth of 20 m.

Note 10: The ejecta-induced free-field settlement provided in Table 11 is an areal average settlement due to ejecta, which is based on the total settlement assessment area, A_T (provided in Table 9 and repeated in Table 14). However, the considered area was not always covered completely with ejecta; thus, it is important to provide the localized ejecta-induced settlement, too. The localized settlement due to ejecta is estimated using photographic evidence only as

$$S_{E,P\_localized} = \frac{V_E}{A_E}$$

where V_E is the total volume of ejecta within A_T and A_E is the total coverage area of ejecta within A_T. Please note that the areal ejecta-induced settlement provided in Table 14 as S_{E,P_areal} is the same as $S_{E,P}$ in Table 11, which was estimated as

$$S_{E,P\_areal} = S_{E,P} = \frac{V_E}{A_T}$$

where V_E is the total volume of ejecta within A_T and A_T is the total settlement assessment area.

Table 14a: Areal and localized ejecta-induced settlement estimates for Patch A (10-, 20-, and 50-m buffers) based on photographic evidence.

Earthquake Event	A_T (m^2)	A_E (m^2)	V_E (m^3)	S_{E,P_areal} (mm)	$S_{E,P\_localized}$ (mm)
Sep-10	20.0	0	0	0	0
Feb-11	20.0	6.9	0.3-0.4	20±5	50±10
Jun-11	20.0	0.9	0.02-0.03	<5	25±10
Dec-11	20.0	0	0	0	0

Notes: $S_{E,P\_areal} = S_{E,P}$ reported in Table 11 = areal ejecta-induced settlement; $S_{E,P\_localized}$ = localized ejecta-induced settlement; A_T = total settlement assessment area; V_E = total volume of ejecta within A_T; A_E = total area of ejecta within A_T; The estimates of both areal and localized ejecta-induced settlement are rounded to the nearest 5; Final plus/minus values are also rounded to the nearest 5.

Table 14b: Areal and localized ejecta-induced settlement estimates for Patch B (20- and 50-m buffers) based on photographic evidence.

Earthquake Event	A_T (m^2)	A_E (m^2)	V_E (m^3)	S_{E,P_areal} (mm)	$S_{E,P\_localized}$ (mm)
Sep-10	13.0	0	0	0	0
Feb-11	13.0	7.6	0.08-0.2	10±5	20±10
Jun-11	13.0	0	0	0	0
Dec-11	13.0	0	0	0	0

Notes: $S_{E,P\_areal} = S_{E,P}$ reported in Table 11 = areal ejecta-induced settlement; $S_{E,P\_localized}$ = localized ejecta-induced settlement; A_T = total settlement assessment area; V_E = total volume of ejecta within A_T; A_E = total area of ejecta within A_T; The estimates of both areal and localized ejecta-induced settlement are rounded to the nearest 5; Final plus/minus values are also rounded to the nearest 5.

Table 14c: Areal and localized ejecta-induced settlement estimates for Patch C (50-m buffer) based on photographic evidence.

Earthquake Event	A_T (m^2)	A_E (m^2)	V_E (m^3)	S_{E,P_areal} (mm)	$S_{E,P\_localized}$ (mm)
Sep-10	46.8	0	0	0	0
Feb-11	46.8	46.8	7.2-11.7	200±50	200±50
Jun-11	46.8	NA	NA	100±25	NA
Dec-11	46.8	46.8	3.6-7.7	120±45	120±45

Notes: S_{E,P_areal} = $S_{E,P}$ reported in Table 11 = areal ejecta-induced settlement; $S_{E,P\_localized}$ = localized ejecta-induced settlement; A_T = total settlement assessment area; V_E = total volume of ejecta within A_T; A_E = total area of ejecta within A_T; The estimates of both areal and localized ejecta-induced settlement are rounded to the nearest 5; Final plus/minus values are also rounded to the nearest 5; NA = Not available.

Table 14d: Areal and localized ejecta-induced settlement estimates for Road (20-m buffer) based on photographic evidence.

Earthquake Event	A_T (m^2)	A_E (m^2)	V_E (m^3)	S_{E,P_areal} (mm)	$S_{E,P\_localized}$ (mm)
Sep-10	266	0	0	0	0
Feb-11	256	45.9	2.7-3.9	15±5	70±10
Jun-11	215	ND	ND	15±5	ND
Dec-11	266	26.5	0.8-1.2	5±5	40±10

Notes: S_{E,P_areal} = $S_{E,P}$ reported in Table 11 = areal ejecta-induced settlement; $S_{E,P\_localized}$ = localized ejecta-induced settlement; A_T = total settlement assessment area; V_E = total volume of ejecta within A_T; A_E = total area of ejecta within A_T; The estimates of both areal and localized ejecta-induced settlement are rounded to the nearest 5; Final plus/minus values are also rounded to the nearest 5; ND = Not evaluated because the coverage area of ejecta could not be estimated with confidence (the large volume of ejecta on the road within the small area plus uncertainty in the origin of ejecta).

Table 14e: Areal and localized ejecta-induced settlement estimates for Road (50-m buffer) based on photographic evidence.

Earthquake Event	A_T (m^2)	A_E (m^2)	V_E (m^3)	S_{E,P_areal} (mm)	$S_{E,P\_localized}$ (mm)
Sep-10	1617	0	0	0	0
Feb-11	1593	186	5.2-7.9	5±5	35±5
Jun-11	1492	ND	ND	5±5	ND
Dec-11	1595	ND	ND	5±5	ND

Notes: S_{E,P_areal} = $S_{E,P}$ reported in Table 11 = areal ejecta-induced settlement; $S_{E,P\_localized}$ = localized ejecta-induced settlement; A_T = total settlement assessment area; V_E = total volume of ejecta within A_T; A_E = total area of ejecta within A_T; The estimates of both areal and localized ejecta-induced settlement are rounded to the nearest 5; Final plus/minus values are also rounded to the nearest 5; ND = Not evaluated because the coverage area of ejecta could not be estimated with confidence (the large volume of ejecta on the road within the small area plus uncertainty in the origin of ejecta).

Summary 2:

- **The best estimate of the localized ejecta-induced free-field ground settlement at the Pinewood Ave site for the SEP 2010, FEB 2011, JUN 2011, and DEC 2011 earthquake is 0 mm, 50±10 mm, 25±10 mm, and 0 mm, respectively.**
- **The best estimate of the localized ejecta-induced settlement of the road at the Pinewood Ave site for the SEP 2010, FEB 2011, and DEC 2011 earthquake is 0 mm, 70±10 mm, and 40±10 mm, respectively. The localized ejecta-induced settlement of the road for the JUN 2011 earthquake could not be estimated with confidence.**